

**PREPARATION OF HOLLOW FIBER  
MEMBRANES  
FOR GAS SEPARATION**

**Shu-Guang Li**



**PREPARATION OF HOLLOW FIBER MEMBRANES  
FOR GAS SEPARATION**

**PROEFSCHRIFT**

ter verkrijging van  
de graad van doctor aan de Universiteit Twente,  
op gezag van de rector magnificus,  
prof. dr. Th.J.A. Popma,  
volgens besluit van het College voor Promoties  
in het openbaar te verdedigen  
op donderdag 13 januari 1994 te 13.15 uur.

door

**Shu-Guang Li**  
geboren op 19 mei 1960  
te Guang Xi, P.R. China

Dit proefschrift is goedgekeurd door de promotor prof. dr. ing. H. Strathmann,  
de co-promotor prof. dr. C.A. Smolders en de assistent-promotor  
dr. ir. Th. van den Boomgaard.



## ACKNOWLEDGEMENT

I would like to express my sincere appreciation to all those people who contributed to this thesis.

First I'd like to give my special thanks to Kees Smolders, Heiner Strathmann, and Thonie van den Boomgaard for their invaluable guidance and support.

I am very grateful to Remco Boom and Astrid Bulte for their valuable suggestions, fruitful discussions and for their kindness.

It is my great pleasure to thank Erik Rolevink and Ineke Pünt for their outstanding technical assistance; to Ingrid Wienk for her revising the English in this thesis.

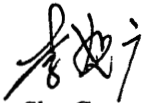
Thanks also to all members of the research group for their understanding, support and friendship.

I appreciate very much the fascinating discussions with Ingo Pinnau (a typical membrane-maker).

I enjoy a lot my stay in the "Membraantechnologie" group in University of Twente. The pleasant atmosphere in this group gives me many warm feelings.

STW (PCM) and Delair Droogtechniek en Luchtbehandeling B.V. are gratefully acknowledged for their financial support of this work.

Finally I'd like to thank my wife, Qiu-Wei, and my daughter, Lu-Yue, for their love, patience and support. Final thanks also to my little son, Tai-Long, just for fun.



Shu-Guang Li

CIP-DATA KONINKLIJKE BIBLIOTHEEK, DEN HAAG

Li, Shu-Guang

Preparation of hollow fiber membranes for gas separation

Shu-Guang Li

Thesis Enschede. - With ref. - With summary in Dutch.

ISBN 90-9006853-8

Key words: membrane, gas separation, hollow fiber.

© Shu-Guang Li, Enschede, the Netherlands, 1993.

All rights reserved.

Printed by Reprodienst at the University of Twente, Enschede.

---

**CONTENTS**

---

**CHAPTER 1 INTRODUCTION**

|  |    |
|--|----|
| 1.1. Gas separation by membranes                   | 1  |
| 1.2. Membrane separation mechanism                 | 6  |
| 1.2.1. Porous membranes                            | 7  |
| 1.2.2. Nonporous membranes                         | 7  |
| 1.3. Preparation of gas separation membranes       | 10 |
| 1.3.1. Melt pressing or extrusion                  | 10 |
| 1.3.2. Solution casting and evaporation            | 10 |
| 1.3.3. Thermal precipitation                       | 11 |
| 1.3.4. Controlled solvent evaporation              | 11 |
| 1.3.5. Interfacial composite                       | 11 |
| 1.4. Membrane formation by immersion precipitation | 14 |
| 1.4.1. A historical review                         | 14 |
| 1.4.2. Membrane formation mechanism                | 15 |
| 1.4.3. Dual bath spinning process                  | 20 |
| 1.5. Structure of this thesis                      | 22 |
| 1.6. References                                    | 23 |

**CHAPTER 2 GELATION OF AMORPHOUS POLYMER IN A MIXTURE OF SOLVENT AND NONSOLVENT**

|  |    |
|--|----|
| 2.1. Abstract  | 29 |
| 2.2. Introduction  | 30 |
| 2.3. Gelation of amorphous polymer                                   | 31 |
| 2.3.1. Guenet's mechanism for gelation of amorphous polymers         | 32 |
| 2.3.2. Berghmans' mechanism for gelation of amorphous polymers       | 33 |
| 2.4. Glass transition temperature of polymer solutions               | 35 |
| 2.5. Experimental  | 37 |
| 2.5.1. Materials   | 37 |
| 2.5.2. Cloud point measurements                                      | 37 |
| 2.5.3. Glass transition temperature of homogeneous polymer solutions | 37 |
| 2.5.4. Glass transition temperature of demixed polymer solutions     | 38 |
| 2.5.5. Membrane preparation  | 38 |

|   |    |
|---|----|
| 2.5.6. Delay time of demixing                                       | 38 |
| 2.6. Results and discussion   | 38 |
| 2.6.1. Glass transition temperatures of solvents                    | 38 |
| 2.6.2. Cloud points   | 39 |
| 2.6.3. $T_g$ depression of PES by different solvents                | 40 |
| 2.6.4. $T_g$ depression of PES by a mixture of NMP and water        | 42 |
| 2.6.5. Determination of the gelation boundary                       | 43 |
| 2.6.6. The ternary phase diagram of H <sub>2</sub> O-NMP-PES system | 44 |
| 2.6.7. Examination of the gelation boundary                         | 46 |
| 2.6.8. Demixing behaviour in relation to vitrification phenomenon   | 47 |
| 2.6.9. Membrane formation   | 49 |
| 2.7. Conclusions  | 51 |
| 2.8. References   | 52 |

**CHAPTER 3      MODELLING OF MEMBRANE FORMATION FROM  
THE SYSTEM H<sub>2</sub>O-NMP-POLYETHERSULFONE**

|  |    |
|--|----|
| 3.1. Abstract  | 53 |
| 3.2. Introduction  | 53 |
| 3.3. Equilibrium thermodynamics  | 56 |
| 3.3.1. Flory-Huggins theory  | 56 |
| 3.3.2. Evaluation of interaction parameters for H <sub>2</sub> O-NMP-PES<br>system | 57 |
| 3.4. Mass transfer   | 58 |
| 3.4.1. Mass transfer model   | 58 |
| 3.4.2. Calculation procedure   | 62 |
| 3.4.3. Evaluation of friction coefficients for H <sub>2</sub> O-NMP-PES<br>system  | 62 |
| 3.5. Calculation of the phase diagram  | 63 |
| 3.5.1. The phase diagram calculated by Zeman and Tkacik                            | 63 |
| 3.5.2. Binodal calculated by using a ternary interaction parameter                 | 64 |
| 3.5.3. The effect of variations of $\chi_T$ on equilibrium properties              | 66 |
| 3.6. Composition path after a very short immersion time                            | 68 |
| 3.6.1. General meaning of a composition path                                       | 68 |
| 3.6.2. Composition path for H <sub>2</sub> O-NMP-PES system                        | 69 |
| 3.6.3. A hypothesis for the formation of nodular structure                         | 71 |
| 3.7. Simulating the kinetic effect on membrane formation                           | 73 |
| 3.8. Conclusions   | 76 |

|                      |    |
|----------------------|----|
| 3.9. List of symbols | 76 |
| 3.10. References     | 77 |

#### **CHAPTER 4      PREPARATION OF HOLLOW FIBER MEMBRANES BY A MODIFIED DUAL BATH SPINNING PROCESS**

|   |     |
|---|-----|
| 4.1. Abstract   | 79  |
| 4.2. Introduction   | 80  |
| 4.3. Theory   | 81  |
| 4.4. Experimental   | 83  |
| 4.4.1. Materials  | 83  |
| 4.4.2. Cloud point and delay time measurements              | 83  |
| 4.4.3. Measurements of the temperature change due to mixing | 83  |
| 4.4.4. Spinning of hollow fibers                            | 84  |
| 4.4.5. Fiber characterization                               | 85  |
| 4.5. Results and discussion                                 |     |
| 4.5.1. Choice of first coagulant                            | 85  |
| 4.5.2. The effect of contact time                           | 95  |
| 4.5.3. The effect of bore liquid                            | 100 |
| 4.5.4. Solvent effect                                       | 102 |
| 4.5.5. The effect of drying procedure                       | 108 |
| 4.6. Conclusions  | 110 |
| 4.7. References   | 111 |

#### **CHAPTER 5      ELIMINATION OF MACROVOIDS IN DUAL-BATH FIBERS BY A THERMAL INVERSION PROCESS**

|   |     |
|---|-----|
| 5.1. Abstract                                 | 113 |
| 5.2. Introduction                             | 114 |
| 5.3. Theory                                   | 115 |
| 5.4. Experimental                             | 117 |
| 5.4.1. Materials                              | 117 |
| 5.4.2. Cloud point measurements               | 117 |
| 5.4.3. Fiber spinning and characterizations   | 117 |
| 5.4.4. Plasma etching                         | 118 |
| 5.5. Results and discussion                   | 119 |
| 5.5.1. The use of different first coagulants  | 119 |
| 5.5.2. Addition of solvent to the bore liquid | 119 |

## *Contents*

|   |     |
|---|-----|
| 5.5.3. Addition of nonsolvent to the polymer solution | 124 |
| 5.5.4. Support layer resistance                       | 127 |
| 5.5.5. Hollow fibers spun with the DB&TIPI process    | 127 |
| 5.5.6. Skin formation in the new spinning process     | 131 |
| 5.6. Conclusions                                      | 134 |
| 5.7. References                                       | 135 |
| <b>SUMMARY</b>  | 137 |
| <b>SAMENVATTING</b>                                   | 139 |
| <b>CURRICULUM VITAE</b>                               | 143 |

---

**CHAPTER 1**

---

**INTRODUCTION**

---

**1-1. GAS SEPARATION BY MEMBRANES**

The fact that rubber membranes (films) are selectively permeable for gases was recognized more than 160 years ago by Mitchell [1,2]. In 1866, Graham postulated a solution-diffusion mechanism for permeation of gases through rubber membranes [3]. He described the permeation of gases as a sequence of three steps (see figure 1): solution of the gas in the upstream membrane surface, diffusion through the membrane and desorption at the downstream membrane surface. Graham also demonstrated that gas fluxes are dependent on the membrane thickness whereas selectivities are not.

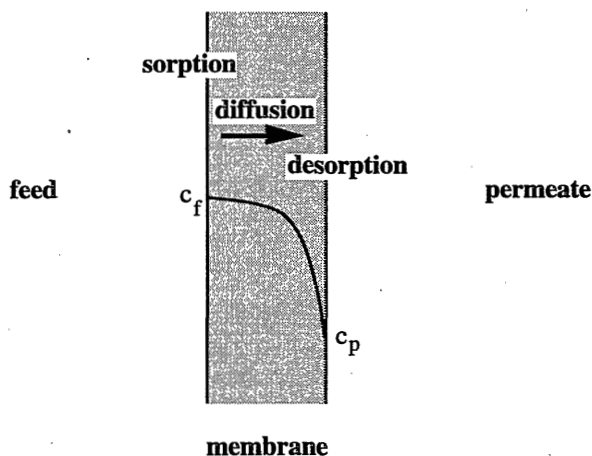


*Figure 1. Schematic illustration of the solution-diffusion mechanism for the permeation of gases through polymeric membranes*

Despite the early recognition of the separating potential of polymer membranes for gas, no large scale applications were introduced until the seventies of this century. It was due to the lack of polymeric membrane materials and membrane structures that combined high selectivities and high transmembrane fluxes. However, large-scale (but non-commercial) application of membrane-based gas separation appeared during World War II for the enrichment of uranium<sup>235</sup>. The separation was achieved by means of porous ceramic membranes [4].

The breakthrough leading to the successful use of gas separation membranes on a large commercial scale was the discovery of integrally-skinned asymmetric cellulose acetate (CA) membranes by Loeb and Sourirajan [5] in 1960. The structure of such a membrane is schematically shown in figure 2. The asymmetric membranes consist of a dense and thin skin layer supported by a porous sublayer of the same material. The skin layer performs the separation with a high flux because it is thin and with a high selectivity due to its high density. The porous sublayer provides the mechanical strength.

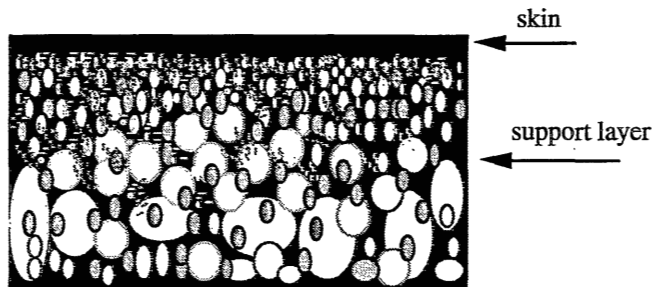


**Figure 2.** A schematic illustration of the structure of integrally-skinned asymmetric membranes.

Those membranes were developed for the application of desalination of sea water. However, the potential to use this type of membrane for gas separation was recognized immediately after the discovery, which resulted in the first asymmetric membrane for gas separation in 1970 [6]. The step from desalination to gas separation was accomplished by the development of methods for the drying of wet desalination membranes without collapsing the porous sublayer and thickening or destructing the dense skin layer [6-9]. At the time also thin-film composite membranes were developed for gas separation [10,11]. A thin-film composite membrane can also be regarded as an asymmetric membrane, which can be prepared by laminating a separately made thin film on a microporous supporting membrane [12] or by forming the thin film directly on a support membrane with a coating technique [11]. The separation properties of the membrane are determined by the thin film.

Commercial membrane systems for gas separation have been available since 1970. Examples are oxygen-enriched air for home medical care by using silicon/polycarbonate copolymer composite membranes [13,14], the separations of acidic gases from natural gas, the recovery of carbon dioxide in the enhanced oil recovery process, gas dehydration and the separation of hydrogen from carbon monoxide by using CA (or a blend of CA and other cellulosic polymers) asymmetric



membranes [15-17]. Membranes in these systems were applied in the form of spiral-wound modules.

The most important innovation for large-scale commercialization of membrane gas separation systems was achieved by Monsanto company [18-21]. The membrane separators, marketed as Prism<sup>®</sup>, were first tested on a pilot scale inside the company in 1975 [22], and were commercially launched in November 1979 [22]. The membrane used in the Prism<sup>®</sup> separator is based on polysulfone formed as hollow fibers. The membrane is asymmetric and coated with a silicon rubber. Unlike the thin-film composite membranes in which the membrane properties are controlled by the top selective layer, the properties of Monsanto's membrane are determined by the supporting membrane. In Monsanto's membrane, the silicon rubber layer does not function as a selective barrier but rather plugs the defects of the supporting membrane. Detailed discussion on this plugging effect will be given later in this chapter.

The success of large-scale membrane systems for gas separation by Monsanto initiated abruptly increased research efforts for the development of superior membrane materials and techniques for the preparation of gas separation membranes. Nowadays, many applications for membrane-based gas separation have been identified [23], as shown in table 1.

**Table 1.** Gas mixtures separated with membrane systems and their applications [23].

| Gas mixture                    | Application  |
|--------------------------------|--|
| H <sub>2</sub> /N <sub>2</sub> | H <sub>2</sub> recovery from purge streams in ammonia plants |
| H <sub>2</sub> /CO             | H <sub>2</sub> ratio adjustment in synthesis gas             |
| H <sub>2</sub> /Hydrocarbons   | H <sub>2</sub> recovery for hydrocarbon processes            |
| CO <sub>2</sub> /Hydrocarbons  | Acid gas treatment<br>Landfill gas upgrading                 |
| H <sub>2</sub> O/Hydrocarbons  | Natural gas dehydration                                      |
| O <sub>2</sub> /N <sub>2</sub> | O <sub>2</sub> enriched air<br>N <sub>2</sub> enriched air   |
| He/N <sub>2</sub>              | He recovery  |
| He/Hydrocarbons                | He separation  |
| Hydrocarbons/Air               | Hydrocarbon recovery<br>Pollution control                    |
| H <sub>2</sub> O/Air           | Air dehydration  |
| H <sub>2</sub> S/Hydrocarbons  | Sour gas treatment   |

Commercial membranes used for the various applications are made of different materials, as listed in table 2. The companies supplying the membrane systems are also listed in this table.

**Table 2** Commercial membrane gas separation suppliers and the membranes from each supplier. (based on Pinnaus' thesis [24] and complemented)

| Company                        | Membrane material                         | Membrane structure | Module type | Ref. |
|--------------------------------|---|--------------------|-------------|------|
| A/G Technology                 | Ethylcellulose                            | ISA                | HF          | [25] |
| Air Products                   | Poly(trimethyl silylpropyne)              | C                  | HF          | [26] |
|                                | Cellulose acetate                         | ISA                | SW          | [27] |
| Allied Signal                  | Cellulose acetate                         | ISA                | SW          | [28] |
|                                | Silicon/poly(ethylene glycol)             | C                  | SW          | [29] |
| Asahi Glass                    | Silicon/fluoropolymer                     | C                  | PF          | [30] |
| Delair                         | Poly(2,6-dimethyl-p-phenylene oxide)      | ISA                | HF          | [31] |
| Dow Chemical                   | Tetrabromopolycarbonate                   | ISA                | HF          | [32] |
|                                | Cellulose acetate                         | ISA                | HF          | [33] |
| Du Pont                        | Polyaramide                               | ISA                | HF          | [34] |
| Envirogenics                   | Cellulose triacetate                      | ISA                | SW          | [35] |
| Grace Membrane Systems         | Cellulose acetate                         | ISA                | SW          | [36] |
| Membrane Technology & Research | Silicone                                  | C                  | SW          | [37] |
|                                | Poly(ether ester amide)                   | C                  | SW          | [38] |
| OECO                           | Silicone/polycarbonate                    | C                  | PF          | [14] |
| Osaka gas                      | Silicone                                  | C                  | SW          | [39] |
| Permea (Air Products)          | Polysulfone/silicone                      | C                  | HF          | [40] |
|                                | Brominated poly(phenylene-oxide)/silicone | C                  | HF          | [41] |
| Ube                            | Polyimide                                 | C                  | HF          | [30] |
| Union Carbide                  | Ethylcellulose                            | C                  | HF          | [42] |
|                                | Cellulose acetate                         | C                  | HF          | [43] |
| UOP                            | Silicone                                  | C                  | SW          | [30] |

C: composite membrane; ISA: integrally-skin asymmetric membrane; HF: hollow fiber; PF: plate & frame; SW: spiral-wound

Gas separation properties of a number of membrane materials are given in table 3.

**Table 3.** Permeability coefficients of a number of polymers from table 2, at 25 °C [30,44]

| Membrane                                  | Permeability coefficient * |            | Selectivity       |                     |
|---|----------------------------|------------|-------------------|---------------------|
|   | $P_{O_2}$                  | $P_{CO_2}$ | $P_{O_2}/P_{N_2}$ | $P_{CO_2}/P_{CH_4}$ |
| Polysulfone                               | 1                          | 6          | 6                 | 30                  |
| Polyimide                                 | 0.1                        | -          | 11                | -                   |
| Cellulose acetate                         | 1                          | 6          | 5.5               | 30                  |
| Cellulose triacetate                      | 1                          | -          | 5.9               | -                   |
| Silicone rubber<br>(polydimethylsiloxane) | 604                        | 3230       | 2.1               | 3                   |

\* units:  $\text{cm}^3 \text{ cm/cm}^2 \text{ s cmHg} \times 10^{-10}$

The definitions for permeability coefficient and selectivity are given later in this chapter.

It can be seen in table 2 that polymers used for the production of commercial membranes include rubbery and glassy polymers. Nowadays for gas separation membranes glassy polymers are used more often than rubbery polymers because of their high selectivities as shown in table 3. The permeability coefficients of glassy polymers are in general much lower than of rubbery polymers, but this can be compensated, to a certain extent, by reducing the membrane thickness (by means of asymmetric structure).

As polymeric membranes are permeable for all gases, although at different rates, high purity of the permeate (or the nonpermeate) usually cannot be achieved in a single pass. To reach a high purity, repeated separation stages or recycling part of the permeate (or nonpermeate) are required. This will increase operation cost since energy intensive compression of feed streams is often needed to provide the driving force for the permeation. So, most of the membrane applications are limited to areas where feed streams are available at high pressure (e.g.  $H_2$  recovery), or the nonpermeate is the product of interest (e.g. removal of water and acidic gases from natural gas), or medium purity is required (e.g.  $O_2$  enrichment for medical use).  $N_2$  enrichment for blanketing usage is one of the most important membrane-based separations mainly because high purity (>99.5 %) is not necessary and  $N_2$  is the nonpermeate [45].

To further extend the applications of membrane-based gas separation, the development of the integration of the three aspects shown in figure 3 is of great importance [45]. For a given separation the maximum achievable selectivity is determined by the membrane material, while the productivity (gas fluxes) is controlled

by the permeability coefficient of the membrane material as well as the membrane thickness. The efficiency of a practical application is highly dependent on module and system design [30,45,46].

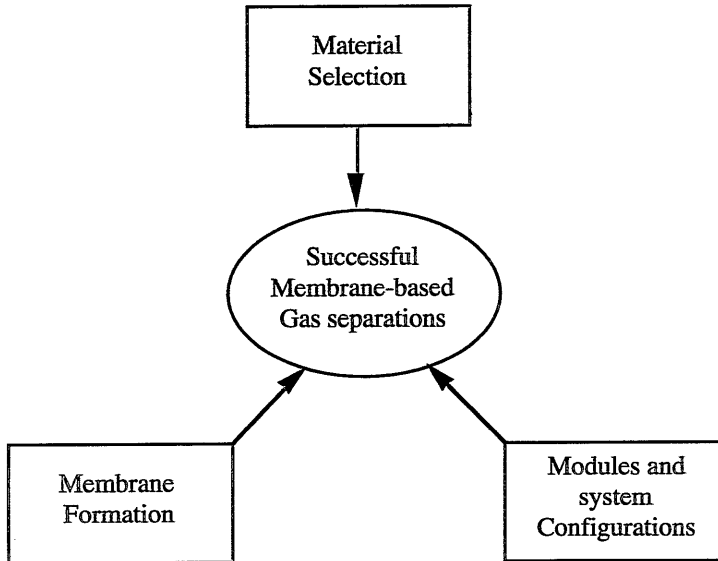


*Figure 3. Critical issues controlling successful membrane-based gas separation [45].*

Membrane materials for gas separations are not limited to polymers. Other materials like ceramic, metal, carbon and glass are also used [47-50]. Ceramic membranes are currently gaining more and more attention because of their applicability in harsh environments. The reader is referred to literature [47] for detailed discussions on these membranes.

This research concerns only the formation of gas separation membranes from polymeric materials.

## **1-2. MEMBRANE SEPARATION MECHANISM**

As described previously, gas permeation through polymeric membranes follows the solution-diffusion mechanism. It is true only for nonporous membranes. Since on a molecular level dynamic "molecular pores" are always present [51], nonporous means here that no permanent or "fixed" pores are present. Gas separation can also be performed using porous membranes. The separation mechanism for porous and the mechanism for nonporous membranes are discussed hereafter.

### 1-2-1. Porous membranes

In order to separate a gas mixture with a porous membrane the pore size of the membrane must be much smaller than the mean free path of the gases. In this case the transport is governed by the Knudsen flow mechanism. Since Knudsen flow is molecular weight dependent (smallest goes most fast), separation will occur when gases with different molecular weights pass through the membrane. The ideal selectivity is reciprocal to the square root of the ratio of the molecular weight of the gases ( $\alpha_{ij}^* = (M_j/M_i)^{1/2}$  [30]). Theoretically (and thus also practically) the achievable selectivity is quite limited since molecular weight ratios of most gases of interest are not very large. Thus in order to reach efficient separation of a gas mixture, a large amount of separation stages are required. Large scale application of this separation process is limited only to the enrichment of uranium<sup>235</sup> from its isotope [4], where a large amount of separation stages (over 10000 stages [30]) are used.

It has to be mentioned here that from carbon and glass materials membranes have been made with pores smaller than 7 Å [49,50]. For gas transport through such small pores, besides the sizes of the gas molecules, the sorption of gas on the pore wall can be important as well on affecting the separation. Much higher selectivity than can be obtained by purely Knudsen flow or by the solution-diffusion mechanism is reported to have been achieved [49,50].

For the separation of gas mixtures containing one easily condensable component, surface diffusion or capillary-condensation can significantly influence the separation as reported in the literature for porous ceramic membranes [47].

### 1-2-2. Nonporous membranes

As already mentioned transport of gases through nonporous polymer films is based on the solution-diffusion mechanism [3]. The permeability of a gas through a membrane is determined by its solubility and diffusivity in the membrane matrix. So, both the nature of the gas and the nature of the polymer will influence the permeability. Conceptually, very efficient separation should be possible this way. The permeability coefficient,  $P$ , can be expressed as a product of a thermodynamic factor  $S$ , called the solubility coefficient, and a kinetic parameter  $D$ , called the diffusion coefficient.

$$P = S D \quad (1)$$

The permeability for a gas is a fundamental property of the polymeric material, so it is independent of the thickness of the membrane [45]. Evaluation of the two coefficients  $S$  and  $D$  in equation (1) is of crucial importance for the understanding of how a gas is dissolved in a polymer matrix and how it "bumps" through the matrix. In

its turn it will give some guidelines for the development of "tailored" materials. This is a subject of substantial researches being on the way as recently reviewed by Koros [45].

The selectivity  $\alpha_{AB}$ , for a binary mixture A and B, defined in terms of the downstream (1) and upstream (2) mole fractions of components A and B is [45]:

$$\alpha_{AB} = (P_A/P_B) \times [(\Delta p_A/p_{A2})/(\Delta p_B/p_{B2})] \quad (2)$$

where  $\alpha_{AB}$  is defined as being larger than 1, which means that in equation (2)  $P_A$  represents the permeability coefficient of the "fast" gas. In case the downstream partial pressures ( $p_{A1}$  and  $p_{B1}$ ) are kept to be negligibly low (e. g. under vacuum), the selectivity equals the ratio of the two permeability coefficients, called the ideal selectivity or the *intrinsic selectivity*. The intrinsic selectivity is a very useful term for the comparison of different materials on an equivalent basis. It depends only on the intrinsic properties of the gases and the polymer. The second term at the right hand side of equation (2) is related to the driving force of an actual operation, called the driving force factor. Based on the definition of A to be the fast gas, this term can never be larger than 1 so that the actual selectivity is in general smaller than the intrinsic selectivity.

According to Fick's first law, the flow rate of a component through the membrane,  $J$ , is related to the permeability  $P$ , the driving force  $\Delta p$  and the membrane thickness  $l$  in the form:

$$J = P \Delta p / l \quad (3)$$

This equation can be rewritten as:

$$P/l = J/\Delta p \quad (4)$$

where  $P/l$  is a pressure normalized flux and is membrane thickness dependent. Very often the flux of a membrane is defined in this form.

From equation (2) and (3) or (4), one can derive that whereas *flow rate is thickness dependent, selectivity is not*. It is obvious that to achieve an efficient separation, one needs to find the "right" membrane material with a high intrinsic selectivity and a high permeability coefficient, and further to prepare the membrane as thin as possible to obtain a high flux. Most of the currently available commercial polymers show a trade-off between selectivity and permeability, e.g., high selectivity is coupled with low permeability and *vice versa* (e.g. see table 3). However, some newly synthesized materials have been made showing drastically increased permeability while

keeping similar or even higher selectivities compared to commercial polymers [45,52-54]. To realize the full potential of those materials the related membranes have to be prepared with a minimized thickness (e.g.  $< 500 \text{ \AA}$ ) and meanwhile to be completely dense.

To meet these critical requirements, preparation of membranes with an asymmetric structure (composite membranes can be seen as asymmetric membranes as well) is probably the only solution. Although the method used by Loeb and Sourirajan [5] followed by careful drying of the formed membranes can be applied to prepare asymmetric gas separation membranes from cellulosic materials, it is very difficult to apply the same method to prepare membranes showing a skin as dense and thin as the Loeb and Sourirajan membrane from non-cellulosic materials [20,40,45]. Defects (tiny pores) are often present in the skin of asymmetric membranes prepared from non-cellulosic materials when the skin is made very thin (e. g.  $< 0.2 \text{ \mu m}$ ). Most gas molecules have kinetic diameters in the range of  $2.6 \text{ \AA}$  to  $5.0 \text{ \AA}$  [45]. The presence of any tiny pores ( $> \sim 5 \text{ \AA}$ ) in the separating layer of gas separation membranes in an area fraction as small as  $10^{-5}$  can result in a large reduction in selectivity [20,45]. These tiny pores can be effectively plugged by using the Monsanto's approach [18,20]. However, since this approach is virtually a sort of post treatment, it inevitably will add a certain complexity to the membrane production process, and therefore it will increase the production cost.

Besides the requirement of a thin and dense skin, the resistance of the sublayer of a gas separation membrane has to be minimized while maintaining the mechanical stability of the membrane. A highly resistant sublayer will reduce not only the flux of the membrane but also the selectivity of the membrane [20]. Since gas separation membranes are often used under high pressures, strong mechanical stability is one of the important requirements to be fulfilled. It is a big challenge for membrane scientists to prepare membranes meeting all mentioned requirements simultaneously in order to broaden the applications of membrane-based gas separation.

Searching for improved or new techniques for the preparation of gas separation membranes is one of the research subjects in membrane science where activities are concentrated. It is accompanied by extensive studies for understanding the membrane formation process.

In the following sections, methods that can be used for the preparation of gas separation membranes are discussed. Furthermore, some basic principles concerning membrane formation are presented.

### 1-3. PREPARATION OF GAS SEPARATION MEMBRANES

Several techniques are available for the preparation of gas separation membranes from polymeric materials:

*For dense symmetrical membranes*

- Melt pressing or melt extrusion
- Solution casting and evaporation

*For asymmetrical membranes:*

- Thermal precipitation
- Controlled solvent evaporation (or dry phase inversion)
- Immersion precipitation (or wet phase inversion)
- Interfacial composite

Immersion precipitation is the most often used technique for the preparation of asymmetric membranes for gas separation (and other membrane-based applications [51]), and can be performed in different ways. Most of the supports for composite membranes are also prepared by using this technique. In this study, immersion precipitation technique is investigated and used, but used in a specific way. So, it is discussed in details in a separate section. Other techniques shown above are described briefly in this section.

#### *1-3-1. Melt pressing or melt extrusion*

Melt pressing and melt extrusion are well developed techniques for the preparation of dense symmetrical membranes in the form of flat sheets (films) [55] or hollow fibers [56]. These membranes are normally used for the characterization of the intrinsic properties of the membrane materials. The two techniques can also be used for membrane preparation from polymers that do not dissolve in solvents under ambient conditions. Two examples of using the melt extrusion technique to prepare gas separation hollow fibers for commercial applications can be found in literature[56,57].

#### *1-3-2. Solution casting and evaporation*

In laboratory work for the preparation of dense membranes for testing the material properties, the solution casting technique (plus evaporation) is often used because it is simple and easy to perform. In this process, a membrane is formed from a polymer solution containing a volatile solvent, by casting a thin film followed by evaporation of the solvent.



### ***1-3-3. Thermal precipitation***

The essence of this process is the usage of a latent solvent. A latent solvent means that it is a good solvent for a polymer at high temperature and becomes a nonsolvent at low temperature. In this process a homogeneous polymer solution containing a latent solvent is prepared at high temperature. By lowering the temperature the loss of solvent power will first cause demixing of the solution and further cooling will lead to crystallization or vitrification of the demixed solution. Usually, this process is used to prepare microfiltration membranes from polyolefins. It is reported, however, that gas separation membranes, probably only flat sheet type, could also be prepared with this process [58]. In this case, the polymer solution is cast on a metal plate. By cooling the plate in a certain way, membranes with a gas tight skin can be obtained. The skin of this type of membrane is formed on the side adjacent to the plate [59]. No large scale application of this technique has been reported for the preparation of gas separation membranes.

### ***1-3-4. Controlled solvent evaporation***

In this case the casting solution contains at least three components, a polymer, a volatile solvent and a less volatile nonsolvent. Evaporation of the solvent first results in liquid-liquid demixing in the solution and further evaporation causes the precipitation of the polymer. In general, membranes are formed with an asymmetric structure consisting of a dense skin on top of a porous sublayer. The skin is formed at the side facing the air. Depending on the amount of nonsolvent in the polymer solution, the formed skin can be porous or nonporous[58]. At low nonsolvent concentration, a thick and gas tight skin can be formed together with a closed cell structure in the sublayer whereas a porous skin is obtained when the nonsolvent concentration is high.

Since this process is relatively slow and since it is difficult to obtain a skin to be thin and dense, it is not practically feasible for large-scale membrane production. However, the combination of this process with the immersion precipitation process, called the dry/wet (phase inversion) process is very often used for the production of gas separation membranes.

### ***1-3-5. Interfacial composite***

Here the term of interfacial composite is used to include all the methods for the preparation of the selective layer of composite membranes. The initial idea [12] to prepare composite membranes was to adhere a thin film made according to the Langmuir-Blodgett technique on top of a porous membrane. The mechanical stability of this type of membrane is rather poor and it is very difficult to produce membranes with

this technique on a large scale. Several other techniques have been developed for the preparation of composite membranes [45,51,55]:

#### *Interfacial polymerization*

With this technique a highly crosslinked and thin film of thickness within 50 nm can be formed on the top surface of a porous support membrane [51,60,61]. First the support membrane is soaked by a liquid containing the reactant. Then one surface of the membrane is brought into contact with another liquid containing the second reactant. The highly crosslinked thin film is formed at the interface due to the reaction of the reactants. Meanwhile a less crosslinked hydrogel layer is formed under this surface layer which fills the pores of the support layer [55]. It has been argued by Baker [55] that although this technique has been successfully used for the production of highly permeable and highly selective reverse osmosis membranes it is not a very interesting technique for the production of gas separation membranes. The reason is that in reverse osmosis membranes the hydrogel layer filling the pores of the support is highly water-swollen and consequently has little resistance for water flow. For gas separation the membrane is dried so that the gel becomes a rigid glass and offers very low gas permeability.

#### *Plasma polymerization*

A dense and thin ( $< 50$  nm) skin can be formed on top of a support membrane by deposition of the products produced in a plasma reactor [51]. The plasma is generated by ionisation of a gas by means of an electrical discharge. The collision of the ionised gas with supplied reactants in the reactor results in the formation of different kinds of radicals which can react with each other. When the molecular weight of the resulting products becomes too high, the products will deposit (*e.g.* on a membrane). Gas separation membranes have been prepared by using this techniques as reported by several authors [62-66]. However, plasma polymerization membranes have not been produced on a commercial scale.

#### *Coating*

By applying a rather diluted polymer solution ( $< 5$  wt %) on top of a porous membrane, a thin film can be formed after evaporation of the solvent. Depending on the porosity of the support membrane as well as the coating material, the final properties of the composite membrane can be determined by the coating material or by the support membrane material. When the porosity is high ( $>10^{-2}$ ), the coating layer will control the membrane properties. When the porosity is low ( $< 10^{-4}$ ) and the coating material is much less selective than the support membrane material, the properties of the composite membrane are controlled by the support membrane. Virtually, the most successfully used membranes in industry for gas separation are prepared with the coating process.

For example, Monsanto's membranes are prepared by coating polysulfone hollow fibers with silicon rubbers [18,20]. The surface porosity of the polysulfone fibers is rather low ( $<10^{-4}$ ). After coating these fibers with a thin layer of silicon rubber, the formed composite membranes showed nearly the intrinsic selectivity of polysulfone [20,30]. Gas transport through small pores follows the Knudsen flow mechanism, and has a much higher permeability (typically six orders of magnitude higher [30,67]) than that of a gas transport through a dense glassy polymer film. Thus the presence of a few pores ( $>10^{-7}$  area fraction of the membrane surface) can drastically reduce the selectivity of the membrane. Plugging of the pores with a silicon rubber coating significantly reduces the gas flow through these pores and consequently enables gas transport through the polysulfone matrix of the skin to be predominant. The advantage of using this plugging coating technique is that it circumvents the difficulty of making membranes with a perfect skin. The gas separation properties of Ube's composite polyimide membrane [30] are controlled by the top coating layer. The advantage of this type of composite membrane is that it enables the use of expensive high performance polymer as the coating material because the required content of a coating material is rather small.

The coating layer can be formed as a dense top layer but also as an asymmetric structure [68]. Under well controlled conditions hollow fibers with an asymmetric coating layer and an asymmetric support layer can even be formed in a single precipitation step [69], instead of using the more standard procedure for making a composite membrane in which the coating layer and the support layer are prepared separately.

In general, preparation of composite membranes allows the formation of the selective top layer and the formation of the support layer to be optimized separately. This makes composite membranes very attractive for practical applications. To optimize the support membrane, important issues involve the number and size of the pores in the surface layer as well as the resistance of the sublayer and the mechanical stability of the support membrane. Most of the support membranes are asymmetric membranes formed by immersion precipitation. In addition, asymmetric membranes with a completely gas tight skin can also be prepared directly with this technique. Understanding of membrane formation by immersion precipitation is of crucial importance for the development of membranes with improved performance.

## 1-4. MEMBRANE FORMATION BY IMMERSION PRECIPITATION

### 1-4-1. A historical review

According to the literature [24], Baranetzky was the first who used the immersion precipitation technique for the preparation of nitrocellulose membranes in 1872 [70]. The first commercial nitrocellulose membranes available for ultrafiltration applications was made by Zsigmondy and Bachmann around 1920 [71]. By modifying the procedures used by Dobry [72,73] and Duclaux and Amat [74] for the preparation of cellulose acetate (CA) ultrafiltration membranes, Loeb and Sourirajan were successful in preparing CA membranes suitable for reverse osmosis (RO) in 1960 [5]. The membranes made by Loeb and Sourirajan exhibited a higher selectivity and a much higher water flux compared to the dense cellulose acetate RO membranes made by Reid et al. [75] in 1959. Speculation was made by Loeb in 1960 [76], and earlier by other authors [77-79], that membranes prepared by immersion precipitation might have an asymmetric structure. The speculation was based on the optical appearance of the membranes and dependence of the permeation on the side of the membranes to be chosen to face the feed stream. The speculation was confirmed by Riley et al. [58] in 1964 who used electron microscopy to examine the structures of the membranes made by Loeb and Sourirajan.

The Loeb and Sourirajan membranes [5] were made by spreading uniformly a thin layer (~200 $\mu\text{m}$ ) of a homogeneous solution consisting of 22.3% cellulose acetate, 66.6% acetone, 10% water and 1.1% magnesium perchlorate on a glass plate. About 200 seconds exposure time was allowed for acetone to evaporate. Next the plate with the solution film was immersed into an iced-water bath for about 1 hour. Subsequently, the film was peeled off and washed in running water for 24 hours, and then dipped into hot water for about 100 seconds for annealing. This membrane showed an asymmetric structure: a dense and thin skin (about 0.25  $\mu\text{m}$ ) supported on a porous sublayer. The dense skin had permselective properties suitable to separate salt from sea water, while it was thin enough for a high water flux. The porous sublayer provided the mechanical stability for the membrane.

In principle, this process can be described as a sequence of five steps:

- preparation of a homogeneous polymer solution;
- casting of a thin film of the solution on a support;
- evaporation of the solvent;
- immersion of the film into a coagulation bath;
- annealing of the obtained membrane.

Although evaporation of the solvent was employed to increase the polymer concentration at the surface in order to obtain a dense skin, in essence the asymmetric

structure is formed due to the immersion precipitation whereas the annealing step was performed to further densify the skin.

Since immersion precipitation is of essential importance for controlling the formation of the asymmetric structure, investigations on membrane formation have been focused mainly on the immersion precipitation process.

#### *1-4-2. Membrane formation mechanism*

The membrane forming system used by Loeb and Sourirajan [5] consisted of four components—a polymer (CA), a solvent (acetone), a nonsolvent (water) and an additive (magnesium perchlorate) which is a nonsolvent for the polymer as well. Conceptually, however, membrane formation by immersion precipitation can be described in terms of a three component system: nonsolvent (1), solvent (2) and polymer (3).

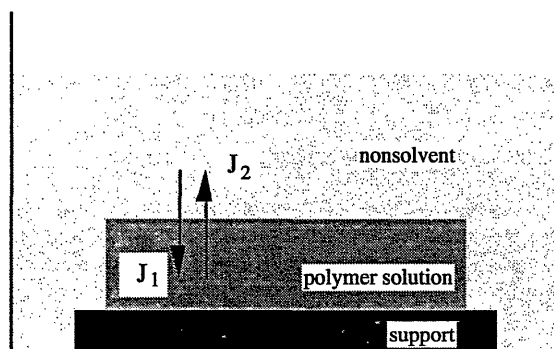


**Figure 4.** Membrane formation by immersion precipitation from ternary system: nonsolvent (1), solvent (2) and polymer (3).

After immersion of a polymer solution into a nonsolvent bath, the solvent diffuses out of the polymer solution while nonsolvent diffuses into the solution, as illustrated in figure 4. This exchange of solvent and nonsolvent in general leads to the change of the polymer solution from a thermodynamically stable state to a metastable or unstable state. Then liquid-liquid demixing takes place in the solution. In case the solvent flux ( $J_2$ ) is larger than the nonsolvent flux ( $J_1$ ), the polymer concentration at the surface of the film will increase. The formed highly concentrated polymer layer at the surface reduces the outdiffusion of the solvent more strongly than the indiffusion of the nonsolvent. Hence, the polymer concentration in the sublayer is lower than the polymer concentration in the top layer at the moment when liquid-liquid demixing sets in. The further replacement of solvent by nonsolvent will result in solidification of the polymer rich phase and in its turn the asymmetric structure of the membrane is fixed.

As the membrane formation is induced by the exchange of the solvent and the nonsolvent, which gives rise to liquid-liquid demixing and solidification of the solution, in literature studies on the mechanism of membrane formation by immersion precipitation include the investigation of mass transfer [80-97], liquid-liquid demixing phenomena [98-108] and solidification mechanisms [109-112].

### ***Mass transfer***

Frommer *et al.*[80] and Altena *et al.*[81] performed casting-leaching experiments to determine the exchange rate of solvent and nonsolvent after immersion. Because of the limitation of the experimental method, information concerning the most important formation period, i.e., the very short period between the moment of immersion and the onset of liquid-liquid demixing, could not be obtained. To gain information about the mass transfer behaviour in this period, several authors [82-89,95] used mathematical models to predict mass transfer during the first stage of membrane formation. With the established models, the composition changes of the polymer solution could be calculated in combination with the calculation of the liquid-liquid demixing boundary (binodal). It has been shown by Reuvers *et al.* [83] and by Tsay *et al.* [87] that accurate description of the thermodynamic properties of a membrane forming system is a fundamental requirement for modelling the membrane formation process.

The model predictions by Reuvers *et al.* [82,83] eventually led to the development of a "tailored" process for the preparation of gas separation membranes—a so-called dual bath spinning process [67,113-115]. This spinning process will be described later.

### ***Liquid-liquid demixing***

Whether liquid-liquid demixing will take place or not in the immersed polymer solution is strongly dependent on the thermodynamic properties of the membrane forming system. The Flory-Huggins theory [116] is often used for the description of the thermodynamics of a membrane forming system, since this theory can be used for highly concentrated polymer solutions and it is simple and easy to understand.

To apply the Flory-Huggins theory to describe the thermodynamic properties of a polymer solution, the Flory-Huggins' interaction parameter data for the solution have to be known. For a ternary system, there are three binary interaction parameters and one ternary interaction parameter [117]. The ternary interaction parameter is often neglected in describing the thermodynamic properties of a membrane forming system [83,87,101,104-106] because of the lack of literature data and the lack of simple means to measure it.

Neglecting the ternary interaction parameter is a reasonable simplification when investigations are only aimed to find the general trends concerning the influence of the

binary interaction parameters on the demixing boundary (binodal) or on the mass transfer behaviour during membrane formation. This simplification virtually has led to very informative results. For example, Altena and Smolders [101] have systematically studied the influences of the interactions of solvent/nonsolvent, solvent/polymer and nonsolvent/polymer on the demixing boundary (binodal) of ternary membrane forming systems. The study showed that the interaction between solvent and nonsolvent, and the interaction between nonsolvent and polymer have a strong effect on the demixing compositions whereas the interaction between the solvent and polymer has only a minor effect.

However, important information relevant to membrane formation may be shadowed by the simplification. An accurate description of the thermodynamic properties of a membrane forming system is essentially important in order to obtain reliable information from the models. This is due to the fact that a slight change in the thermodynamic properties can have a significant effect on the mass transfer behaviour as is shown by different authors [83,87]. Therefore, in this study the acceptability of neglecting the ternary interaction parameter of a ternary membrane forming system is investigated.

### ***Solidification***

Solidification is defined as structure fixation of a polymer matrix. In literature several mechanisms [109-112] are proposed to be responsible for the structure fixation:

- vitrification;
- gelation or crystallization.

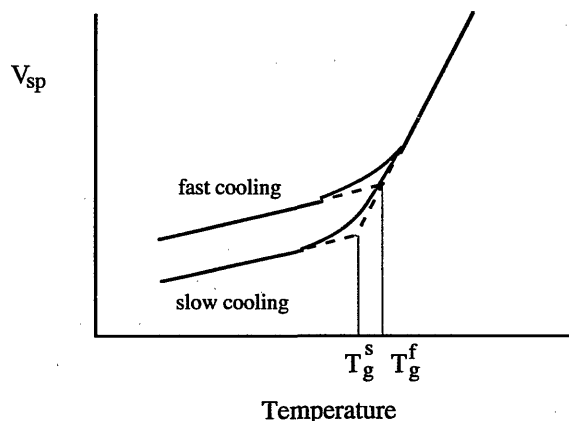


**Figure 5.** Schematic illustration of the change in specific volume of an amorphous polymer with temperature at two different cooling rates.  $T_g^s$  and  $T_g^f$  represent the glass transition temperature of the polymer at a slow and a fast cooling rate, respectively. According to Hiemenz [118].

### *Vitrification*

Vitrification is a thermodynamically nonequilibrium process. It describes the frozen amorphous state of a polymer without any long term ordering. Because no ordering is required in this process, it can be very fast. To show its kinetic behaviour, we consider the situation of cooling an amorphous polymer from a liquid state to a glassy state. Figure 5 schematically shows the change in specific volume of an amorphous polymer with temperature at two different cooling rates. This figure clearly shows that vitrification of an amorphous polymer occurs earlier when the polymer is cooled fast. For semicrystalline polymers, however, the crystallinity can be more or less hindered or even completely suppressed at fast cooling rate.

The presence of a solvent in a polymer will reduce the  $T_g$  of the polymer (solution). In general, the  $T_g$  of a polymer solution decreases with increase of the solvent concentration. Vitrification of a polymer solution can be realized in two different ways, by cooling the solution or by evaporating the solvent at a constant temperature. The change of  $T_g$  of a polymer solution with cooling rate exhibits the same behaviour as cooling a pure polymer as indicated in figure 5. By analogy, at a constant temperature, fast evaporation of the solvent from a polymer solution will lead to vitrification to occur at an earlier stage (related to a lower polymer concentration) compared to slow evaporation.

In the immersion precipitation process, vitrification of the polymer solution is realised by depletion of solvent and meanwhile diffusion of nonsolvent into the polymer solution. This process is analogous to evaporation of solvent from a polymer solution. Therefore, it can be expected that fast exchange of solvent and nonsolvent during immersion precipitation will cause vitrification to be induced at a lower polymer concentration. Here one can see the totally different kinetic behaviour of vitrification and crystallization. In a quickly changed environment crystallization is more or less hindered whereas vitrification is promoted.

### *Gelation and crystallization*

The term (physical) gelation is very often used to describe the skin formation of membranes by immersion precipitation [102,103,112,119,120]. It is suggested that gelation might suppress liquid-liquid demixing due to kinetic hindering of nucleation and growth imposed by the high viscosity of the gelled skin layer [102,112,119]. However, this suggestion has never been verified experimentally for membrane formation by immersion precipitation.

A conventional image of a gel is something like a predominantly liquid-containing soft, elastic, wobbly but coherent object [121]. Actually, gels cover a much wider spectrum from one phase or homogeneous solutions (where entropy of the mix is the main factor responsible for maintaining of the solvent) to two phase or heterogeneous



rigid porous structures (where capillary forces are responsible for solvent maintaining) [122]. So, the general features for gels are their infinite viscosities (responsible for the loss of their fluidity) and their three-dimensional loose network.

A gel is created by the formation of some sort of connecting elements (junctions) in the initial liquid. The junctions can be formed either by chemical cross-links or by physical associations of the materials in the initial liquid. Chemical cross-linking, the covalent bonding of polymer chains by means of a chemical reaction, is unlikely to occur during membrane formation by immersion precipitation, therefore, it will not be considered here. In case that physical associations are responsible for gel formation, the formed gel is thermally reversible, and so the gel formation process (gelation) is called thermoreversible gelation or physical gelation.

The mechanisms for physical gelation are system-dependent and a universal mechanism may not exist [123,124]. However, for semicrystalline polymers it is often found that gelation is initiated by the formation of microcrystallites (localized interchain crystallization [125]) [51,123,126,127]. These microcrystallites, which are small size ordered regions, are in fact the nuclei of the crystallization process but without the ability to grow further due to the presence of solvent. Since these microcrystallites connect various polymeric chains together, a three dimensional network can be formed. The formation of these microcrystallites depends on the time allowed for crystallization from the solution.

For membrane preparation, often semicrystalline polymers are used. Due to the fact that membrane formation is generally a fast process, only polymers that are capable of crystallizing rapidly (*e.g.* polyethylene, polypropylene, aliphatic polyamides, *etc.*) will exhibit an appreciable amount of crystallinity during phase inversion [51]. Other semicrystalline polymers contain low to very low crystallinity in the formed membranes. For example, it has been found that solutions of PPO (poly(2,6-dimethyl-1,4-phenyleneoxide)) in various solvents or mixtures of solvent and nonsolvent can form gels initiated by crystallization of PPO [109,111]. However, PPO ultrafiltration membranes made from those solutions hardly contain any crystalline material [109,111]. Considering the fact that the skin of a membrane is formed in a very short time scale (in seconds or much less), it is unlikely that any crystallinity may exist in the skin of most membranes. It was stated by Kesting [58] that in most cases the skin of reverse osmosis membranes is amorphous and the presence of crystallinity may actually be detrimental for the membranes. Apparently, gelation by means of crystallization cannot be accepted as a general explanation for skin formation. Gelation in semicrystalline polymers can also take place by other means like hydrogen-bonding [128] or some sort of special interaction (difficult to verify) between the polymer and the solvent [129]. However, gelation by these means is a very slow process. A certain settling time (hours or days) has to be allowed for gelation to occur [129].

Gelation can take place in amorphous polymer solutions as well (e.g. atactic polystyrene (aPS) [130-134]). The formation of junctions in a gel formed from amorphous polymer can be caused by special interactions between the polymer and the solvent [131,132] or by vitrification (in combination with liquid-liquid demixing) [133,134]. Wijmans *et al.* [102] and Gaides *et al.* [112] proposed a viscosity related mechanism to be responsible for gelation in amorphous polymer systems, based on their studies on the membrane forming system polysulfone (an amorphous polymer)/dimethylacetamide/water. Using a falling ball method, Gaides *et al.* [112] found that above a certain polymer concentration a solution loses its fluidity characterized by the incapability of falling of a stainless steel ball in the solution. A serious question arises concerning the definition of gelation as a viscosity phenomenon: how to distinguish a gel from a highly concentrated polymer solution. To answer this question one has to look at the definition for a gel. Unfortunately, a commonly accepted definition for gels does not exist [121]. In a common sense, however, it is difficult to accept that a highly viscous solution is a gel since the gelation boundary for such a gel is poorly defined. It can be expected that with the change of the size (or the weight) of the ball the gelation boundary will change as well, which obviously will cause some confusion. If it would be allowed to define a gel based on viscosity phenomenon, providing that the gelation boundary is defined by the usage of a "standard ball", one will question the practical value of such a definition since it is difficult to imagine that the effect of such a gel on liquid-liquid demixing will be much different from the effect of a slightly less viscous solution.

Apparently, a clear picture concerning gelation mechanism in membrane formation and its relevance to membrane formation is still missing. In this study we will clarify the concept of gelation in the membrane formation process by immersion precipitation and we will explain the general role of gelation in structure formation of the membrane. As discussed previously, crystallization is not necessarily responsible for gelation and the structure fixation during membrane formation. It becomes clear that the use of an amorphous polymer in the study of membrane formation will give more general information concerning the formation of the membrane. This is one of the reasons for choosing an amorphous polymer in this study.

#### ***1-4-3. Dual bath spinning process***

The dual bath spinning process was developed by Van't Hof [67,113], which is based on the model predictions by Reuvers [82,83]. It was found by Reuvers [82,83] that membranes suitable for gas separation are generally formed following a delayed demixing process. Delayed demixing means that after immersion of a polymer solution into a nonsolvent bath it takes a certain time for demixing to occur. Membranes formed

by delayed demixing often possess a thick skin and a closed cell structure in the sublayer. In a practical point of view, these membranes are not acceptable because of their low fluxes. Another type of demixing process, i.e., the instantaneous demixing process, usually results in membranes suitable to be used in ultrafiltration or microfiltration. The structures of these membranes are characterized by a slightly porous and thin skin and an open cell structure of the sublayer. The idea of the dual bath spinning process is to use the combination of the two formation processes to produce hollow fibers with a dense and thin skin as well as a highly porous substructure. The spinning process was designed to first contact the polymer solution with a nonsolvent (the first coagulant), which can induce delayed demixing, for a short time (a time shorter than the delay time), in order to increase the polymer concentration at the interface without significantly changing the solution in the sublayer. Immersion of this polymer solution with a highly concentrated top layer into a second nonsolvent bath (the second coagulant) where instantaneous demixing occurs will lead to the formation of a membrane with a dense and thin skin in combination with a highly porous sublayer.

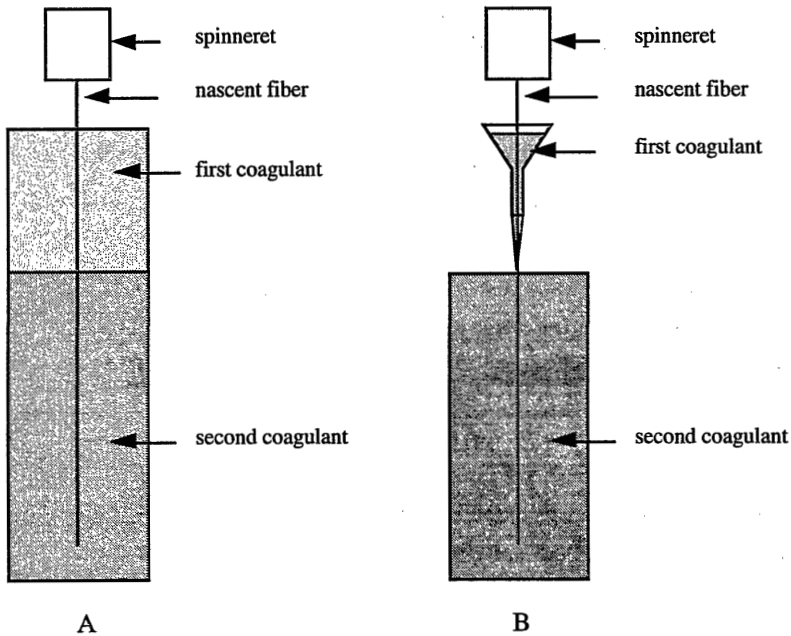


**Figure 6.** The two different processes used by Van't Hof [67,113] to perform the dual bath spinning process for the preparation of hollow fibers for gas separation.

The spinning was performed by Van't Hof in two different processes as shown in figure 6. In process A), a first coagulant with a density lower than the density of the

second coagulant (water) must be used. In addition the two coagulants must be immiscible or poorly miscible with each other. In his case for the spinning of polyethersulfone (PES) hollow fibers from a solution of PES/N-methylpyrrolidone (NMP)/glycerol (a nonsolvent additive), 1-pentanol was used as the first coagulant. The disadvantage of this process is apparent; it adds extra limitations for the choice of the first coagulant. Furthermore, the saturation of the first coagulant by water quickly reduces the selectivity of the resulting fiber. For example, hollow fibers with high selectivities could be obtained within the first two hours of spinning. After two hours of spinning the formed fiber became nonselective.

In process B), in which a funnel was used to maintain the first coagulant, the disadvantages encountered in A) could be eliminated. In principle, various types of first coagulants could be used. By using glycerol as the first coagulant, defect-free hollow fibers could be obtained from a polymer solution of PES/NMP/glycerol. The advantage of the dual bath spinning process is that completely defect-free hollow fibers could be obtained without the necessity of coating.

In principle, the dual bath spinning process has a very high potential to be developed into a commercially valuable process for the production of high performance gas separation hollow fibers. However, the fiber obtained by Van't Hof did not yet reveal the expected performance. This means that although the intrinsic selectivity of the membrane material could be achieved, the flux of the fiber was rather low. The low flux is caused by the formation of a relatively thick skin (about 1  $\mu\text{m}$  thick). It was stated by Van't Hof [113] that the formation of the thick skin was due to the difficult control of a short contact time between the first coagulant and the spinning solution, since a short contact time is critical for the formation of a thin skin. Another problem that has to be solved is that fibers prepared with the dual bath spinning process contained macrovoids in the sublayer. The presence of macrovoids can reduce the mechanical strength of the fiber.

## 1-5. STRUCTURE OF THIS THESIS

Aim of this thesis is to extend the knowledge on membrane formation and to further develop the dual bath spinning process for the preparation of gas separation hollow fibers with both high selectivity and high flux.

Studies on the membrane formation mechanism are presented in chapter 2 and chapter 3. Investigations for the preparation of gas separation hollow fibers are described in chapter 4 and chapter 5.

In chapter 2, the gelation mechanism for membrane formation by immersion precipitation is studied. Berghmans' approach [134] for gelation of amorphous polymer

in binary systems will be extended to a ternary membrane forming system. The gelation study is carried out for the system PES/NMP/water. It will be shown what mechanism is responsible for the cease of liquid-liquid demixing in this system.

A study on the thermodynamic properties and the mass transfer behaviour of the system PES/NMP/water is described in chapter 3. It is shown that the use of a ternary interaction parameter in the Flory-Huggins theory in combination with the use of binary interaction parameters can give a quite accurate description of the thermodynamic properties of the system. Based on the thermodynamic consideration, mass transfer behaviour of the system during membrane formation is studied by adopting Reuvers [82,83] model for membrane formation by immersion precipitation.

The dual bath spinning process is modified with the use of a triple orifice spinneret. Spinning is performed by using various first coagulants. The results are presented in chapter 4. Vitrification is related to the performance of the resulting fibers.

In chapter 5, studies on the elimination of macrovoids in the sublayer of hollow fibers made with the dual bath process are presented. The mechanism proposed by Smolders *et al.* [135] for macrovoids formation is used to understand macrovoid formation during the dual bath spinning process.

## 1-6. REFERENCES

1. Mitchell, J.K., *Am. J. Med.*, 7, 36 (1830)
2. Mitchell, J.K., *Royal Inst. J.*, 2, 101 and 307 (1831)
3. Graham, T., *Phil. Mag.*, 32, 401 (1866)
4. Hwang, S.T. and Kammermeyer, "Membranes in Separations", Wiley, New York, 1975, Chapter 13.
5. Loeb, S. and Sourirajan, S., *Adv. Chem. Ser.*, 38, 117 (1962)
6. Gantzel, P.K. and Merten, U., *I&EC Proc. Res. Dev.*, 9, 331 (1970)
7. Vos, K.D. and Burris, F.O., *I&EC Proc. Res. Dev.*, 8, 84 (1969)
8. Stern, S.A.; Sen, S.K. and Rao, A.K., *J. Macromol. Sci. -Phys.*, B, 10, 507 (1974)
9. Schell, W.J., *ACS Div. Fuel Chem., Preprints*, 20, 253 (1975)
10. Ward III, W.J.; Browall, W.R. and Salemme, R.M., *J. Membr. Sci.*, 1, 99 (1976)
11. Riley, R.L., *U. S. Pat.*, 3,648,845 (1972)
12. Riley, R.L.; Lonsdale, H.K.; Lyons, C.R. and Merten, U., *J. Appl. Polym. Sci.*, 11, 2143 (1967)
13. Lundstrom, J.E., *U. S. Pat.*, 3,767,737 (1973)
14. Matson, S.L.; Ward III, W. J.; Kimura, S.G. and Browall, W.R., *J. Membr. Sci.*, 29, 79 (1986)
15. Schell, W.J. and Houston, C.D., *U. S. Pat.*, 4,134,742 (1979)
16. Coady, A.B. and Davis, J.A., *Chem. Eng. Progr.*, 78, 44 (1982)

17. Schell, W.J. and Houston, C.D., *ACS Symp. Ser.* 223, Washington, D. C., 1983
18. Henis, J.M.S. and Tripodi, M.K., *U. S. Pat.*, 4,230,463 (1980)
19. Henis, J.M.S. and Tripodi, M.K., *Sep. Sci. Techn.*, 15, 1059 (1980)
20. Henis, J.M.S. and Tripodi, M.K., *J. Membr. Sci.*, 8, 233 (1981)
21. Henis, J.M.S. and Tripodi, M.K., *Science*, 220, 11 (1983)
22. Backhouse, I.W., in "*Membranes in gas separation and enrichment-BOC Priestley Conference (4th : 1986: Leeds)*", The Royal Society of Chemistry (Ed.), Whitstable Litho Ltd., Whitstable, Kent, 1986
23. Spillman, R.W., *Chem. Eng. Progr.*, 85, 41 (1989)
24. Pinnau, I., *PhD Thesis*, University of Texas at Austin, U.S.A., 1991
25. Gollan, A.Z., *U. S. Pat.*, 4,681,605 (1987)
26. Puri, P.S., *U. S. Pat.*, 4,756,932 (1988)
27. Schell, W.J., *J. Membr. Sci.*, 22, 217 (1985)
28. Li, N.N.; Funk, E.W.; Chung, Y.A.; Kulkarni, S.S.; Swamikannau, A.X. and White, L.S., Department of Energy Report No, DE-AC07-82ID 12422 (1987)
29. Kulprathipanja, S. and Kulkarni, S.S., *U. S. Pat.* 4,608,060 (1986)
30. Fritzsche, A.K. and Kurz, E., in Porter, M.C. (Ed), "*Handbook of Industrial Membrane Technology*", Noyes Publications, Park Ridge, New Jersey, 1990
31. Albers, J.H.M.; Smid, J. and Kusters, A.P.M., *U. S. Pat.*, 5,129,920, 1992
32. Sanders, E.S., Clark, D.O. and Jensvold, J.A., *U. S. Pat.*, 4,838,904 (1989)
33. Crull, A., Buisiness Opportunity Report C-062, Business Communications Co., Inc., Stamford, CT (1985)
34. Ekiner, O.M.; Hayes, R.A. and Manos, P., *U. S. Pat.*, 4,863,496 (1989)
35. Mazur, W.H. and Chan, M.C., *Chem. Eng. Prog.*, 78, 38 (1982)
36. Cooley, T.E. and Dethloff, W.L., *Chem. Eng. Prog.*, 81, 45 (1985)
37. Baker, R.W., *U. S. Pat.*, 4,553,983 (1985)
38. Blume, I. and Pinnau, I., *U. S. Pat.*, 4,963,165 (1990)
39. *Chemical week*, 135, p. 38 (July 24, 1984)
40. Kesting, R.E.; Cruse, C.A.; Fritzsche, A.K.; Malon, R.F.; Murphy, M.K. and Handermann, A.C., *Eur. Pat. Application*, 0259288 (1987)
41. Zampini, A., *U. S. Pat.*, 4,488,886 (1984)
42. Bikson, B.; Gigla, S. and Kharas, G., *U. S. Pat.*, 4,767,422 (1988)
43. Bikson, B. and Nelson, J. K., *U. S. Pat.*, 4,826,599 (1989)
44. Werner, U., in "*Membranes in gas separation and enrichment-BOC Priestley Conference (4th : 1986: Leeds)*", The Royal Society of Chemistry (Ed.), Whitstable Litho Ltd., Whitstable, Kent, 1986
45. Koros, W.J. and Fleming, G.K., *J. Membr. Sci.*, 83, 1 (1993)
46. McLean, D.L.; Stookey, D.J. and Metzger, T.R., *Hydrocarbon Process*, 62 (8), 47 (1983)

47. Uhlhorn, R.J.R. and Burggraaf, in R. Bhave (Ed.), "*Inorganic membranes*", Nortrand and Reinholdt, New York, 1990
48. Baker, R.W.; Louie, J.; Pfromm, P.H. and Wijmans, J.G., *U. S. Pat.*, 4,857,080 (1989)
49. Soffer, A.; Koresh, J.E. and Saggy, S.S., *U. S. Pat.*, 4,685,940 (1987)
50. Koresh, J.E. and Soffer, A., *Sep. Sci. Technol.*, 22, 973 (1987)
51. Mulder, M.H.V., "*Basic principles of membrane technology*", Kluwer Academic Publishers, Dordrecht, The Netherlands, 1991
52. Hayes, R.A., *U. S. Pat.*, 4,717,394 (1988)
53. Stern, S.A.; Mi, Y.; Tamamoto, H. and St. Clair, A.K., *J. Polym. Sci., Polym. Phys. Ed.*, 17, 1887 (1989)
54. Anand, J.N.; Bales, S.E.; Feay, D.C. and Jeanes, T.O., *U. S. Pat.*, 4,840,646 (1989)
55. Baker, R.W.; Cussler, E.L.; Eykamp, W.; Koros, W.J. and Strathmann, H., *Membrane separation systems: Recent developments and future directions*, Noyes Dta Corp., Park Ridge, New Jersey, 1991
56. Skiens, W.E.; Lipps, B.J.; Mclain E.A. and Dubocq, D.E., *U. S. Pat.*, 3,798,185 (1974)
57. Antonson, C.R.; Gardner, R.J.; King, C.F. and Ko, D.Y., *I&EC, Proc. Res. Dev.*, 16, 463 (1977)
58. Kesting, R.E., *Synthetic polymeric membranes—a structure perspective*, 2nd ed., John Wiley and Sons, New York, 1985
59. Castro, A.J., *U. S. Pat.*, 4,247,498 (1981)
60. Cadotte, J.E., in Lloyd, D.R. (Ed.), "*Materials science of synthetic membranes*", ACS, Washington, D.C., 1985
61. Riley, R.L.; Fox, R.L.; Lyons, C.R.; Milstead, C.E.; Seroy, N.W. and Tagami, M., *Desalination*, 19, 113 (1976)
62. Osada, Y., in Osada, Y. and Nakagawa, T. (Ed.), "*Membrane science and technology*", Marcel Dekker, Inc., New York, 1992
63. Stancell, A.R. and Spencer, A.T., *J. Appl. Polym. Sci.*, 16, 1505 (1972)
64. Terada, I.; Haraguchi, T. and Kajiyama, T., *Polym. J.*, 18 (7), 529 (1986)
65. Kawakami, M.; Yamashita, Y.; Iwamoto, M. and Kagawa, S., *J. Membr. Sci.*, 19, 249 (1984)
66. Sakata, J. and Yamamoto, M., *J. Appl. Polym. Sci. Appl. Polym. Symp.*, 42, 339 (1988)
67. Van't Hof, J.A., *PhD Thesis*, University of Twente, the Netherlands, 1988
68. Bikson, B. and Nelson, J., *U. S. Pat.*, 4,826,599 (1989)
69. Ekiner, O.A.; Hayes, R.A. and Manos, P., *U. S. Pat.*, 5,085,676 (1992)
70. Baranetzky, J., *Pogg. Ann. Phys.*, 147, 195 (1872)
71. Zsigmondy, R. and Bachmann, W., *U. S. Pat.*, 1,421,341 (1922)
72. Dobry, A., *Bull. Soc. Chim.*, 3, 312 (1936)
73. Dobry, A., *U. S. Pat.*, 2,059,934 (1936)
74. Duclaux, J. and Amat, M., *Comptes Rendus*, 206, 1475 (1938)
75. Reid, C.E. and Breton, E.S., *J. Appl. Polym. Sci.*, 1, 133 (1959)

76. Loeb, S. in Turbak, A.F. (Ed), "Synthetic membranes", ACS Symp. Ser., 153, Washington, D.C., 1981
77. Bechhold, H. and Silbereisen, K., *Biochem. Z.*, 199, 1 (1928)
78. Zsigmondy, R. and Bachmann, W., *Z. Anorg. u. Allg. Chemie*, 103, 119 (1918)
79. Goetz, A. and Tsuneishi, N., *J. Am. Wat. Works. Association*, 43, 943 (1951)
80. Frommer, M.A. and Lancet, D., in Lonsdale, H.K. and Podall, H.E.(Ed.), "Reverse osmosis membrane research", Plenum Press, New York, 1972
81. Altena, F.W.; Smid, J.; van den Berg, J.W.A.; Wijmans, J.G. and Smolders, C.A., *Polymer*, 26, 1531 (1985)
82. Reuvers, A. J.; Van den Berg, J. W. A. and Smolders, C. A., *J. Membrane Sci.* 34, 45 (1987)
83. Reuvers, A. J. and Smolders, C. A., *J. Membrane Sci.* 34, 67 (1987)
84. Radovanovic, P.; Thiel, S. W. and Hwang, S.-T., *J. Membrane Sci.* 65, 213 (1992)
85. Radovanovic, P.; Thiel, S. W. and Hwang, S.-T., *J. Membrane Sci.* 65, 231 (1992)
86. Boom, R. M., *PhD Thesis*, University of Twente, the Netherlands, 1992
87. Tsay, C. S. and McHugh, A. J., *J. Polym. Sci., Polym Phys. Ed.* 28, 1327 (1990)
88. Tsay, C. S. and McHugh, A. J., *J. Polym. Sci., Polym Phys. Ed.* 29, 1261 (1991)
89. Tsay, C. S. and McHugh, A. J., *Chem. Eng. Sci.* 46, 1179 (1991)
90. McHugh, A.J. and Tsay, C.S., *J. Appl. Polym. Sci.*, 46, 2011 (1992)
91. Yilmaz, L. and McHugh, A.J., *J. Membr. Sci.*, 28, 287 (1986)
92. McHugh, A.J. and Yilmaz, L., *J. Polym. Sci., Polym. Phys. Ed.*, 23, 1271 (1985)
93. McHugh, A.J. and Yilmaz, L., *J. Membr. Sci.*, 43, 319 (1989)
94. Gaides, G.E. and McHugh, A.J., *J. Membr. Sci.*, 74, 83 (1992)
95. Cohen, C.; Tanny, G. B. and Prager, S., *J. Polym. Sci., Polym Phys. Ed.* 17, 477 (1979)
96. Tkacik, G. and Zeman, L., *J. Membr. Sci.*, 31, 273 (1987)
97. Kang, Y.S.; Kim, H.J. and Kim, U.Y., *J. Membr. Sci.*, 60, 219 (1991)
98. Strathmann, H.; Scheible, P. and Baker, R.W., *J. Appl. Polym. Sci.*, 15, 811 (1971)
99. Guillotin, M.; Lemoyne, C.; Noël, C. and Monnerie, L., *Desalination*, 21, 165 (1977)
100. Koenhen, D.M.; Mulder, M.H.V. and Smolders, C.A., *J. Appl. Polym. Sci.*, 21, 199 (1977)
101. Altena, F.W. and Smolders, C.A., *Macromolecules*, 15, 1491 (1982)
102. Wijmans, J.G.; Kant, J.; Mulder, M.H.V. and Smolders, C.A., *Polymer*, 26, 1539 (1985)
103. Reuvers, A.J.; Altena, F.W. and Smolders, C.A., *J. Polym. Sci., Polym Phys. Ed.*, 24, 793 (1986)
104. Yilmaz, L. and McHugh, A.J., *J. Appl. Polym. Sci.*, 31, 997 (1986)
105. Li, S.-G.; Jiang, C.-Z. and Zhang, Y.-Q., *Desalination*, 62, 79 (1987)
106. Zeman, L. and Tkacik, G., *J. Membr. Sci.*, 36, 119 (1988)
107. Swinyard, B.T. and Barrie, J.A., *Brit. Polym. J.*, 20, 317 (1987)
108. Lau, W.W.Y.; Guiver, M.D. and Matsuura, T., *J. Membr. Sci.*, 59, 219 (1991)
109. Wijmans, J.G.; Rutten, H.J.J. and Smolders, C.A., *J. Polym. Sci., Polym Phys. Ed.*, 23, 1941 (1985)



110. Altena, F.W.; Schröder, J.S.; van de Hulst, R. and Smolders, C.A., *J. Polym. Sci., Polym. Phys. Ed.*, 24, 1725 (1986)
111. Burghardt, W.R.; Yilmaz, L. and McHugh, A. J., *Polymer*, 28, 2085 (1987)
112. Gaides, G. E. and McHugh, A. J., *Polymer*, 30, 2118 (1989)
113. Van't Hof, J. A.; Reuvers, A. J.; Boom, R. M.; Rolevink, H. H. M and Smolders, C.A., *J. Membr. Sci.*, 70, 17 (1992)
114. Koops, G. H.; Li, S.-G.; Boomgaard, Th. v. d.; Mulder, M. H. V. and Smolders, C. A., *Dutch Patent* 91.02151 (1991)
115. Li, S.-G.; Koops, G. H.; Mulder, M. H. V.; Boomgaard, Th. v. d. and Smolders, C.A., To be published in *J. Membrane Sci.*
116. Flory, P.J., "*Principles of polymer chemistry*", Cornell University Press, Ithaca, 1953
117. Pouchly, J.; Zivney, A. and Solc, K., *J. Polym. Sci. Polym. Symp.* 23, 245 (1968)
118. Hiemenz, P.C., "*Polymer chemistry-The basic concepts*", Marcel Dekker Inc., New York, 1984
119. Broens, L.; Altena, F.W.; Smolders, C.A. and Koenhen, D.M., *Desalination*, 32, 33 (1980)
120. Mulder, M.H.V.; Hendrikman, J.O.; Wijmans, J.G. and Smolders, C.A., *J. Appl. Polym. Sci.*, 30, 2805 (1985)
121. Callister, S.; Keller, A. and Hikmet, R.M., *Makromol. Chem. Macromol. Symp.*, 39, 19 (1990)
122. Muhr, A.H. and Blanshard, J.M.V., *Polymer*, 23, 1012 (1982)
123. Hikmet, R.M.; Callister, S. and Keller, A., *Polymer*, 29, 1378 (1988)
124. Guenet, J.-M., in Cheremisinoff, N.P. (Ed), "*Handbook of polymer science and technology*", Vol. 1, Marcel Dekker Inc., New York, 1989
125. Keller, A., in Hiltner, A. (Ed), "*Structure-property relationships of polymer solids*", Plenum Press, New York, 1983
126. Guenet, J.-M.; Lotz, B. and Wittmann, J.-C., *Macromolecules*, 18, 420 (1985)
127. Domszy, R.C.; Alamo, R.; Edwards, C.O. and Mandelkern, L., *Macromolecules*, 19, 310 (1986)
128. Yang, Y. C. and Geil, P. H., *J. Macromol. Sci. Phys.* B22, 463 (1983)
129. Schneider, T.; Wolf, B.A.; Kasten, H. and Kremer, F., *Macromolecules*, 24, 5387 (1991)
130. Tan, M.-M.; Moet, A.; Hiltner, A. and Baer, E., *Macromolecules*, 16, 28 (1983)
131. Francois, J.; Gan, J. Y. S. and Guenet, J.-M., *Macromolecules*, 19, 2755 (1986)
132. Guenet, J.-M.; Klein, M. and Menelle, A., *Macromolecules*, 22, 493 (1989)
133. Hikmet, R. M.; Callister, S. and Keller, A., *Polymer*, 29, 1378 (1988)
134. Arnauts, J. and Berghmans, H., *Polym. Commun.* 28, 66 (1987)
135. Smolders, C. A.; Reuvers, A. J.; Boom, R. M. and Wienk. I. M., *J. Membr. Sci.*, 73, 259 (1992)



---

**CHAPTER 2**

---

**GELATION OF AMORPHOUS POLYMER IN A MIXTURE  
OF SOLVENT AND NONSOLVENT**

---

S.-G. Li, Th. van den Boomgaard, C.A. Smolders, H. Strathmann

**2-1. ABSTRACT**

Berghmans' mechanism for gelation of binary systems consisting of an amorphous polymer in a solvent has been extended to ternary systems. The gelation phenomenon of an amorphous polymer, polyethersulfone (PES), in mixtures with a solvent and a nonsolvent has been studied.  $T_g$  depression of PES caused by N-formylpiperidine (FP), dimethylsulfoxide (DMSO), N, N-dimethylacetamide (DMAC) or N-methylpyrrolidone (NMP) as well as by mixtures of NMP and water was investigated. It was found that the  $T_g$  depression of PES caused by NMP was the same as that caused by mixtures of NMP and water as far as the related polymer solutions were homogeneous. Cloud point data for the system  $H_2O$ -NMP-PES and for the system MPD (2-methyl-2,4-pentanediol)-NMP-PES were measured with a titration method at 25 °C.

The ternary phase diagram for the system  $H_2O$ -NMP-PES was obtained. This is shown to be relevant in the membrane formation process from this system by immersion precipitation. In the phase diagram four regions were distinguished: a homogeneous solution region, a liquid-liquid two-phase region and a single phase glass region as well as a liquid-glass two-phase region.

For the systems  $H_2O$ -NMP-PES and  $H_2O$ -DMAC-polysulfone (PSF), membranes were made from highly concentrated polymer solutions by immersion precipitation. The membrane formation processes showed that as far as the initial polymer solutions were in the homogeneous solution region instantaneous demixing always took place when the solutions were immersed into a water bath.

Membranes were also prepared from the system MPD-NMP-PES. It was found that dense and transparent membranes can be formed from this system by immersion precipitation. These experiments clearly indicated that, by immersion precipitation, membranes can also be formed without undergoing liquid-liquid demixing.

## 2-2. INTRODUCTION

A membrane prepared by the immersion precipitation process often shows an asymmetrical structure consisting of a dense and thin skin supported by a porous sublayer [1]. The performance of such a membrane is mainly controlled by the properties of the skin. It is proposed in literature [2,3] that the formation of the skin and the formation of support layer follow different mechanisms. The skin was thought to be formed by gelation or crystallization prior to liquid-liquid demixing and the porous support layer was formed by liquid-liquid demixing followed by gelation or crystallization. Therefore the gelation process is the key point for understanding the membrane formation mechanism by immersion precipitation.

For the preparation of asymmetric membranes by immersion precipitation, glassy polymers are used. Although some of the polymers used are crystallizable, in general the rate of crystallization is very slow compared to the membrane formation process. Thus, the effect of crystallization on the formation of the membrane could often be neglected [4-6]. Consequently, the study on gelation of amorphous polymers gives general information on the formation of a membrane by immersion precipitation. In this study two completely amorphous polymers, polyethersulfone (PES) and polysulfone (PSF), are used.

The gelation phenomenon of a typical membrane-forming system consisting of  $H_2O$ -DMAC-PSF has been investigated by Wijmans *et al.* [7] and by Gaides and McHugh [8]. From DSC measurements in which no local ordering could be found for concentrated PSF solutions (up to 60% PSF), Wijmans [7] proposed that gelation during membrane formation of amorphous polymer systems by immersion precipitation occurs by crossing a viscosity boundary. Gaides [8] was able to measure this viscosity boundary by using a falling ball method. This viscosity boundary was also defined by Gaides as the gelation boundary of the system. According to Gaides [8], the ternary phase diagram of a system consisting of an amorphous polymer, a solvent and a nonsolvent is schematically shown in figure 1.

In figure 1, in the ternary phase diagram a binodal, a vitrification boundary and a gelation boundary are present. Above the vitrification boundary, a polymer solution is a glass. In between the vitrification boundary and the gelation boundary a polymer solution is a gel as defined by Gaides. The problem of defining the gelation boundary by a viscosity boundary is that it is difficult to distinguish a gel from a highly concentrated polymer solution. Is such a gel strong enough to assure a permanent structure in the final membrane or is such a gel still affected by the demixing behaviour of the system?

Apparently, the actual role of gelation in the structure formation process of a membrane by immersion precipitation is not clear yet. This is due to the absence of a

clear picture concerning the gelation mechanism in the membrane formation process. The purpose of this chapter is to clarify the concept of gelation in a membrane formation process by immersion precipitation and to explain the general role of gelation in the structure formation of the membrane.

A mechanism concerning the gelation of an amorphous polymer in mixtures of a solvent and a nonsolvent is proposed in this chapter, which is derived from Berghmans mechanism [9] for the gelation of binary systems consisting of an amorphous polymer and a solvent. The gelation mechanism for a ternary system proposed here will be used to describe the membrane formation process by immersion precipitation.

In literature, investigations on the gelation phenomenon are usually dealing with binary systems. Especially, systematic investigations on the physical gelation of amorphous polymers are focusing on atactic polystyrene (aPS) in different solvents. So, in this article the basic concepts concerning gelation of amorphous polymers are derived from aPS systems known in literature.

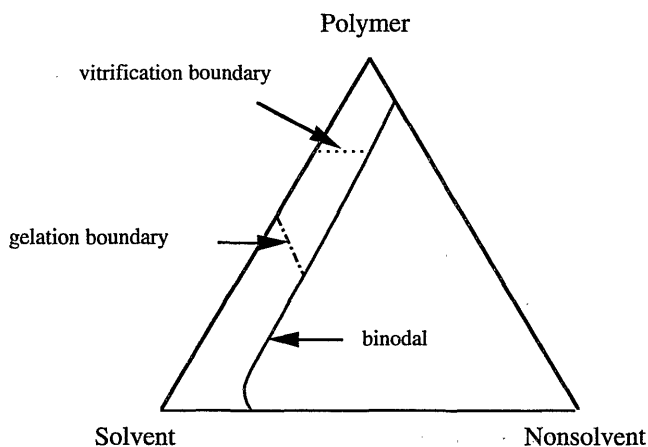


**Figure 1.** A schematic ternary phase diagram for an amorphous polymer-solvent-nonsolvent system, proposed by Gaides [8]. The gelation boundary was regarded by Gaides as a viscosity boundary as measured by the falling ball method.

### 2-3. GELATION OF AMORPHOUS POLYMERS

The discovery of physical gelation of aPS in different solvents [10,11] was puzzling because physical gelation of synthetic polymer had been thought to correspond to junction formation resulting from crystallization [12] or special interaction between the polymer chains, such as hydrogen bonding [13], and aPS is thought uncrystallizable and incapable of localized intermolecular associations [14]. To examine the origin and nature of the junctions in gels of aPS systems a lot of studies have been carried out [15-21].

Two different mechanisms have been proposed corresponding to the gel formation.

### 2-3-1. Guenet's mechanism for gelation of amorphous polymers

Guenet *et al.* [17-19] suggested that the formation of a polymer-solvent complex is responsible for the gelation. This means that without solvent, physical links (junction) cannot be created, a statement in agreement with the fact that aPS cannot crystallize from the bulk. Their experiments [17] and Xie's experiments [21] clarified that the gelation of the aPS/CS<sub>2</sub> system is a first-order transition. Evidence of the presence of ordered structures in the aPS/CS<sub>2</sub> system has been confirmed by neutron diffraction technique[19].

General observations of gelation following Guenet's mechanism are schematically shown in figure 2, data are from Tan [11].

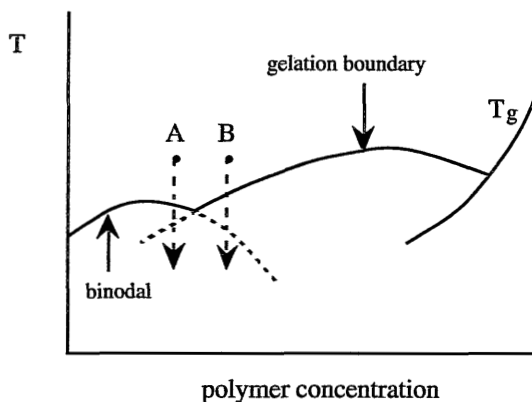


**Figure 2.** A schematic binary phase diagram showing the general experimental observations of gelation following Guenet's mechanism. Point A and point B are arbitrarily chosen points used to explain the gelation behaviour of the system. (see text)

By cooling a polymer solution denoted as A in figure 2 the solution first passes the binodal and consequently becomes turbid. By further cooling of the turbid solution, it transforms into a turbid gel when it passes the gelation boundary. Upon cooling solution B, a clear gel is formed after crossing the gelation boundary, which becomes turbid when cooled down further. According to the mechanism depicted in figure 2, gelation of amorphous polymer has the following characteristics:

- 1)  $T_{gel}$  is concentration dependent;
- 2) Liquid-liquid demixing is not necessary for the formation of a gel
- 3) Liquid-liquid demixing can still take place after gel formation, which is due to the fact that only a small part of the polymer chains are involved in formation of the

junctions. Yu *et al.* [22] used the forced rayleigh scattering technique to investigate the chain diffusion of aPS in CS<sub>2</sub>. Their results show that most of the polymer chains still move rather freely in the gel state and less than 20% of the chains is involved in the junctions of the gel structure.

4)A gel can also be formed after liquid-liquid demixing, but it is not clear how gelation can stop the continuing demixing process.

According to Guenet's mechanism, a gel can be formed only in a system in which some sort of complex between the polymer and the solvent can be formed, which indicates that special interactions must exist in the system.

### **2-3-2. Berghmans' mechanism for gelation of amorphous polymers**

Berghmans' mechanism [9] is rather simple. According to this mechanism, gelation results from liquid-liquid phase separation arrested by vitrification of the polymer rich phase. This mechanism has been demonstrated morphologically by Hikmet *et al.* [14] and analysed thermodynamically by Frank *et al.* [15].

Berghmans' mechanism for gelation of amorphous polymers is shown schematically in figure 3.

In figure 3, the binodal of the system intersects with the vitrification boundary of the system. By cooling down a homogeneous solution noted as A in figure 3, the solution separates into two phases after the binodal is crossed. Upon further cooling, the composition of the polymer rich phase finally reaches point B. At this particular point (Berghmans point), the polymer rich phase vitrifies and consequently the structure of the demixed solution is fixed. If the cooling speed is not infinitely slow a porous glass will be formed. Such a porous glass is defined as a gel by Berghmans. From the above descriptions, it is clear that for such a gelation process the pores in the final gel are created by liquid-liquid demixing and the formation of the junctions constructing the network of the gel is related to vitrification.

According to this mechanism, gelation of amorphous polymer has the following characteristics:

1)Gelation arises in a system characterized by the intersection of the binodal and the glass transition boundary in the temperature-concentration phase diagram.

2)For homogeneous polymer solutions with concentrations lower than the concentration related to Berghmans point,  $T_{gel}$  of the solutions is constant, independent on the initial concentrations of the polymer solutions.

3)Liquid-liquid demixing is necessary for the formation of a gel. Actually, such a gel is a porous glass.

4)Liquid-liquid demixing will cease as soon as gelation starts.

In this mechanism, gelation occurs without the necessity of special interaction between polymer and solvent. In literature, a lot of systems can be found [23-25], which form gels following Berghmans' mechanism.

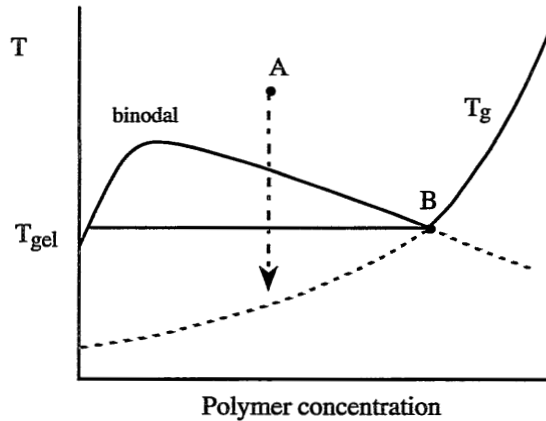


**Figure 3.** A schematic binary phase diagram used to explain Berghmans' mechanism for gelation of amorphous polymers.  $T_g$  is the vitrification temperature.  $T_{gel}$  is the gelation temperature. B is Berghmans' Point which represents the intersect point of the binodal and the  $T_g$  boundary of the system.

In our opinion, compared to Guenet's mechanism Berghmans' mechanism is a more general mechanism for gelation of amorphous polymers during membrane formation by immersion precipitation. Gelation following Guenet's mechanism is a rather slow process. Normally, a certain settling time (a few hours or a few days) has to be allowed for a solution to become a gel following Guenet's mechanism. The time scale (in minutes or seconds) for a membrane formation process does not allow the formation of such sort of a gel. In addition, in Guenet's mechanism special interaction must exist between the polymer and the solvent to form a gel. This is obviously not the case for membrane formation systems because membranes can be made from a polymer by using all kinds of available solvents. Therefore, in this study Berghmans' mechanism will be used to investigate the gelation phenomenon during membrane formation by immersion precipitation.

In figure 3, it can be seen that the *gelation boundary is actually a specified tieline whose polymer rich phase is located at Berghmans' point*. This mechanism can be transferred to a ternary system consisting of a polymer, a solvent and a nonsolvent. A schematic ternary phase diagram representing Berghmans gelation mechanism is shown in figure 4.

In figure 4, four regions exist. Solutions in region I are in a homogeneous, one phase liquid state. In region II, solutions will separate into two liquid phases, one



polymer lean phase and one polymer rich phase. In region III, the polymer rich phase of a demixed polymer solution reaches its glass state. In region IV, all solutions are in one phase glass state. This phase diagram will be used later on to discuss the membrane formation process by immersion precipitation process.

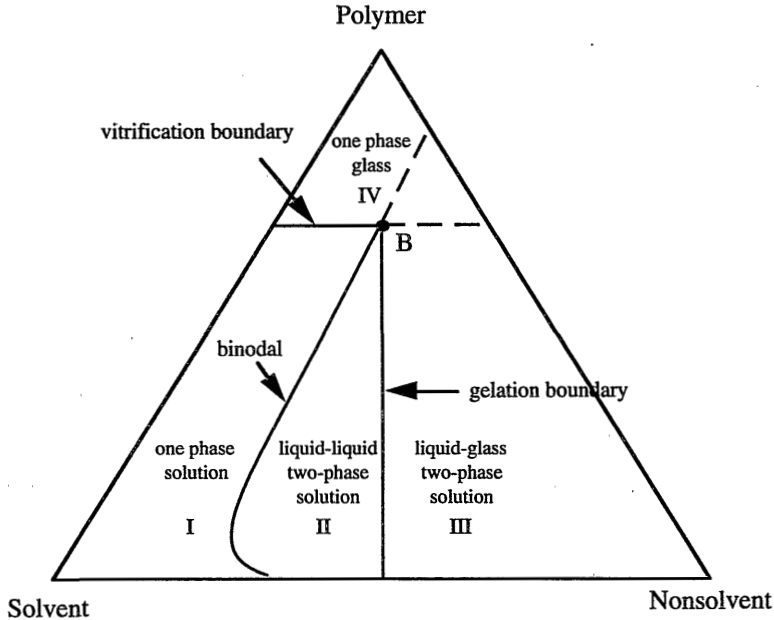


**Figure 4.** A schematic ternary phase diagram used to describe Berghmans' mechanism for ternary systems. Solutions in region I are in a homogeneous liquid state. In region II, polymer solutions separate into two liquid phases. Region III is a two-phase glass region consisting of one liquid phase which is the polymer lean phase and one glass phase. Solutions in region IV are in a homogeneous glass state. Point B is the Berghmans' point for a ternary system.

## 2-4. GLASS TRANSITION TEMPERATURE OF POLYMER SOLUTIONS

Different theories concerning the glass transition temperature depression of a polymer by a low molecular weight diluent are proposed in literature. It has been shown by Burghardt *et al.* [26] that the Kelley-Bueche [27] equation can be used to describe the glass transition temperature depression of a membrane forming system quite well. The Kelley-Bueche equation (1) is based on the free volume concept.

$$T_g = \frac{R\phi_2 T_{g2} + \phi_3 T_{g3}}{R\phi_2 + \phi_3} \quad (1)$$

The subscripts 2 and 3 in equation 1 denote the solvent and the polymer, respectively.  $\phi_i$  is the volume fraction of component  $i$  and  $T_{gi}$  is the glass transition temperature of component  $i$ . Parameter  $R$  is related to the thermal expansion coefficients of the components. But, this parameter is often used as a fitting parameter.

The Kelley-Bueche equation has been generalized for ternary systems by Burghardt and can be used to describe nonsolvent-solvent-polymer systems. For mixtures of two diluents, 1 and 2, the following expression was obtained.

$$T_g = \frac{R_1\phi_1 T_{g1} + R_2\phi_2 T_{g2} + \phi_3 T_{g3}}{R_1\phi_1 + R_2\phi_2 + \phi_3} \quad (2)$$

In equations (1) and (2), to calculate the glass transition temperature of the system the glass transition temperature of the individual components has to be known.  $T_g$  of a polymer normally can be found in literature, but literature data on  $T_g$  of low molecular weight solvents are rather limited.

Equation 3 is an empirical equation for the estimation of  $T_g$  of solvents which was obtained by Fedors [28].

$$\gamma = \frac{T_m + T_b}{T_g + T_b} \quad (3)$$

In this equation,  $T_m$ ,  $T_b$  and  $T_g$  are the melting temperature, boiling temperature and glass transition temperature of a solvent, respectively. From literature data available for 64 solvents, Fedors found that  $\gamma$  in equation 3 was nearly a constant, 1.15. The deviation of  $\gamma$  is from 1.09 to 1.30 for the 64 solvents. This equation can be modified further to obtain equation 4:

$$\gamma^* = \frac{T_m + T_b}{T_g + T_b} + 0.6 \times \frac{T_b - T_m}{T_b + T_m} \quad (4)$$

In equation 4 the mean value of  $\gamma^*$  was found to be 1.36. The deviation of  $\gamma^*$  is from 1.30 to 1.41 for the 64 solvents, which is smaller than the deviation of  $\gamma$  in equation 3.

## 2-5. EXPERIMENTAL

### 2-5-1. *Materials*

The polymers used were polyethersulfone (PES) (5200P, from ICI) and polysulfone (PSF) (Udle 3500, from Amoco).  $T_g$  of PES as determined by DSC, is 225 °C. FP, DMSO, DMAC, NMP and MPD were purchased from MERCK (synthesis grade) and used as received.  $T_g$  of pure solvents DMSO, DMAC and water are obtained from literature [28]: 150 K for DMSO, 146 K for DMAC and 137 K for water.  $T_g$  of FP and NMP was calculated with equation 4.

### 2-5-2. *Cloud point measurements.*

Cloud point data were measured by means of a titration method. Pure nonsolvent was slowly added to a solution of polymer and solvent. The solution was kept at a constant temperature. Every drop of nonsolvent added to the solution caused local coagulation. Further addition of nonsolvent was performed after the solution became homogeneous again. This procedure was continued until permanent turbidity was detected visually.

### 2-5-3. *Glass transition temperature of homogeneous polymer solutions.*

Differential scanning calorimetry (DSC) measurements were carried out with a liquid-nitrogen-cooled Perkin-Elmer DSC-II apparatus coupled with a Thermal Analysis Data System (TADS). Indium ( $T_m = 156.6$  °C) was used for temperature calibration. Samples of PES in a pure solvent were made by adding 40-50 mg 20 % (w/w) PES solutions into volatile sample pans followed by evaporating the solvents at 100 °C to the required concentration. The sample pans were then tightly sealed. The sealed pans were stored at 100 °C for at least one week before performing DSC scanning. Samples of PES in mixtures of NMP and water were prepared by weighing the appropriate amount of PES powder and of a mixture of NMP/water (9/1, w/w) into volatile sample pans. The tightly sealed sample pans were annealed at 100 °C for one week to ensure the achievement of homogeneous solutions. All the sealed sample pans were weighed before and after annealing. Only samples without leaking were used for DSC measurements. The homogeneity of the solution could be checked by DSC scanning. For samples with poor homogeneity, the DSC scanning showed a very broad  $T_g$  signal. For those samples with poor homogeneity, annealing in the DSC apparatus at a temperature of about 60 °C above their approximated  $T_g$  for 20 minutes normally could make the solutions become homogeneous. The glass transition temperature of a

solution was measured by quenching the solution to  $-40\text{ }^{\circ}\text{C}$  followed by heating it at a speed of  $20\text{ }^{\circ}\text{C}/\text{min}$ .  $T_g$  was recorded as the middle point of the transition for the second run. After DSC measurements the sample pans were weighed again to ensure that no leaking had occurred.

#### ***2-5-4. Glass transition temperature of demixed polymer solutions.***

The glass transition temperature of the polymer rich phase of a demixed polymer solution was measured by DSC. Demixed polymer solutions were prepared by homogenizing the polymer solutions containing 10% PES and various NMP/water ratios at  $110\text{ }^{\circ}\text{C}$  for three weeks followed by cooling the solutions down to room temperature at a speed of about  $3\text{ }^{\circ}\text{C}/\text{min}$ . The demixed solutions were then kept at room temperature for another three weeks. The solutions were contained in glass tubes with a diameter of 8 mm. After centrifugation for one week, a certain amount (25-35 mg) of the polymer rich phase of each of the solutions was taken from the glass tubes and sealed into DSC sample pans for the  $T_g$  measurements of the samples. After DSC measurements the sample pans were weighed again to ensure that no leaking occurred.

#### ***2-5-5. Membrane preparation.***

For membranes cast from highly concentrated polymer solutions ( $> 40\text{ wt }%$ ), a small casting knife was used. The initial thickness of the cast solution was  $200\text{ }\mu\text{m}$ , which was controlled by the casting knife. The solution was cast on a small glass plate with a dimension of  $60\text{ mm} \times 40\text{ mm} \times 1\text{ mm}$  (length  $\times$  width  $\times$  thickness). The amount of solution cast on the glass plate was measured by weighing. A highly concentrated polymer solution could be prepared by casting a 20% PES solution on the glass plate followed by evaporation of the solvent to the required concentration. The demixing behaviour of the polymer solution when immersed into a water bath was observed.

#### ***2-5-6. Delay time of demixing***

Delay time measurements were performed in a similar procedure as described in literature [29].

## **2-6. RESULTS AND DISCUSSION**

### ***2-6-1. Glass transition temperatures of solvents***

Glass transition temperatures of DMSO and DMAC are obtained from literature. For NMP and FP, no literature data on  $T_g$  are available. So,  $T_g$  of NMP and FP were calculated with equation 4. Table 1 gives  $T_g$ ,  $T_m$  and  $T_b$  of the four solvents and water.

Although the melting temperatures and the boiling temperatures of the four solvents and water are quite different, the glass transition temperatures are rather similar, which is shown in table 1. It can be seen that glass transition temperatures calculated from equation 4 are more close to the experimental values than that from equation 3.

**Table 1.**  $T_g$ ,  $T_m$  and  $T_b$  of different solvents

| Solvents | $T_m$ (K) | $T_b$ (K) | $T_g$ (K), calc. from equa. 3 | $T_g$ (K), calc. from equa. 4 | $T_g$ (K) from literature [28] |
|----------|-----------|-----------|-------------------------------|-------------------------------|--------------------------------|
| FP       | 242       | 495       | 146                           | 144*                          |                                |
| DMSO     | 291.5     | 462       | 193                           | 153                           | 150*                           |
| DMAC     | 253       | 439       | 163                           | 138                           | 146*                           |
| NMP      | 248.6     | 477       | 154                           | 143*                          |                                |
| water    | 273       | 373       | 189                           | 137                           | 137                            |

\* data used in this study

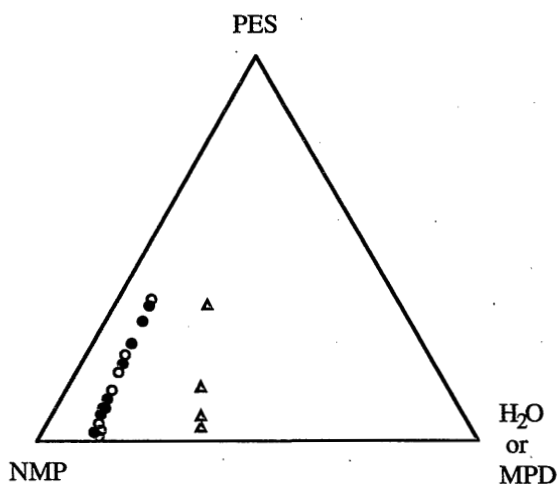


**Figure 5.** Cloud point data for  $H_2O$ -NMP-PES and MPD-NMP-PES systems at 25 °C. (●) cloud point data measured in this study for  $H_2O$ -NMP-PES system, (○) data from literature [30] for the same system, (Δ) data measured in this study for MPD-NMP-PES system.

### 2-6-2. Cloud points

The cloud points of  $H_2O$ -NMP-PES and MPD-NMP-PES systems shown in figure 5 have been measured with the titration method at 25 °C. For reason of comparison, literature data [30] for  $H_2O$ -NMP-PES system are also plotted in this

figure. It is clear that the agreement between literature data and the data measured here is very good. The binodal of MPD-NMP-PES is located more close to the nonsolvent corner compared to the binodal of H<sub>2</sub>O-NMP-PES system. According to calculations performed by Altena [31], a small polymer-nonsolvent interaction parameter (i.e. a rather mild interaction) or a large solvent-nonsolvent interaction parameter displays a binodal which is located close to the polymer-nonsolvent axis.

### **2-6-3. $T_g$ depression of PES by different solvents**

Samples of PES in NMP were first examined with DSC, in which the PES concentrations ranged from 40% to 85%. For solutions with PES concentrations smaller than 50%, no transition signals were detected in the experimental range of -40 °C to 150 °C. Only for solutions with PES concentration larger than > 55%,  $T_g$  transition signal was detected. From these DSC experiments it can be concluded that no crystallization or local ordering existed in the PES-NMP solutions.

Wijmans [7] demonstrated that for the system H<sub>2</sub>O-DMAC-PSF, the DSC scan of a highly concentrated PSF solution showed a melting peak near the melting temperature of DMAC. This melting behaviour of the solution was not observed in our experiments when homogeneous solution samples were examined. It is believed that the melting peak observed in Wijmans experiment was due to the sample preparation method. In Wijmans experiment, the highly concentrated polymer solution was prepared by separation of the polymer rich phase from a demixed polymer solution. In our experiments it was found to be very difficult to completely separate a demixed polymer solution, with a polymer rich phase of relatively high polymer concentration, into two phases by centrifugation. Usually, a small amount of polymer lean phase was trapped in the polymer rich phase; even after a long time of centrifugation, which was indicated by the fact that the polymer rich phase remained turbid. So, the polymer solution used by Wijmans might not have been homogeneous or when it was homogeneous at room temperature it might have separated into two phases upon cooling down below room temperature. The melting peak observed by Wijmans then would be corresponded by the trapped polymer lean phase, which was actually confirmed by Wijmans' own experiment that the related polymer lean phase showed a melting peak exactly in the same position.

Highly concentrated and homogeneous binary components solutions consisting of PES and a solvent were made by using the evaporation method. Figure 6 shows the  $T_g$  depression of PES by FP, DMSO, DMAC and NMP. In figure 6, it could be seen that among the solvents, the  $T_g$  of PES is depressed most strongly by NMP. The  $T_g$  depression of PES by the different solvents is in the consequence of NMP > DMAC > DMSO > FP.

Equation 1 was used to describe the  $T_g$  depression of PES by the various solvents. The fitting parameter  $R$  for the solvents are shown in table 2. The polymer concentrations related to the  $T_g$  at 298 K are also shown in this table. Gaides *et al.* [8] measured the  $T_g$  depression of PSF by DMAC. They found that the PSF-DMAC solution became glass at 298 K when the PSF concentration was 82%. This is much higher than the PES concentration in DMAC, which is 67%. The PSF concentration of 82% is in weight fraction, calculated from the volume fraction data as given by Gaides.

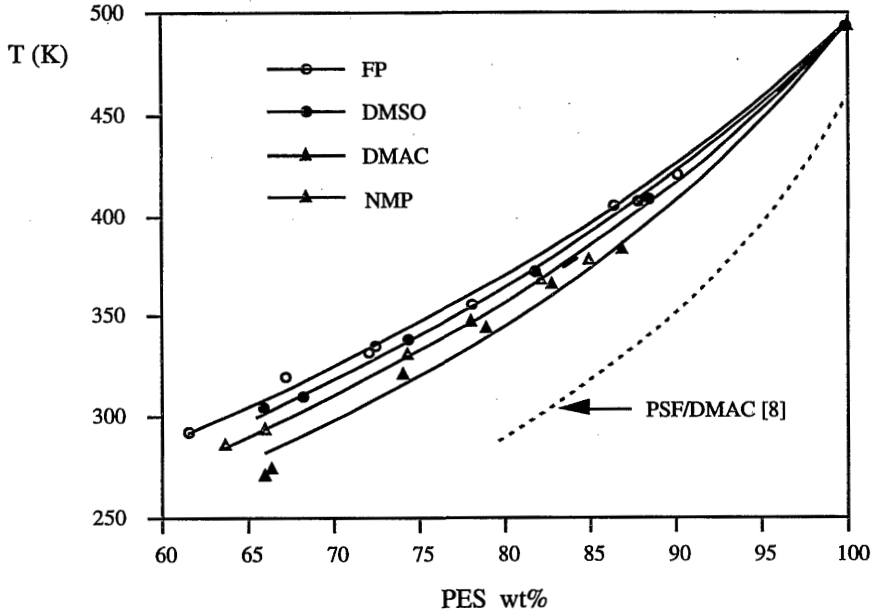


**Figure 6.**  $T_g$  depression of PES by various solvents. The dashed curve represents the  $T_g$  depression of PSF by DMAC [8].

**Table 2.** The Kelley-Bueche parameter  $R$  (equation 1) for the  $T_g$  depression of PES by various solvents together with the PES concentration related to  $T_g$  at 298 K.

| Solvents | $R$  | PES concentration at $T_g = 298$ K |
|----------|------|------------------------------------|
| FP       | 2.21 | 63                                 |
| DMSO     | 2.45 | 64                                 |
| DMAC     | 2.62 | 67                                 |
| NMP      | 2.98 | 70                                 |

#### 2-6-4. $T_g$ depression of PES by a mixture of NMP and water

Samples of homogeneous solution of PES in mixtures of NMP and water were prepared by weighing appropriate amount of PES powder and mixture of NMP and water into DSC sample pans followed by heating at elevated temperature for a certain time. The evaporation method could not be used here because the evaporation process would change the ratio of NMP to water.

Figure 7 shows the  $T_g$  depression behaviour of PES by a mixture of NMP/water (9/1) compared to that by pure NMP. It is clear that the  $T_g$  depression of PES by a mixture of NMP and water is the same as by pure NMP. In general, it is expected that the  $T_g$  depression of PES by NMP would be different from that by water, because the interaction between PES-NMP and PES-water is significantly different. So the  $T_g$  depression of PES by pure NMP should be different from the  $T_g$  depression of PES by mixtures of NMP and water as well. However, in the experiments the amount of water added into the polymer solution was quite limited, which might be the reason why no

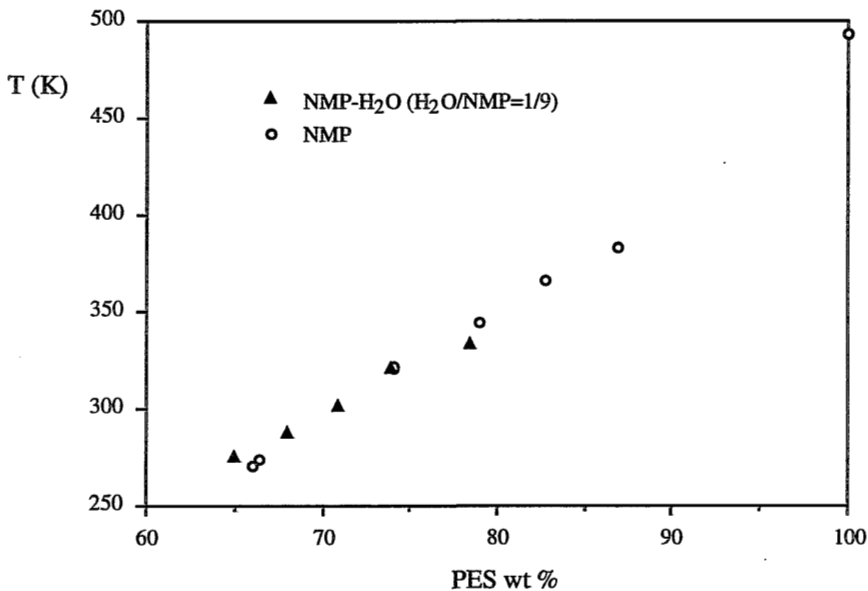


**Figure 7.** Comparison of  $T_g$  depression of PES by pure NMP and by a mixture of NMP and water (9/1).

difference was found between the  $T_g$  depression of PES by pure NMP and by a mixture of water and NMP. According to the cloud point data shown in figure 5, to be in the homogeneous region the water content in a highly concentrated polymer solution has to be rather low. For example, in the homogeneous region polymer solutions with



PES concentrations higher than 60% have water concentrations less than 6%. From the results shown in figure 7 and the cloud point data shown in figure 5, it can be concluded that regarding in the homogeneous region the  $T_g$  depression of PES by mixtures of NMP and water could be considered as the same as by pure NMP, which means that for homogeneous polymer solutions showing  $T_g$  at room temperature (298 K), the PES concentration in pure NMP is the same as in mixtures of NMP and water.

### ***2-6-5. Determination of the gelation boundary***

According to Berghmans mechanism for gelation of amorphous polymers, the gelation boundary is actually a specified tieline whose high (polymer) concentration end locates at the Berghmans point (see figure 4). In principle, for a ternary system at a certain temperature (for example, at 298 K) this tieline can be measured by separation of the two equilibrium phases, whose polymer rich phase shows a  $T_g$  at 298 K, from each other through centrifugation, followed by analysis of the compositions of the two phases. As discussed previously, when the polymer concentration of the polymer rich phase is relatively high it is extremely difficult to completely separate the demixed polymer solution into two phases. The gelation boundary can be measured in a different way. First, the Berghmans point (the intersection point of the binodal and the vitrification boundary) can be obtained from cloud point data and vitrification data of the system. Knowing the overall composition of a demixed polymer solution with a polymer rich phase whose  $T_g$  is at the desired temperature (here, it is 25 °C), then the gelation boundary can be generated by connecting the just mentioned overall composition point with the Berghmans point, providing that the two phases of the demixed polymer solution are in equilibrium.

In this study, a series of demixed polymer solutions were prepared by using a constant polymer concentration (10%) and varying the ratio of water to NMP. The procedure to make the solution can be found in the experimental part.

Glass transition temperatures of the polymer rich phase of the demixed solutions were measured. Table 3 gives the results. The PES concentrations of the polymer rich phase were examined as well by complete evaporation of NMP and water, the data are also shown in table 3.

From the data shown in table 3, it can be interpolated that the overall water concentration of the demixed polymer solution with  $T_g = 25$  °C of its polymer rich phase is about 21.5%. The related PES concentration of the polymer rich phase of the solution, determined by complete evaporation of NMP and water, is about 56%, which is much lower than the PES concentration at Berghmans point (70%). The discrepancy between those two data is caused by underestimation of the PES concentrations shown

in table 3 due to trapped polymer lean phase in the polymer rich phase. The trapped lean phase could not be removed from the polymer rich phase by centrifugation. All the polymer rich phase samples used for the DSC measurement were found to be turbid.

**Table 3.** *Glass transition temperatures and PES concentrations of the polymer rich phase of demixed polymer solutions of 10 % PES and various NMP/ water ratios.*

| Water concentration in the demixed solution (w/w %) | T <sub>g</sub> (°C) | polymer concentration of the polymer rich phase (w/w %)* |
|---|---------------------|--|
| 20  | 20.5                | 58   |
| 22  | 27.2                | 55   |
| 24  | 30.5                | 53   |
| 26  | 38.0                | 49   |
| 30  | 60.0                | 40   |

\*: underestimated data, see text for the reasons.

The DSC scans of the polymer rich phase samples showed a melting peak near the melting point of NMP, which is a further experimental proof that the melting peak found by Wijmans [7] was caused by trapped polymer lean phase.

As expected, table 3 shows that a higher amount of water in the polymer solution resulted in a higher glass transition temperature of the polymer rich phase. Due to random trapping of polymer lean phase, decrease of the polymer concentration of the polymer rich phase with increase of the water concentration in the solution might simply be an experimental coincidence. In principle, if the two equilibrium phases could be completely separated from each other the polymer concentration of the polymer rich phase should increase with increase of the water concentration in the demixed solution.

#### **2-6-6. The ternary phase diagram of H<sub>2</sub>O-NMP-PES system**

The ternary phase diagram of the system H<sub>2</sub>O-NMP-PES at 25 °C can be generated from the data presented above, and is shown in figure 8.

Figure 8 clearly shows that the vitrification boundary (of H<sub>2</sub>O-NMP-PES system) intersects the binodal (of the system), which means that Berghmans mechanism for gelation holds for this system. In this phase diagram, there are three boundaries: a binodal, a vitrification boundary and a gelation boundary. These three boundaries divide the phase diagram into four regions. The definition of the four regions is shown

in figure 4. Region I is a one-phase liquid region. Region II is a two-phase liquid region. Liquid-liquid demixing occurs when the composition of a polymer solution is within this region. The area of this region is controlled by the binodal and by the gelation boundary. Region III is a two-phase glass region. Within this region liquid-liquid demixing ceases because the polymer rich phase of a demixed polymer solution vitrifies. Region IV is a one-phase glass region. Liquid-liquid demixing cannot take place within this region, which is demonstrated experimentally later.

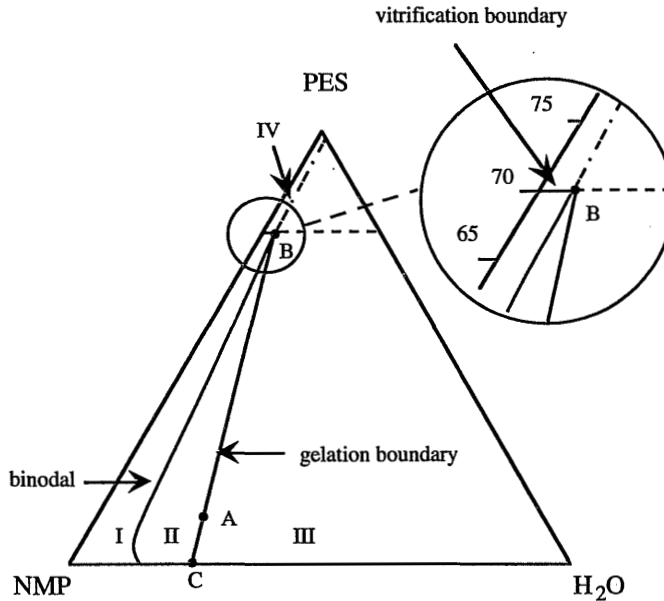


**Figure 8.** Ternary phase diagram of the system  $H_2O$ -NMP-PES at 25 °C. Point A in the figure represents the over all composition of a demixed polymer solution with 10% PES and 21.5% water in NMP. The  $T_g$  of the polymer rich phase of this demixed solution is at 25 °C. There are four regions in the diagram. The definition of the four regions is given in figure 4. Point B is Berghmans point. Point C is the intersection point of the gelation boundary with the solvent-nonsolvent axis, which has a composition of 76/24 (NMP/water, w/w).

Point C in figure 8 is the point where the gelation boundary intersects with the solvent-nonsolvent axis. The composition of this point obtained by extrapolation is 76/24 of NMP/water (w/w). In principle, point C is the critical point determining the maximum solvent concentration in a coagulation bath that can be used to prepare a solidified membrane. Using a mixture of NMP and water with a NMP concentration higher than 76% as the coagulation bath, solidified PES membranes cannot be obtained from the ternary system since the polymer concentration of the polymer rich phase will be lower than the vitrification concentration, as is proven in this work and is shown in the following section.

### 2-6-7. Examination of the gelation boundary

As described previously, the extension of Berghmans' gelation mechanism to ternary system consisting of a polymer, a solvent and a nonsolvent leads to the definition of point C in figure 8. This point defines the maximum solvent concentration in the coagulation bath that can be used to obtain a solidified membrane. For the system H<sub>2</sub>O-NMP-PES this point has been determined based on cloud point data and DSC measurements. It has been further tested by membrane casting experiments.

**Table 4.** *The elongation of membranes formed from a polymer solution of 30% PES and 6% water in NMP immersed into coagulation baths with various NMP concentrations.*

| NMP concentration<br>in the coagulation bath (wt %) | elongation of the film<br>(L/L <sub>0</sub> )* |
|---|--|
| 0   | 1  |
| 60  | 1  |
| 65  | 1  |
| 70  | 1  |
| 75  | 1  |
| 77.5  | ∞  |
| 80  | ∞  |

\*: L<sub>0</sub> is the initial film length and L the final film length.

Membranes were cast from a polymer solution of 30 % PES and 6 % water in NMP immersed in different coagulation bath with various NMP concentrations. The elongation behaviour of those membranes was measured in a simple way. After immersion of the cast solution into a coagulation bath for two days, a film with a dimension of 100 mm x 10 mm was cut from each of the formed membranes. The elongation of each film was measured by hanging a clamp of 35 g at one end of the film. Table 4 gives the results.

During the experiments, it was found that when the NMP concentration in the coagulation bath is  $\geq 77.5$  %, the films were broken immediately by hanging the clamp. Below 75 % NMP no elongation was observed under the experimental conditions. This experiment clearly shows that for this system vitrification is the only mechanism responsible for the structure fixation of the membranes. From the data presented in table 4, it can be concluded that the maximum NMP concentration in the coagulation bath in order to obtain a solidified membrane is in between 75 and 77.5 %, which is in

very good agreement with the datum obtained from figure 8. The very good agreement indicates that the method we used to determine the gelation boundary gives rather accurate results.

### ***2-6-8. Demixing behaviour in relation to vitrification phenomenon***

The demixing behaviour of binary component solutions of PES-NMP and PSF-DMAC in water bath was observed, and is presented in table 5.

***Table 5. Demixing behaviour of highly concentrated polymer solutions in water bath***

| polymer solution | demixing behaviour in water |
|------------------|-----------------------------|
| 30 % PES in NMP  | instantaneous demixing      |
| 62 % PES in NMP  | instantaneous demixing      |
| 65 % PES in NMP  | instantaneous demixing      |
| 72 % PES in NMP  | no demixing (no turbidity)  |
| 74 % PES in NMP  | no demixing (no turbidity)  |
| -----            |                             |
| 30 % PSF in DMAC | instantaneous demixing      |
| 60 % PSF in DMAC | instantaneous demixing      |

Table 5 shows that for polymer solutions of  $\text{PES}\% \leq 65\%$ , instantaneous demixing took place in the solutions when immersed into a water bath. For solutions with PES concentration higher than 72% no demixing occurred. At concentrations above 70% PES in NMP the solution is in a glass state at room temperature (see figure 8). Combining the data presented in figure 8 with the experimental observations shown in table 5, it is clear that instantaneous demixing can always take place in a PES solution immersed into a water bath as far as the initial polymer solution is in a liquid state. No liquid-liquid demixing can occur in a solution which is in a glass state. Data from Gaides [8] on the system  $\text{H}_2\text{O}$ -DMAC-PSF show that the solution is in a liquid state at room temperature when PSF concentration is below 82%. This explains why instantaneous demixing was observed when solutions of 30% PSF or 60% PSF in DMAC was immersed into a water bath.

The experiments presented in table 5 clearly show that liquid-liquid demixing cannot be prohibited by the high viscosity of a highly concentrated polymer solution. Liquid-liquid demixing can be prevented only when the composition of the polymer solution is higher than the vitrification concentration of the system.

It is noticed that the polymer solution of 60% PSF in DMAC is located in between the vitrification boundary and the "gelation" boundary of the system according to Gaides' experimental data [8]. So, in terms of a viscosity boundary this solution was defined as a "gel" by Wijmans [7] and Gaides [8]. However, the demixing behaviour of such a "gel" does not show any difference when compared to the demixing behaviour of a "normal" solution in a water bath. Instantaneous demixing can still take place in the "gel". Here one can question the practical value to define a gelation boundary in terms of a viscosity boundary concerning its relevance for the understanding of the membrane formation mechanism by immersion precipitation.

The weight of a film made out of a 74% PES solution was measured before and after immersion. The immersion time was 2 hours. The data are given in table 6. It can be seen that after immersion the weight of the film decreased, although the film remained transparent. This experiment indicates that even though no liquid-liquid demixing could occur in a vitrified polymer solution, the exchange of solvent and nonsolvent between the solution and the coagulation bath does take place. The result of the exchange was that the loss of solvent from the polymer solution was higher than the uptake of nonsolvent by the polymer solution which gave rise to the densification of the final film.

**Table 6.** *The weight of a polymer film from a solution of 74% PES in NMP, measured before and after immersion into water bath for 2 hours*

| before immersion | after immersion |
|------------------|-----------------|
| 51 mg            | 46 mg           |

Table 7 shows the demixing behaviour of PES-NMP solutions in a MPD bath. All the polymer solutions presented in this table are in a liquid state according to the data shown in table 2. It was found, however, that when the PES concentration was higher than 30% no liquid-liquid demixing could occur in the solution when MPD was used as the coagulant. The only explanation for these observations is that for polymer solutions with PES concentration higher than 30% during the membrane formation process the composition path of the system crosses the vitrification boundary before traversing the binodal of the system. An indication for this was that a stiff and transparent film was obtained. For polymer solutions with a lower PES concentration (< 20%), the composition path traverses the binodal before the vitrification boundary of the system is reached so liquid-liquid demixing of the solution was observed.

**Table 7.** Demixing behaviour of PES-NMP solutions in MPD bath

| polymer solution | demixing behaviour in MPD |
|------------------|---------------------------|
| 20 % PES in NMP  | delayed demixing          |
| 30 % PES in NMP  | no demixing               |
| 40 % PES in NMP  | no demixing               |

### 2-6-9. Membrane formation

Based on the experimental results for the system H<sub>2</sub>O-NMP-PES and literature data for the system H<sub>2</sub>O-DMAC-PSF [7, 8], it is shown that Berghmans mechanism for gelation of amorphous polymers holds for these two membrane-forming systems. Actually, this mechanism can be applied to a wide range of systems [32] as far as the binodal of the system intersects its vitrification boundary. For semicrystalline polymer systems crystallization may induce the formation of a gel, however, the time scale (in seconds or even much less) of a membrane formation process does not allow crystallization to progress, especially for the skin formation. For example, it has been found that solutions of PPO (poly(2,6-dimethyl-1,4-phenyleneoxide)) in various solvents or mixtures of solvent and nonsolvent can form gels initiated by crystallization of PPO [26]. However, PPO ultrafiltration membranes made from those solutions hardly contain any crystalline material [26]. From the above considerations, it becomes evident that Berghmans mechanism can be regarded as a gelation mechanism generally occurring in the membrane formation process.

The formation of the porous sublayer of a membrane is actually a gelation process; vitrification of a demixed solution which intends to evolve into a macroscopic two-layer, final state. Demixing induced by the replacement of solvent in the polymer solution by nonsolvent, initially takes place by the creation of a large number of nuclei of polymer diluted phase. This is immediately followed by the coalescence of the nuclei in an attempt to reach the macroscopic two-layer, final state. In a metastable stage, however, the demixing process is frozen by vitrification. The final porosity of the membrane is then controlled by the overall composition of the system at the moment that vitrification sets in. In quantitative terms the familiar lever rule should apply defining the relative amounts of concentrated and diluted phases. The continuity of the diluted phase is related to the overall composition, but more strikingly determined by the fact that at which stage of demixing the vitrification is realized. To say more precisely, if vitrification occurs in an earlier stage of demixing, the degree of continuity should be higher because in an earlier stage, the number of nuclei is larger and consequently the frequency of coalescence is higher. For binary systems [14,25] it has

been proven that the cease of demixing by vitrification at an earlier stage indeed results in a better interconnected porous structure.

The above statements can be illustrated with a generalized phase diagram as shown in figure 9. Point A represents the initial composition of a casting solution. The arrows 1 and 2 represent two possible composition paths if a polymer film with composition A is immersed into a nonsolvent bath.

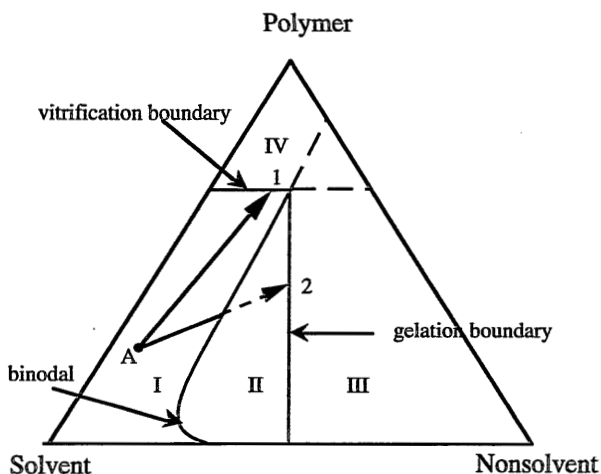


**Figure 9.** A generalized ternary phase diagram used to describe Berghmans' mechanism in relation to membrane formation. Point A is the initial composition of a casting solution. The arrows 1 and 2 represent two possible composition paths if a polymer film with composition A is immersed into a nonsolvent bath. The definition of the four regions (I, II, III, IV) are shown in figure 4.

From figure 9, it can be seen that for path 1 the polymer solution undergoes a glass transition and consequently the solution becomes a homogeneous, dense glass. Of course, in this situation no gelation is involved. The resulting membrane will show the intrinsic polymer properties for gas separation. This situation has been observed in our experiments, as shown in table 7. For path 2 gelation dominates the formation of the membrane. Liquid-liquid demixing starts when the path crosses the binodal. The demixing will continue as far as the composition path remains in region II (definition in figure 4). The time associated with the dotted part of path 2 determines when vitrification will set in after demixing. Here, this time is defined as *gelation time*.

In region II of figure 9, liquid-liquid demixing proceeds. The area of this region is determined by both the binodal and the gelation boundary. When the area is small, it implies that after demixing only a small amount of nonsolvent diffusing into the polymer solution is sufficient to induce vitrification, which means that the gelation time is short. For the system H<sub>2</sub>O-NMP-PES, this region is rather small, characterized by a



very steep gelation boundary as shown in figure 8. Experiments showed that membranes prepared from this system vitrified very quickly, as was noticed by a simple touch test. It appears that, because the gelation boundary is just a specific tieline, knowledge about the tieline in relation to the thermodynamic properties of the system is of great importance concerning the structure formation of a membrane. This has not been recognized in literature so far. Apparently, from the above analysis, the importance of determining the gelation boundary emerges.

In practice, the composition path shifts with time during the formation of a membrane by immersion precipitation [29]. So, more likely path 1 in figure 9 may represent the skin formation and path 2 the sublayer formation because the ratio of solvent outflow and nonsolvent inflow is higher for the skin formation than for the sublayer. If so, the resulting membrane will show a homogenous, dense, glassy skin and a porous sublayer. It appears then that depending on the composition path gelation is not necessarily responsible for the formation of a dense skin.

## 2-7. CONCLUSIONS

Berghmans gelation mechanism has been extended to ternary membrane forming systems consisting of a polymer, a solvent and a nonsolvent. Based on this mechanism, the gelation boundary is defined as a specific tieline whose polymer concentrated end is located at Berghmans' point.

A method has been developed to measure the gelation boundary of a ternary system. In this method, the gelation boundary is generated based on the cloud point data and vitrification data of homogeneous solutions as well as demixed solutions.

The phase diagram of the system  $H_2O$ -NMP-PES at 25 °C has been measured. In the phase diagram four different regions can be distinguished: I) a homogeneous liquid region, II) a two-phase liquid-liquid region, III) a two phase liquid-glass region and IV) a homogeneous glass region.

Membrane casting experiments of the system  $H_2O$ -NMP-PES and  $H_2O$ -DMAC-PSF showed that vitrification is the only mechanism responsible for the fixation of the membrane structure. It was also shown that liquid-liquid demixing of these systems can only be prevented by vitrification at high enough polymer concentration.

It has been experimentally proven that the skin of a membrane made by immersion precipitation can be formed by vitrification without undergoing liquid-liquid demixing. For the system MPD-NMP-PES, the formation of membranes can even be completely dominated by vitrification without liquid-liquid demixing taking place.

## 2-8. REFERENCES

1. Loeb, S. and Sourirajan, S., *Adv. Chem. Ser.*, 38, 117 (1962)
2. Koenhen, D. M.; Mulder, M. H. V. and Smolders, C. A., *J. Appl. Polym. Sci.* 21, 199 (1977)
3. Broens, L.; Altena, F. W.; Smolders, C. A. and Koenhen, D. M., *Desalination* 32, 33 (1980)
4. Altena, F. W.; Schroder, J. S.; Van de Huls, R. and Smolders, C. A., *J. Polym. Sci., Polym. Phys. Ed.* 24, 1725 (1986)
5. Reuvers, A. J.; Altena, F. W. and Smolders, C. A., *J. Polym. Sci., Polym. Phys. Ed.* 24, 793 (1986)
6. Wijmans, J. G.; Rutten, H. J. J. and Smolders, C. A., *J. Polym. Sci., Polym. Phys. Ed.* 23, 1941 (1985)
7. Wijmans, J. G.; Kant, J.; Mulder, M. H. V. and Smolders, C. A., *Polymer*, 26, 1539 (1985)
8. Gaides, G. E. and McHugh, A. J., *Polymer*, 30, 2118 (1989)
9. Arnauts, J. and Berghmans, H., *Polym. Commun.* 28, 66 (1987)
10. Wellinghoff, S.; Shaw, J. and Baer, E., *Macromolecules*, 12, 932 (1979)
11. Tan, M.-M.; Moet, A.; Hiltner, A. and Baer, E., *Macromolecules*, 16, 28 (1983)
12. Bassett, D. C.; Keller, A. and Mitsuhashi, S., *J. Polym. Sci.* A1, 763 (1963)
13. Yang, Y. C. and Geil, P. H., *J. Macromol. Sci. Phys.* B22, 463 (1983)
14. Hikmet, R. M.; Callister, S. and Keller, A., *Polymer*, 29, 1378 (1988)
15. Frank, F. C. and Keller, A., *Polym. Commun.* 29, 186 (1988)
16. Koltisko, B.; Keller, A.; Litt, M.; Baer, E. and Hiltner, A., *Macromolecules*, 19, 1207 (1986)
17. Francois, J.; Gan, J. Y. S. and Guenet, J.-M., *Macromolecules*, 19, 2755 (1986)
18. Gan, J. Y. S.; Francois, J. and Guenet, J.-M., *Macromolecules*, 19, 173 (1986)
19. Guenet, J.-M.; Klein, M. and Menelle, A., *Macromolecules*, 22, 493 (1989)
20. Boyer, R. F.; Baer, E. and Hiltner, A., *Macromolecules*, 18, 427 (1985)
21. Xie, X.-M.; Tanioka, A. and Miyasaka, K., *Polymer*, 31, 281 (1990)
22. Lee, J.; Kim, H.; and Yu, H., *Macromolecules*, 21, 858 (1988)
23. Tsai, F.-J. and Torkelson, J. M., *Macromolecules*, 23, 775 (1990)
24. Aubert, J. H., *Macromolecules*, 23, 1446 (1990)
25. Castro, A. J., *U. S. Pat.*, 4,247,498, 1981
26. Burghardt, W. R.; Yilmaz, L. and McHugh, A. J., *Polymer*, 28, 2085 (1987)
27. Kelley, F. N. and Bueche, F., *J. Polym. Sci.* 50, 549 (1961)
28. Fedors, R. F., *J. Polym. Sci. Polym. Lett. Ed.* 17, 719 (1979)
29. Reuvers, A. J. and Smolders, C. A., *J. Membr. Sci.* 34, 67 (1987)
30. Zeman, L. and Tkacik, G., *J. Membr. Sci.* 36, 119 (1988)
31. Altena, F. W. and Smolders, C. A., *Macromolecules*, 15, 1491 (1982)
32. Vandeweerdt, P.; Berghmans, H. and Tervoort, Y., *Macromolecules*, 24, 3547 (1991)

---

**CHAPTER 3**

---

**MODELLING OF MEMBRANE FORMATION FROM THE  
SYSTEM H<sub>2</sub>O-NMP-POLYETHERSULFONE**

---

S.-G. Li, Th. van den. Boomgaard, C.A. Smolders, H. Strathmann

**3-1. ABSTRACT**

Membrane formation from the system H<sub>2</sub>O (1)-NMP (2)-polyethersulfone (PES; 3) has been modelled in this study. The Flory-Huggins theory has been used to describe the thermodynamic properties of the system. It has been found that to properly describe the thermodynamic equilibrium properties of the system, a ternary interaction parameter has to be employed in the theory. With the set of interaction parameters of  $\chi_{12} = 0.718 + 0.669 u_2$ ,  $\chi_{13} = 2.73$ ,  $\chi_{23} = 0.5$  and  $\chi_T = -0.69$ , the calculated binodal and tie lines are in a very good agreement with the experimental data. Reuvers' model for membrane formation by immersion precipitation has been used to evaluate the mass transfer behaviour of the system during membrane formation. Calculations show that for the system H<sub>2</sub>O-NMP-PES, at the interface of the membrane liquid-liquid demixing and vitrification may both take place instantaneously. This means that at the interface these two processes interfere with each other. The calculations give rise to an explanation for nodular structure formation from this system. The results of simulating various friction coefficients on membrane formation by immersion precipitation are also presented.

**3-2. INTRODUCTION**

Today the majority of commercial membranes with applications ranging from microfiltration to gas separation are prepared by immersion precipitation process. The most simple membrane forming system by immersion precipitation is a ternary system consisting of a polymer, a solvent and a nonsolvent. In general, systematic modelling of membrane formation by immersion precipitation is focusing on ternary systems.

In literature, several authors [1-9] published models for membrane formation by immersion precipitation. Cohen *et al.* [1] were the first to systematically model the membrane formation process from a ternary system. With this model, composition changes in the polymer solution during membrane formation can be calculated. Reuvers *et al.* [2,3,4] further developed this model by taking into account the diffusion

processes in both polymer solution and coagulation bath. In Reuvers model, only binary data are taken into account. It was shown that for the systems  $H_2O$ -acetone-cellulose acetate (CA) and  $H_2O$ -dioxane-CA, using binary data from thermodynamics and kinetics membrane formation could be predicted, which was well in accordance with the experiments. Reuvers model was also used by Radovanovic [5,6] to investigate the membrane formation process of the system propanol-DMAC-polysulfone. By using experimentally obtained friction coefficients, observed membrane formation phenomena for the system propanol-DMAC-polysulfone could be satisfactorily predicted. By extending the model presented by Reuvers to a quaternary system, Boom [7] was able to describe the membrane formation process from the system PES-PVP-NMP- $H_2O$  qualitatively.

According to the model of Reuvers two types of demixing processes can be distinguished. The first type is delayed demixing and the second is instantaneous demixing. For the delayed demixing process, it takes a certain time for phase separation to occur after immersion of the solution into a nonsolvent bath. For the instantaneous demixing process, phase separation takes place immediately after immersion. The two processes result in quite different membrane properties. A membrane formed by delayed demixing generally shows a dense skin and a sublayer of isolated pores (a closed cell structure). A membrane formed by instantaneous demixing has a porous skin (suitable for ultrafiltration) as well as a relatively open sublayer. From the model presented by Reuvers, the mechanism of the formation of those two different membranes can be understood.

In principle, this model is an approximation valid only during a very short time after immersion, when the polymer solution can still be considered as an infinitely thick film. As soon as the composition at the other side of the film, away from the interface, changes due to the exchange of solvent and nonsolvent, this model can no longer be used. In recent years, Tsay *et al.* [8-10] further developed Reuvers' model, so that the model remains valid until demixing starts. With the model modified by Tsay, the delay time of demixing of the system  $H_2O$ -acetone-CA could be predicted more accurately. However, this model gave some unexpected results which were in contradiction with the generally accepted assumption and also experimental observation that after immersion of a polymer solution into a nonsolvent bath, the polymer concentration at the interface will increase with time until the top layer solidifies. The model calculations of Tsay showed a decrease of the polymer concentration at the interface with time. This unexpected result might be due to the high sensitivity of the model to the diffusion coefficients of the system, which are difficult to measure accurately in a highly concentrated polymer solution.

In all previously described models, the thermodynamic properties of the membrane forming system are described by using Flory-Huggins theory because this

theory can be used for highly concentrated polymer solutions and it is relatively simple. The model calculations showed that the thermodynamic properties of the membrane forming system have a very strong effect on the demixing behaviour during membrane formation. So an accurate description of the thermodynamic properties of the system is essential for modelling the membrane formation process.

The thermodynamic properties of H<sub>2</sub>O-NMP-PES system have been investigated by Zeman and Tkacik [11]. From literature data on the vapor-liquid equilibrium of H<sub>2</sub>O-NMP system and light scattering and refractive index measurements for NMP/PES system, it was found that the interaction parameters  $\chi_{12}$  and  $\chi_{23}$  are concentration-dependent. An indirect estimation of the interaction parameter  $\chi_{13}$  was also made by the authors, which was considered to be concentration-independent. It was found by Zeman and Tkacik that the theoretical phase diagram predicted from the Flory-Huggins theory with constant interaction parameters  $\chi_{12} = 1.0$ ,  $\chi_{23} = 0.5$  and  $\chi_{13} = 1.5$  agreed very well with the cloud point curve measured at low polymer concentration. However, for the high polymer concentration range the calculated binodal differed considerably from the experimentally obtained cloud point curve. It will be shown later in this study that the use of this set of interaction parameters for describing the thermodynamic properties of the system H<sub>2</sub>O-NMP-PES is not suitable to describe the demixing behaviour during membrane formation. It will also be shown that the tie lines calculated by using this set of parameters differ significantly from the tie lines measured at high polymer concentration. It was found that the use of concentration-dependent  $\chi_{12}$  and  $\chi_{23}$  in the phase diagram calculation does not lead to a better agreement between the calculated data and experimental data. Actually, it can be concluded that the equilibrium thermodynamic properties of this system can not be described satisfactorily by using binary interaction parameters only, even if concentration-dependence of all the three parameters is taken into account. Apparently, for this system a ternary interaction parameter has to be postulated.

In this work it is shown that the use of a ternary interaction parameter in combination with the use of binary interaction parameters obtained from literature gives a very good agreement between the predicted phase diagram and the measured cloud point curve. It is further demonstrated that mass transfer modelling based on an accurate expression of the thermodynamic properties of the system can give important information concerning the structure formation of the related membrane. For the modelling of mass transfer during membrane formation, we focus on the composition changes at the first moment of immersion, so Reuvers model can be applied.

### 3-3. EQUILIBRIUM THERMODYNAMICS

#### 3-3-1. Flory-Huggins theory

In this study, we use Pouchly's [12] extension of the Flory-Huggins theory for ternary polymer solutions, in which a ternary interaction term is included to describe the Gibbs free energy of mixing:

$$\frac{\Delta G_m}{RT} = \sum_{i=1}^3 n_i \ln \phi_i + \chi_{12}(u_2)n_1\phi_2 + \chi_{13}(\phi_3)n_1\phi_3 + \chi_{23}(\phi_3)n_2\phi_3 + \chi_T(u_2, \phi_3)n_1\phi_2\phi_3 \quad (1)$$

where  $\Delta G_m$  is the Gibbs free energy of mixing of the system, R and T are the universal gas constant and temperature, respectively. In addition,  $n_i$  and  $\phi_i$  are moles and volume fraction of component i, and  $u_2 = \phi_2/(\phi_1 + \phi_2)$ . The three components are denoted as: nonsolvent (1), solvent (2) and polymer (3).  $\chi_{ij}$  is the interaction parameter between component i and component j. Originally, Pouchly treated all four interaction parameters in the equation as concentration-dependent. In our study  $\chi_{12}$  is considered as concentration-dependent and the other three interaction parameters as concentration-independent. The reason for this is that it is often observed that the interaction parameter between two low molecular weight components varies considerably with the composition change [4,13].  $\chi_T$  is the ternary interaction parameter, which comprises all non-binary effects. Based on these considerations, the definition of the chemical potential:

$$\frac{\Delta \mu_i}{RT} = \frac{\partial}{\partial n_i} \left( \frac{\Delta G_m}{RT} \right)_{n_j, j \neq i} \quad (i, j = 1, 2, 3) \quad (2)$$

leads to the following expressions for the chemical potential of the components:

$$\begin{aligned} \frac{\Delta \mu_1}{RT} = & \ln \phi_1 - s\phi_2 - r\phi_3 + (1 + \chi_{12}(u_2)\phi_2 + \chi_{13}\phi_3)(1 - \phi_1) - s\chi_{23}\phi_2\phi_3 \\ & + \chi_T\phi_2\phi_3(1 - 2\phi_1) - \phi_2u_2(1 - u_2) \frac{d\chi_{12}(u_2)}{du_2} \end{aligned} \quad (3)$$

$$\frac{s\Delta\mu_2}{RT} = s \ln \phi_2 - \phi_1 - r\phi_3 + (s + \chi_{12}(u_2)\phi_1 + s\chi_{23}\phi_3)(1 - \phi_2) - \chi_{13}\phi_1\phi_3 + \chi_T\phi_1\phi_3(1 - 2\phi_2) - \phi_1u_2(1 - u_2)\frac{d\chi_{12}(u_2)}{du_2} \quad (4)$$

$$\frac{r\Delta\mu_3}{RT} = r \ln \phi_3 - \phi_1 - s\phi_2 + (r + \chi_{13}\phi_1 + s\chi_{23}\phi_2)(1 - \phi_3) - \chi_{12}(u_2)\phi_1\phi_2 + \chi_T\phi_1\phi_2(1 - 2\phi_3) \quad (5)$$

where  $\Delta\mu_i$  is the chemical potential of component  $i$ ;  $s = \underline{v}_1M_1/(\underline{v}_2M_2)$ ;  $r = \underline{v}_1M_1/(\underline{v}_3M_3)$ ,  $\underline{v}_i$  and  $M_i$  are the specific volume and the molecular weight of component  $i$ , respectively.

The requirements for phase equilibrium (the binodal curve) are:

$$\Delta\mu_i \text{ (concentrated phase)} = \Delta\mu_i \text{ (diluted phase)} \quad i=1,2,3 \quad (6)$$

For the computation of the binodal curve, the program developed by Boom [7] is used.

### 3-3-2 Evaluation of interaction parameters for H<sub>2</sub>O-NMP-PES system

The interaction parameters  $\chi_{12}$ ,  $\chi_{23}$  and  $\chi_{13}$  for H<sub>2</sub>O-NMP-PES system can be obtained from literature [7,11]. Based on data by Zeman and Tkacik [11], Boom [7] derived the following expression for  $\chi_{12}$  as a concentration-dependent parameter:

$$\chi_{12}=0.718 + 0.669 u_2 \quad (7)$$

Light scattering measurements [11] for PES/NMP solutions in the concentration range of 5-30 weight percent polymer yielded a concentration-dependent  $\chi_{23}$  in the range of 0.36-0.55. However, a constant value of 0.5 for  $\chi_{23}$  was suggested by Zeman and Tkacik [11], which was also used by Boom [7]. It will be used in this study as well, thus:

$$\chi_{23}=0.5 \quad (8)$$

It has been shown by different authors [3,8,13] that the binodal of a ternary system is not very sensitive to the variation of  $\chi_{23}$ , so the assumption of  $\chi_{23}$  being constant is acceptable.

Based on different experiments two quite different data for  $\chi_{13}$  have been obtained by Zeman and Tkacik [11]. From swelling measurements, a value of 2.73 was obtained for  $\chi_{13}$ , but from light scattering measurements for H<sub>2</sub>O-NMP-PES solutions

an indirect estimation resulted in a value of 1.6 for  $\chi_{13}$ . For water-CA system [13],  $\chi_{13}$  is 1.4, and for water-polysulfone [13],  $\chi_{13}$  is 3.7. Compared to those values it is reasonable to choose  $\chi_{13}=2.73$  for water-PES system, since it is expected that PES is less hydrophilic than CA and less hydrophobic than polysulfone. So, we use:

$$\chi_{13}=2.73 \quad (9)$$

Zeman and Tkacik [11] argued that for thermodynamic analysis of the equilibrium properties of the system H<sub>2</sub>O-NMP-PES the use of constant interaction parameters of  $\chi_{12}=1.0$ ,  $\chi_{23}=0.5$  and  $\chi_{13}=1.5$  gives the best fit for the experimental data. However, their results show that the calculated binodal fits measured cloud point data at low polymer concentration range only. It will be shown later in this study that for the system H<sub>2</sub>O-NMP-PES a reasonable agreement between theoretically predicted and experimentally obtained data, including both the cloud point data and tie line data, cannot be obtained by simply using binary interaction parameters. Therefore, a ternary interaction parameter has to be used in the calculations.

Experimental datum for  $\chi_T$  of the system H<sub>2</sub>O-NMP-PES is not available in literature. In our study, we simply treat  $\chi_T$  as a fitting parameter. The fitting procedure was performed by first choosing a reasonable set of binary interaction parameters from literature as mentioned above, then systematically varying  $\chi_T$  to see if both the calculated binodal and the tie lines fit the experimental data. The fitting results will be shown later.

### 3-4. MASS TRANSFER

Reuvers model [2,3,4] is used to study mass transfer during membrane formation for the system H<sub>2</sub>O-NMP-PES. The model is summarized as follows:

#### 3-4-1. Mass transfer model

##### *Diffusion in the polymer solution*

We start from the continuity equations in terms of volume fluxes relative to the laboratory fixed frame of reference:

$$\frac{\partial \phi_i}{\partial t} = -\frac{\partial \tilde{J}_i}{\partial x} \quad i = 1,2,3 \quad (10)$$

in which  $\phi_i$  is the volume fraction of component  $i$ , and  $t$  and  $x$  are the time and the spatial coordinate, respectively. The volume fluxes  $\tilde{J}_i$  are relative to the laboratory fixed frame of reference.



By introducing a new spatial coordinate,  $m$ , to account for the moving interface between the polymer solution and the coagulation bath (see figure 1):

$$m(x,t) = \int_0^x \phi_3(x,t) dx \quad (11)$$

and by using the polymer component as the reference component, the continuity equations (10) can be converted to:

$$\frac{\partial(\phi_i / \phi_3)}{\partial t} = - \frac{\partial J_i}{\partial m} \quad i = 1,2 \quad (12)$$

where the volume fluxes  $J_i$  are relative to the motion of the polymer, which are defined as:

$$J_i = \phi_i(v_i - v_3) \quad i = 1,2 \quad (13)$$

in which  $v_i$  is the velocity of component  $i$  relative to the laboratory frame. The fluxes  $J_i$  are related to the chemical potential gradients in the form:

$$J_i = - \sum_{j=1}^2 \left\{ \underline{v}_i L_{ij} \frac{\partial \mu_j}{\partial m} \right\} \quad i = 1,2 \quad (14)$$

where  $\mu_i$  is the chemical potential, and  $\underline{v}_i$  the specific volume of component  $i$ . The  $L_{ij}$  are called phenomenological coefficients.

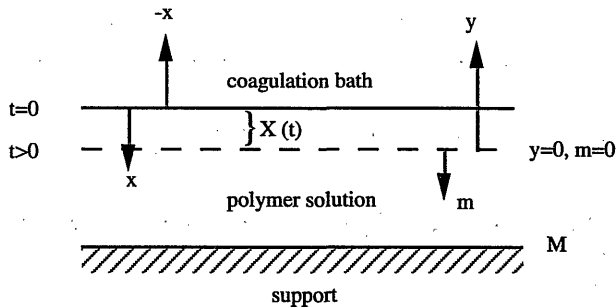


**Figure 1.** Schematic representation of the polymer solution, the coagulation bath and the position coordinates used.

Combining equations (12) and (14), the diffusion equations describing a ternary membrane forming system can be obtained:

$$\frac{\partial(\phi_i / \phi_3)}{\partial t} = \frac{\partial}{\partial m} \left\{ \sum_{j=1}^2 v_i \phi_3 L_{ij} \frac{\partial \mu_j}{\partial m} \right\} \quad i = 1, 2 \quad (15)$$

The composition changes in a polymer solution can be calculated with equations (15). Before this could be done, however, expressions relating the compositions ( $\phi_i$ ) to the phenomenological coefficients  $L_{ij}$  and expressions relating the compositions to the chemical potentials  $\mu_i$  have to be found first. The Flory-Huggins theory is used to correlate the chemical potentials and compositions. To find the expressions for  $L_{ij}$ , the Maxwell-Stefan equations [2] are used:

$$\frac{\partial \mu_i}{\partial x} = \sum_{j=1}^3 c_j R_{ij} (v_j - v_i) \quad i = 1, 2, 3 \quad (16)$$

where  $c_j$  is the concentration of component  $j$  and  $v_j$  is the velocity relative to the laboratory frame.  $R_{ij}$  is the friction coefficient between component  $i$  and  $j$ .

The relation between  $L_{ij}$  and  $R_{ij}$  is derived by Reuvers [2]:

$$L_{ij} = \frac{\beta_{ij}}{\alpha} \quad i, j = 1, 2 \quad (17)$$

where  $\beta_{12} = \beta_{21} = c_1 c_2 R_{12}$ ,  $\beta_{11} = c_1 (c_1 R_{12} + c_3 R_{23})$ ,  $\beta_{22} = c_2 (c_2 R_{12} + c_3 R_{13})$  and  $\alpha = c_3 (c_2 R_{12} R_{23} + c_1 R_{12} R_{13} + c_3 R_{13} R_{23})$ .

It is assumed by Reuvers [2] that the friction coefficients  $R_{ij}$  are dependent only on the two components  $i$  and  $j$ . Thus, the friction coefficients  $R_{ij}$  can be obtained from measured data in binary systems.

The binary friction coefficient  $R_{12}$  can be related to the Fick diffusion coefficient  $D$  and the chemical potential  $\mu_1$  in the binary solvent-nonsolvent mixture:

$$R_{12}(\phi_1, \phi_2) = R_{12}(u_1) = \frac{v_2 u_1}{D(u_1)} \frac{d\mu_1}{du_1}, \quad \text{where } u_1 = \frac{\phi_1}{\phi_1 + \phi_2} \quad (18)$$

The binary friction coefficient  $R_{23}$  can be obtained from the binary sedimentation coefficient  $s_3$  [4]:

$$R_{23}(\phi_2, \phi_3) = R_{23}(\omega_3) = \frac{(1 - \omega_3) v_3 (\rho v_2 - 1)}{\omega_3} \frac{1}{s_3(\omega_3)} \quad (19)$$

where  $\omega_3 = \phi_3 / (\phi_2 + \phi_3)$ , and  $\rho$  is the density of the binary polymer-solvent mixture.

The friction coefficient  $R_{13}$  is assumed by Reuvers [4] to be proportional to  $R_{23}$  in a relation of:

$$R_{13} = (\nu_1 / \nu_2) R_{23} \times 10^{C\phi_3} \quad (20)$$

where the proportionality constant C is used as an adjustable parameter.

#### *Diffusion in the coagulation bath*

By assuming no polymer dissolved in the coagulation bath, the diffusion in the bath can be described by the following equations:

$$\frac{\partial \phi_i}{\partial t} = \frac{\partial}{\partial y} \left\{ D(\phi_i) \frac{\partial \phi_i}{\partial y} \right\} - \frac{\partial \phi_i}{\partial y} \frac{\partial X(t)}{\partial t} \quad (21)$$

where X is the position of the interface in the stationary coordinate and y is a position coordinate relative to the moving interface (see figure 1), defined by

$$y = -x + X(t) \quad (22)$$

To solve equations (15) and equation (21), initial and boundary conditions are required.

#### *Initial conditions*

The initial conditions can be described as follows:

$$\phi_{ib}(y,0) = \phi_{ib}^0 \quad \text{for} \quad y > 0 \quad (23)$$

$$\phi_{ip}(m,0) = \phi_{ip}^0 \quad \text{for} \quad 0 \leq m \leq M \quad (24)$$

The subscript b and p refer to the bath and the polymer solution, respectively. M is the total volume of polymer per unit area of the casting solution.

#### *Boundary conditions*

The boundary conditions are:

$$\mu_{ib}(y=0,t) = \mu_{ip}(m=0,t) \quad i = 1,2 \quad (25)$$

$$J_{ib}(y=0,t) = J_{ip}(m=0,t) \quad i = 1,2 \quad (26)$$

$$\partial \phi_i / \partial m = 0 \quad \text{at} \quad m = M \quad i = 1,2 \quad (27)$$

The complete derivation of the presented equations can be found in literature [4]. With this set of equations, we are able to calculate the concentration profiles for a short time after the polymer solution has been brought into contact with the coagulation bath.

### 3-4-2. Calculation procedure

The numerical procedure used to generate the composition path for a very short time (e.g. 0.1 second) is as follows:

- 1). Choosing the interface compositions located on the binodal curve;
- 2). Calculating the composition profiles in the polymer solution;
- 3). Calculating the nonsolvent flux into the solution and the solvent flux out of the solution;
- 4). Using the fluxes obtained in step 3 to calculate the composition profiles in the coagulation bath;
- 5). Calculating the solvent flux into the bath and nonsolvent flux out of the bath;
- 6). Comparing the fluxes of step 5 and step 3;
- 7). Repeating the whole procedure by choosing a set of different interface compositions, until the fluxes of step 3 and step 5 are equal.

The final outputs of the calculations are the results of step 2, in which the compositions are presented as a function of the distance to the interface. The concentration profiles of the three components then can easily be generated by plotting the composition of each of the components against the film thickness.

### 3-4-3. Evaluation of friction coefficients for $H_2O$ -NMP-PES system

The friction coefficient  $R_{12}$  for water-NMP mixtures can be assumed to be constant [7]. Then  $R_{12}$  can be correlated to the mutual diffusion coefficient  $D(u_1=1)$  of infinitely diluted NMP in water by the following relation:

$$R_{12} = \frac{v_1 RT}{M_2 D(u_1=1)} \quad (28)$$

where  $v_1$  is the specific volume of water at temperature  $T$ .  $R$  is the universal gas constant.  $M_2$  is the molecular weight of NMP.  $D(u_1=1)$  was measured with the Taylor dispersion method [14,15], which resulted in  $D(u_1=1)=9.46 \times 10^{-10} \text{ m}^2/\text{s}$  at  $25^\circ\text{C}$ .

Since no literature data are available for the diffusivity of PES in NMP, the relation from Radovanovic [5] for the diffusivity of polysulfone in DMAC is used for the estimation of  $R_{23}$ :

$$\frac{v_3 RT}{M_2 R_{23}} = 18.0 * 10^{-9-4.386\phi_3} \quad (29)$$

It was described by Boom [7] that this relation approximately agrees with the experimental data on  $H_2O$ -NMP-PES system.

For  $R_{13}$ , we use the assumption made by Reuvers [2] that it is proportional to  $R_{23}$  in a relation described by equation (20).

### 3-5. CALCULATION OF THE PHASE DIAGRAM

#### 3-5-1. *The phase diagram calculated by Zeman and Tkacik [11]*

From a theoretical point of view, it must be noticed that cloud point curve and binodal curve coincide only when the polymer components are monodisperse [4]. The effect of the polydispersity of a polymer on phase equilibrium is most pronounced at low polymer concentrations near the critical point. The polymer we used as well as the one used in literature [11] are polydisperse, so the cloud point data would not represent the real binodal of the system. However, it has been shown by Reuvers [4] that at high polymer concentration the measured cloud point curve of a polydisperse polymer approaches the real binodal of the system, and furthermore it has been confirmed by different authors [8,13] that the calculated binodal at high polymer concentration hardly depends on the molecular weight of the polymer. Thus a cloud point curve can be used to approximate the binodal of the related system.

It is suggested by Zeman and Tkacik [11] that the use of interaction parameters of  $\chi_{12}=1.0$ ,  $\chi_{23}=0.5$  and  $\chi_{13}=1.5$  gives reasonably well theoretical predication of the binodal of the system  $H_2O$ -NMP-PES. The binodal calculated with this set of interaction parameters is shown in figure 2. This figure clearly shows that the agreement between the calculated binodal and measured cloud point data is rather good at relatively low polymer concentrations. However, at high concentrations, the calculated binodal differs significantly from the cloud point data. Even worse is that from cloud point data it can be deduced that with the increase of polymer concentration the water concentration at the cloud point decreases, the theoretical prediction, however, gives the opposite trend. This strongly indicates that the interaction parameters suggested by Zeman and Tkacik are not suitable to be used to describe the thermodynamic equilibrium properties of  $H_2O$ -NMP-PES system.

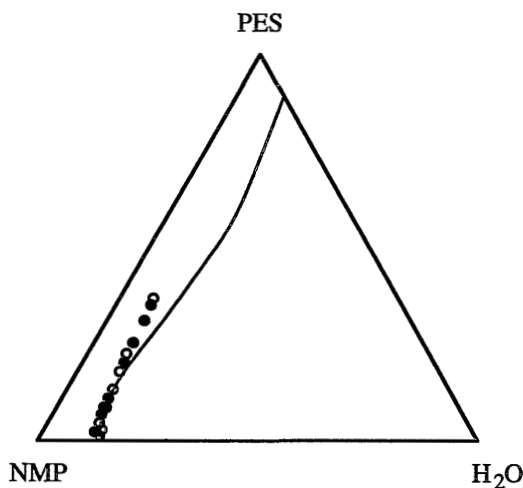


**Figure 2.** Comparison of measured cloud point data with the binodal calculated by Zeman and Tkacik [11]. (o) Cloud point data from literature [11]; (●) Cloud point data measured in this work [16]. Interaction parameters used for the binodal calculation are:  $\chi_{12}=1.0$ ,  $\chi_{23}=0.5$  and  $\chi_{13}=1.5$ .

### 3-5-2. Binodal calculated by using a ternary interaction parameter

As shown in figure 2 the set of interaction parameters suggested in literature [11] cannot be used to properly describe the thermodynamic equilibrium properties of the system H<sub>2</sub>O-NMP-PES. Therefore the originally measured binary interaction parameters were used to calculate the binodal of the system. Here  $\chi_{12}$  and  $\chi_{23}$  are concentration-dependent and  $\chi_{13}$  is constant, having a value of 1.60 or 2.73. However, the binodal calculated from these interaction parameters differs even more from the measured cloud point data. For a theoretical consideration, it was further attempted to see if it would be possible to fit the cloud point data with the Flory-Huggins theory simply by using one of the three interaction parameters as a fitting parameter and using measured data for the others. The best agreement with the cloud point data was obtained by choosing  $\chi_{23}$  as a fitting parameter while applying measured data for  $\chi_{12}$  and  $\chi_{13}$ , as shown in figure 3. The obtained fitting value for  $\chi_{23}$  is -1.3. Figure 3 clearly shows that although the calculated binodal fits the measured cloud point data very well, the calculated tie lines are not in agreement with the measured ones. It can therefore be concluded that an accurate prediction of the thermodynamic equilibrium properties of H<sub>2</sub>O-NMP-PES system with the Flory-Huggins theory is not possible, when only binary interaction parameters are used.

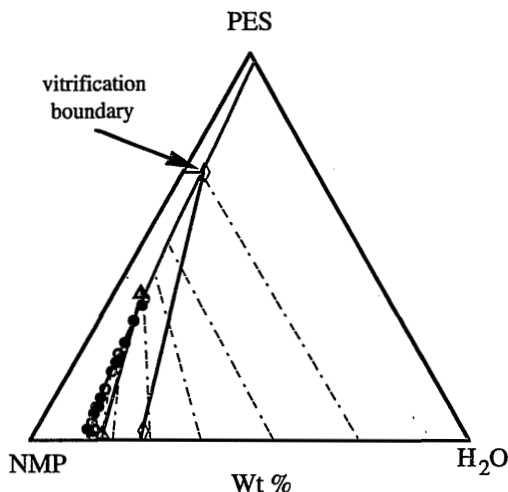


**Figure 3.** Comparison of calculated binodal and tie lines with experimental data. (o) Cloud point data from literature [11]; (●) Cloud point data measured in this work [16]; (Δ—Δ) Measured tie line from literature [11]; (◊—◊) Tie line measured in this work [16]. Dashed lines are calculated tie lines. Interaction parameters used for the binodal calculation:  $\chi_{12}=0.718+0.669 u_2$ ;  $\chi_{13}=2.73$ ;  $\chi_{23}=-1.3$ . The vitrification boundary was also measured in this work [16].

The above discussion indicates that the ternary interaction term cannot be neglected when the thermodynamic equilibrium properties of the system H<sub>2</sub>O-NMP-PES are described by the Flory-Huggins theory. To obtain the ternary interaction parameter ( $\chi_T$ ) of this system, a fitting procedure was used, in which experimental data on cloud point and tie lines were fitted by using binary interaction parameters obtained from the literature while treating  $\chi_T$  as a fitting parameter. The best fit is obtained by using a value of -0.69 for  $\chi_T$ . Figure 4 shows that in this case both the calculated binodal and tie lines agree very well with measured data. This agreement is the result of the fitting procedure where only the ternary interaction parameter  $\chi_T$  has been used as a fitting parameter. The physical meaning of  $\chi_T$  is not clearly defined by Pouchly [12] who used this parameter as a concentration-dependent fitting parameter to correlate the preferential sorption data of the system benzene-methanol-polymethylmethacrylate. In this stage, it is not clear why the ternary term has to be used to describe the system H<sub>2</sub>O-NMP-PES.

Altena [17] had attempted to obtain the ternary interaction parameter as a concentration-dependent parameter for a membrane forming system, H<sub>2</sub>O-dioxane-CA, by fitting osmotic pressure and preferential sorption data. It was found that  $\chi_T$  of the system was only slightly dependent on the concentration and the values were in the range of -0.3 to -0.5.

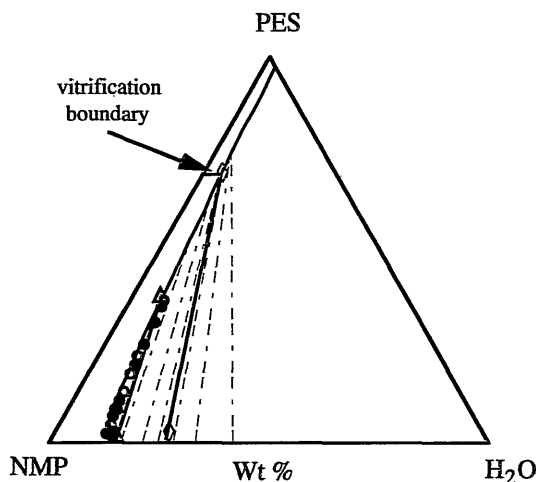


**Figure 4.** Comparison of calculated binodal and tie lines with experimental data. (o) Cloud point data from literature [11]; (●) Cloud point data measured in this work [16]; (Δ—Δ) Measured tie line from literature [11]; (◇—◇) Tie line measured in this work [16]. Dashed lines are calculated tie lines. Interaction parameters used for the binodal calculation:  $\chi_{12}=0.718+0.669 u_2$ ;  $\chi_{13}=2.73$ ;  $\chi_{23}=0.5$  and  $\chi_T=-0.69$ . The vitrification boundary was also measured in this work [16].

The good agreement between our calculated results and measured data implies that the used expressions for describing the thermodynamic equilibrium properties of the system H<sub>2</sub>O-NMP-PES give a very good approximation of reality.

### 3-5-3. The effect of variations of $\chi_T$ on equilibrium properties

The effect of varying the ternary interaction parameter  $\chi_T$  on the thermodynamic equilibrium properties of a ternary polymer solution is studied. For reasons of simplicity constant interaction parameters were used. At two different values of  $\chi_{13}$ , while keeping  $\chi_{12}$  and  $\chi_{23}$  constant, the effect of changing  $\chi_T$  can be seen in figure 5, diagram a) and b). At a higher value of  $\chi_{13}$ , the location of the binodal becomes less sensitive to the changing of  $\chi_T$ . This is similar to the observation of Altena [13] that the binodal hardly changes with changing  $\chi_{12}$  and  $\chi_{23}$  when  $\chi_{13}$  has a high value. A high value of  $\chi_{13}$  means a poor affinity between the nonsolvent and the polymer.

The effect of varying  $\chi_T$  is very drastic at a high value of  $\chi_{12}$ , as can be seen by comparing diagram a) and c) or by comparing diagram d) and e) in figure 5. This indicates that in case of a high value of  $\chi_{12}$  the ternary interaction term may not be neglected even when  $\chi_{13}$  is large, as shown in diagram f). One interesting observation is that the binodals approach each other at high polymer concentration for a high value of  $\chi_{12}$ .



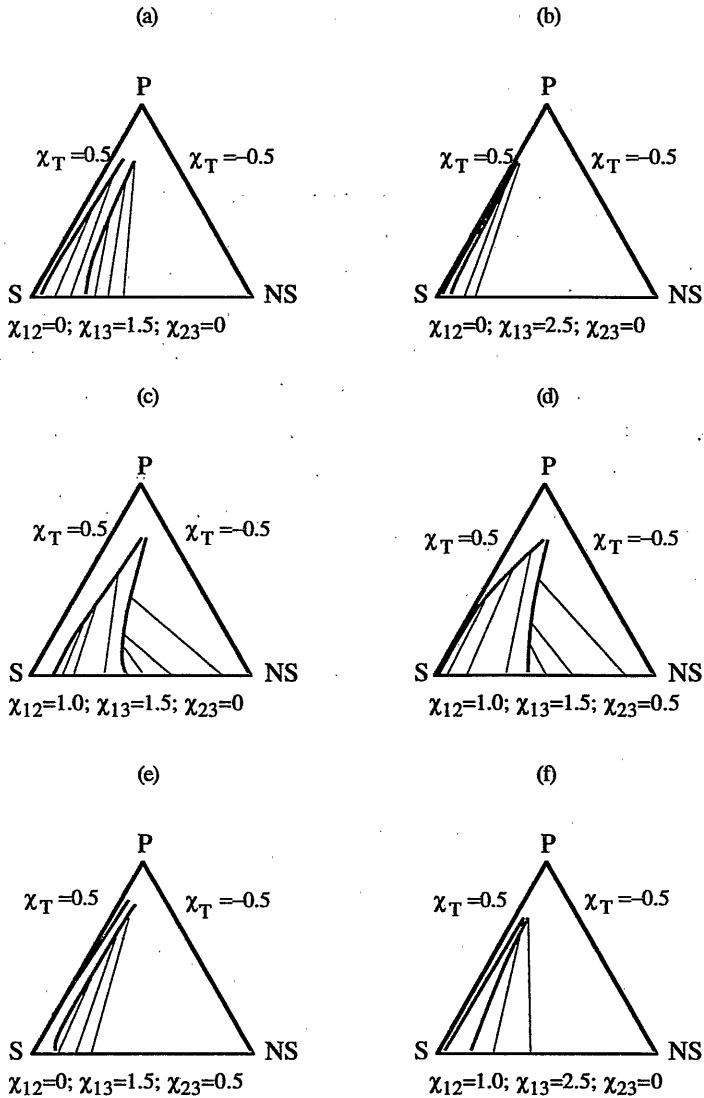


**Figure 5.** Schematic diagrams demonstrating the effect of varying the ternary interaction parameter  $\chi_T$  on the equilibrium properties of ternary polymer solutions.

It appears that the variation of the numerical value of the ternary interaction parameter has a similar effect on the calculated binodal as the binary interaction parameters  $\chi_{23}$  and  $\chi_{13}$ ; *i. e.*, a low value favours the mixing tendency of the related system, which can be concluded from figure 5. It also becomes apparent in figure 5 that at a lower value of  $\chi_T$  the tie lines are less steep. This means that to reach a high polymer concentration in the polymer rich phase after demixing, more nonsolvent is required in the solution.

According to the results presented in figure 5 and the results obtained by Altana [13], a general phenomenon can be observed that when the binodal is closer to the polymer-solvent axis, the related tie lines are steeper. Relating this general phenomenon with the gelation mechanism for membrane formation by immersion precipitation proposed in chapter 2, it can be concluded that when the amount of a nonsolvent required to induce liquid-liquid demixing in a polymer solution is small, characterized by a binodal close to the polymer-solvent axis, the amount of the nonsolvent required to induce vitrification after demixing is also small, reflected by the steep tie lines.

### 3-6. COMPOSITION PATH AFTER A VERY SHORT IMMERSION TIME

Previously, it has been discussed that the model presented by Reuvers for the description of mass transfer behaviour of membrane formation by immersion precipitation is valid only when the polymer solution can be considered as infinitely thick or to say it differently, when the compositions at the bottom side of the solution are unchanged. So, our calculations with this model were limited to a very short immersion time (*e.g.* 0.1 second).

#### 3-6-1. General meaning of a composition path

The concentration profiles generated by solving the diffusion equations can give information about the concentration distribution along the film as a function of time, which is important for understanding the structure formation of the membrane. However, such type of concentration profiles gives no information concerning whether liquid-liquid demixing will start in the solution. Therefore, the compositions of the solution along the film thickness at a certain time are plotted in a ternary phase diagram. In this way, a so called composition path can be obtained and it is easy to see whether the binodal of the system is crossed by the composition path or not.

For the reason of easy understanding the physical meaning of a composition path calculated from Reuvers' model, two important assumptions made in the model are summarized as follows:

- Liquid-liquid demixing takes place by means of nucleation and growth. The demixing will occur immediately after the composition path enters the binodal (metastable) region. This assumption was experimentally shown to be valid for the system CA-acetone-H<sub>2</sub>O by Reuvers [2].
- Thermodynamic equilibrium is established instantaneously at the interface after immersion, which means that all initial composition paths (related to

an infinitely short time) will connect the point of the initial composition with a point on the binodal in a ternary phase diagram.

With these assumptions it then can be understood that a composition path calculated by the model represents the succession of compositions from the bottom of the solution (the point of the initial composition) to the interface (the point on the binodal) at a fixed moment. For an infinitely thick film the composition path also represents the succession of compositions in the solution from the initial composition to the composition for  $t \rightarrow \infty$  at a fixed position in the film.

### ***3-6-2. Composition path for H<sub>2</sub>O-NMP-PES system***

The calculated "initial" composition path for the system H<sub>2</sub>O-NMP-PES at 25 °C is shown in figure 6. The initial polymer concentration of the solution is chosen to be 26 wt %. It is shown in this figure that the composition path (related to an immersion time of 0.1 second in a pure water bath) crosses the binodal rapidly, which means that instantaneous demixing will occur for this system. This has been found experimentally by Boom [7].

In figure 6, the vitrification boundary of the system (see chapter 2) is indicated as well. The calculation of the composition path results in a polymer concentration at the interface, between the polymer solution and the coagulation bath, above the vitrification boundary. This means that the skin formation of the membrane being formed is affected both by liquid-liquid demixing and by vitrification simultaneously. This might be an indication for the formation of nodular structure [18, 19], which will be discussed in the next section.

Calculations were also carried out to see whether the calculated minimum NMP concentration in the water bath necessary to induce delayed demixing would be in accordance with experimental findings. It was measured by Boom [7] that for a solution of 20 wt % PES in NMP, delayed demixing occurs when the NMP concentration in the water bath is in the range of 65–75 wt %. Our calculations showed, however, that the minimum NMP concentration is 53 wt %. The discrepancy between the experimental data and the calculated one is believed to be caused by the lack of accurate friction coefficient data for PES-NMP and PES-H<sub>2</sub>O systems.

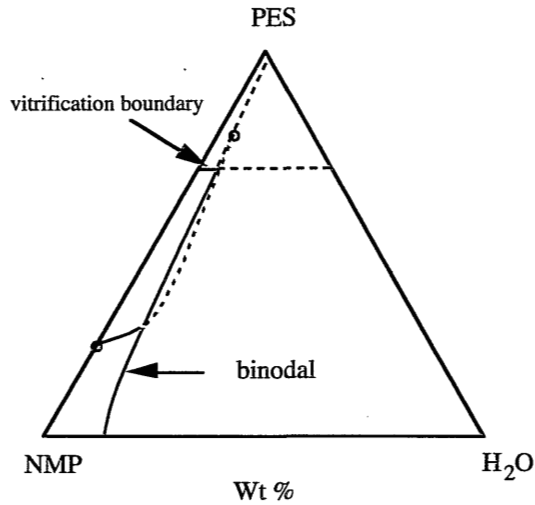


**Figure 6.** The calculated composition path for a solution of 26 wt % PES in NMP immersed in a water bath. The two circles represent the initial composition and the composition reached at the interface. Interaction parameters used for the calculation:  $\chi_{12}=0.718+0.669 u_2$ ;  $\chi_{13}=2.73$ ;  $\chi_{23}=0.5$  and  $\chi_1=-0.69$ .

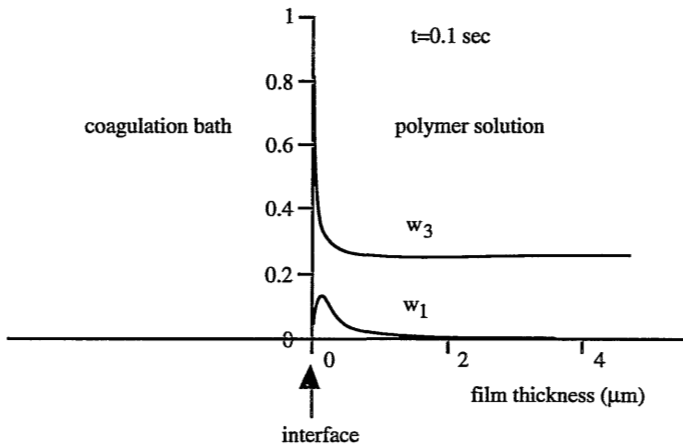


**Figure 7.** Calculated concentration profiles in the solution of 26 wt % PES in NMP immersed in a pure water bath. Only concentration profiles in the film side are presented. The initial film thickness is  $100\mu\text{m}$ .

The concentration profiles related to the composition path presented in figure 6 are shown in figure 7. It can be seen that the polymer concentration gradient near the interface is extremely high. Experiments [7] showed that membranes formed from this system normally exhibit an asymmetric structure consisting of a dense skin supported by a porous sublayer. Figure 7 gives the reason for the formation of the asymmetric

structure. It is also shown that in the region close to the interface water diffuses against its concentration gradient due to the chemical potential driving force. For the situation described in figure 6 and figure 7, the calculated diffusion rate of NMP out off the solution is about three times higher than the diffusion rate of water into the solution.

The composition path for this system is also calculated by using the set of interaction parameters suggested by Zeman and Tkacik [11] to describe the thermodynamic properties of the system. The results are presented in figure 8. Here we can see that the composition path does not enter the liquid-liquid demixing region, indicating a delayed demixing, which is in contradiction with the experimental observations. Therefore we can conclude that the set of interaction parameters suggested in literature [11] cannot be used to properly describe the thermodynamic properties of the system H<sub>2</sub>O-NMP-PES. It should be mentioned here that the interaction parameters are used not only for the calculation of the binodal but also for the calculation of the chemical potential driving force in the diffusion equations.

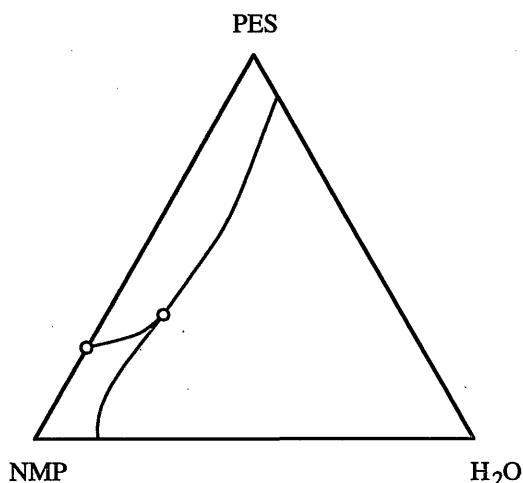


**Figure 8.** *The calculated composition path for a solution of 26 wt % PES in NMP immersed in a water bath by using the interaction parameters suggested in literature [11].*

### 3-6-3. A hypothesis for the formation of nodular structure

In literature, the mechanism for the formation of nodular structure in asymmetric membranes formed by immersion precipitation is not yet understood. A literature review about nodular structure formation is published by Wienk [18]. In this section we propose a hypothesis about nodular structure formation for the system H<sub>2</sub>O-NMP-PES based on the calculated composition path of this system as presented in the previous section.

It is shown in figure 6 that after immersion of a polymer solution, near the interface both liquid-liquid demixing and vitrification take place instantaneously. It has to be emphasised that the vitrification composition is reached from the interior side of the binodal, as shown in figure 6.

For liquid-liquid demixing to take place by means of nucleation and growth, the concentration fluctuation in the solution must be high enough to overcome the surface energy barrier for the creation of a new phase (nucleation) [7,20]. In the polymer concentration range for membrane formation, the formed stable nuclei must be composed of the polymer lean phase. So if nucleation would occur, characterized by the formation of stable nuclei, in the region close to the interface isolated pores should be expected because of the high polymer concentration. Apparently nucleation itself cannot be used to explain the formation of nodular structure.

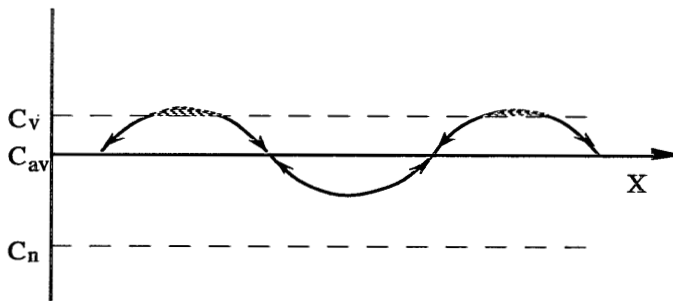


**Figure 9.** Schematic demonstration of polymer concentration fluctuation in the metastable region interfered by vitrification.  $C_v$  is the assumed vitrification composition and  $C_{av}$  is the average composition of the solution.  $C_n$  denotes the composition of a critical nucleus (the smallest stable nucleus). The small arrows indicate the potential diffusion direction of the polymer during concentration fluctuation. The shadowed area represent the "frozen" polymers.  $X$  is a space coordinate

It is expected that in the metastable region the concentration fluctuation will be much higher than in the stable region. Our hypothesis for nodular structure formation is demonstrated schematically in figure 9. In the region inside the binodal and close to the intersection point (Berghmans point) of the binodal and the vitrification boundary, it is very much possible that before the completion of nucleation of the polymer lean phase, locally the polymer concentration has reached the vitrification composition due to the pronounced concentration fluctuation. So the solution "freezes" at the early stage of nucleation and nucleation will not be able to complete. The "frozen islands" will form nodules and in between those nodules pores with sizes smaller than the critical size of a stable nucleus will be created as a result of incomplete nucleation of the polymer lean phase. Because of the incomplete nucleation, the polymer lean locations are

interconnected, which results in a structure similar to a structure formed by spinodal demixing.

### 3-7. SIMULATING THE KINETIC EFFECT ON MEMBRANE FORMATION

With the change of one component in a ternary membrane forming system, both thermodynamic and kinetic parameters of the system will change and consequently the properties of the resulting membrane may vary significantly. In literature, studies [3,8, 13] concerning the thermodynamic effects on membrane formation have been carried out. In this section we will only examine the specific influence of the kinetic parameters on the initial membrane formation process by means of model calculations. For the thermodynamic parameters the data for the system H<sub>2</sub>O-NMP-PES will be used.

To examine the effects of independent changes in the three friction coefficients on the initial membrane formation process, we use the three friction coefficients for the system H<sub>2</sub>O-NMP-PES as reference, which are denoted as  $R_{12}^0$ ,  $R_{13}^0$  and  $R_{23}^0$ , respectively.

In figure 10, the model calculation results are presented. In this figure the dashed curves and the thin curves represent the binodal and the composition path for the reference system (H<sub>2</sub>O-NMP-PES), respectively. The thick curves are calculated composition paths by using different sets of friction coefficients as indexed in the figure.

From diagram a) and diagram b) of figure 10, it can be seen that an increase of the friction coefficient of  $R_{12}$  or  $R_{13}$  will increase the tendency toward delayed demixing. Its physical background is not difficult to understand. When  $R_{12}$  and  $R_{13}$  are high, the diffusion of nonsolvent into the polymer solution will be slow, which will favor delayed demixing to occur. In general, it can be expected that a nonsolvent with a high viscosity as well as a large molecular size will intend to induce delayed demixing in a polymer solution.

Delayed demixing will clearly occur, however, when  $R_{23}$  is low, as shown in diagram c) of figure 10, which means a high diffusivity of solvent in the polymer solution favors delayed demixing. Its physical meaning is not clear at this stage, but in practice this behaviour could be observed. A close examination of the literature data [4] on the systems H<sub>2</sub>O-acetone-CA and H<sub>2</sub>O-dioxane-CA shows that the thermodynamic parameters of those two systems are very similar and characterized by nearly the same binodals [4]. Also, the friction coefficient for acetone-water is about the same as for dioxane-water [4]. However, the friction coefficient for acetone-CA is about six times lower than that for dioxane-CA and indeed delayed demixing was observed for the

system H<sub>2</sub>O-acetone-CA and instantaneous demixing for the system H<sub>2</sub>O-dioxane-CA [4].

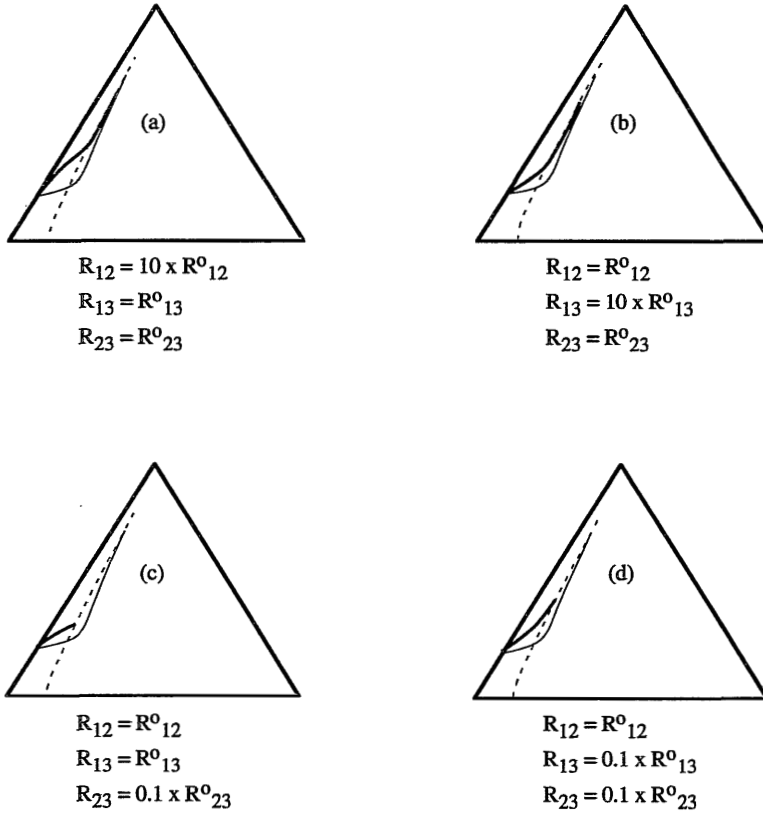


**Figure 10.** Schematic illustrations of the effects of changing friction coefficients on membrane formation.  $R_{ij}^0$  are the friction coefficients for the system H<sub>2</sub>O-NMP-PES. Dashed curves and thin curves represent the binodal and initial composition path for the system H<sub>2</sub>O-NMP-PES. Thick curves are calculated initial composition paths from the indexed sets of friction coefficients.

In the model derived by Reuvers [2], it was assumed that  $R_{13}$  is proportional to  $R_{23}$ . By taking this assumption, model calculations to evaluate the effect of changing  $R_{23}$  were also performed. Diagram d) of figure 10 gives the results. It can be seen that the results are similar to that presented in diagram c) of the same figure.

The polymer concentration profiles related to the composition paths of figure 10 are presented in figure 11. As can be seen in this figure the polymer concentration profile of a system showing delayed demixing is smoother than that of a system showing instantaneous demixing. It is also shown in this figure that the interfacial



polymer concentration reached at the very early moment after immersion is lower in a delayed demixing process than in an instantaneous demixing process. The same phenomenon was observed by Reuvers [4] in studying the effects of changing interaction parameters on membrane formation.

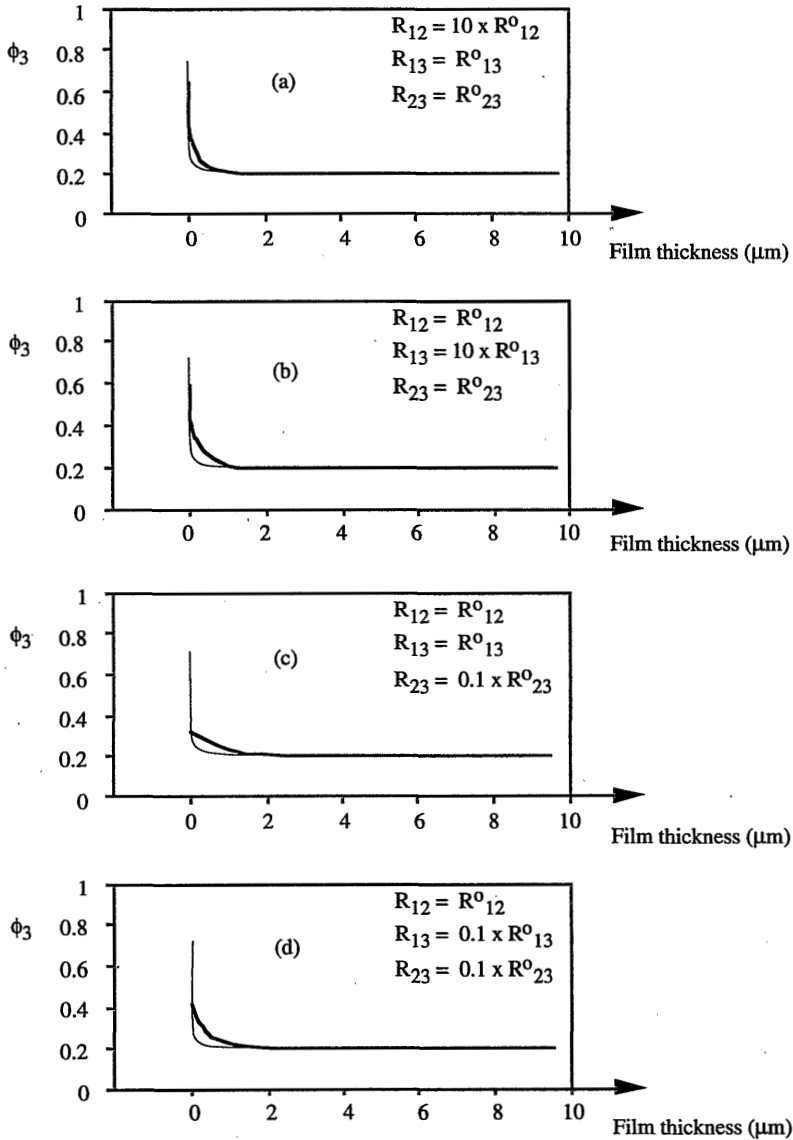


**Figure 11.** Polymer concentration profiles related to the composition paths shown in figure 10. Thin curves are calculated polymer concentration profile for  $\text{H}_2\text{O-NMP-PES}$  system. Thick curves are calculated polymer concentration profiles by using the indexed sets of friction coefficients.  $R_{ij}^0$  are the friction coefficients for  $\text{H}_2\text{O-NMP-PES}$  system.

### 3-8. CONCLUSIONS

It has been shown that in order to properly describe the thermodynamic equilibrium properties of the system H<sub>2</sub>O-NMP-PES, a ternary interaction parameter has to be used. By fitting measured cloud point data and measured tie lines, the ternary interaction parameter for H<sub>2</sub>O-NMP-PES system has been obtained to be -0.69, while literature data for the three binary interaction parameters are applied.

Model calculations showed that a ternary interaction parameter has the same physical meaning as a binary interaction parameter, which means that a low value favors the mixing tendency of the system.

With the mass transfer model derived by Reuvers for membrane formation by immersion precipitation, composition paths and concentration profiles at the very early moment of immersion have been calculated for the system H<sub>2</sub>O-NMP-PES. These calculations showed that both liquid-liquid demixing and vitrification may take place instantaneously in this system.

Based on model calculations for the system H<sub>2</sub>O-NMP-PES, a hypothesis for nodular structure formation in the top layer of asymmetric membranes is proposed. Local vitrification of the polymer solution induced by concentration fluctuation in the region inside the binodal and close to Berghmans point is probably responsible for the formation of nodular structure.

The effects of independent changes of friction coefficients on the initial membrane formation process were simulated. It is shown that increasing values of friction coefficients  $R_{12}$  and  $R_{13}$  promote the tendency towards delayed demixing, whereas an increasing value of  $R_{23}$  has the opposite effect.

### 3-9. LIST OF SYMBOLS

|               |  |
|---------------|--|
| $\phi_i$      | volume fraction of component i                                     |
| $\phi_{ib}$   | volume fraction of component i in the coagulation bath             |
| $\phi_{ib}^0$ | initial volume fraction of component i in the coagulation bath     |
| $\phi_{ip}$   | volume fraction of component i in the polymer solution             |
| $\phi_{ip}^0$ | initial volume fraction of component i in the polymer solution     |
| $\omega_3$    | $\phi_3/(\phi_2+\phi_3)$   |
| $\mu_i$       | chemical potential of component i (J/mole)                         |
| $\mu_{ib}$    | chemical potential of component i in the coagulation bath (J/mole) |
| $\mu_{ip}$    | chemical potential of component i in the polymer solution (J/mole) |
| $\chi_{ij}$   | Flory-Huggins interaction parameters                               |
| $\chi_T$      | ternary interaction parameter                                      |
| $\rho$        | solution density (kg/m <sup>3</sup> )                              |

|               |  |
|---------------|--|
| $c_i$         | concentration of component i ( $\text{kg}/\text{m}^3$ )  |
| $J_i$         | volume flux of component i relative to the polymer fixed frame of reference ( $\text{m}^3/\text{m}^2 \text{ s}$ )    |
| $\tilde{J}_i$ | volume flux of component i relative to the laboratory fixed frame of reference ( $\text{m}^3/\text{m}^2 \text{ s}$ ) |
| $L_{ij}$      | phenomenological coefficient between component i and j   |
| $m$           | spatial coordinate corrected for movement of the interface (m)   |
| $M$           | total volume of polymer per unit area of polymer film (m)  |
| $M_i$         | molecular weight of component i ( $\text{g}/\text{mole}$ )   |
| $r$           | $v_1 M_1 / (v_3 M_3)$  |
| $s$           | $v_1 M_1 / (v_2 M_2)$  |
| $R_{ij}$      | friction coefficient between component i and j   |
| $t$           | time (s)   |
| $u_1$         | $\phi_1 / (\phi_1 + \phi_2)$   |
| $u_2$         | $1 - u_1$  |
| $v_i$         | velocity of component i relative to the laboratory fixed frame of reference (m/s)                                    |
| $v_i$         | specific volume of component i ( $\text{m}^3/\text{kg}$ )  |
| $w_i$         | weight fraction of component i   |
| $x$           | spatial coordinate in the polymer solution (m)   |
| $X(t)$        | distance between the interface on t and the interface on $t = 0$ (m)   |
| $y$           | spatial coordinate in the coagulation bath (m)   |

### 3-10. REFERENCES

1. Cohen, C.; Tanny, G. B. and Prager, S., *J. Polym. Sci., Polym Phys. Ed.* 17, 477 (1979)
2. Reuvers, A. J.; Van den Berg, J. W. A. and Smolders, C. A., *J. Membr. Sci.* 34, 45 (1987)
3. Reuvers, A. J. and Smolders, C. A., *J. Membr. Sci.* 34, 67 (1987)
4. Reuvers, A. J., *PhD Thesis*, University of Twente, the Netherlands, 1987
5. Radovanovic, P.; Thiel, S. W. and Hwang, S.-T., *J. Membr. Sci.* 65, 213 (1992)
6. Radovanovic, P.; Thiel, S. W. and Hwang, S.-T., *J. Membr. Sci.* 65, 231 (1992)
7. Boom, R. M., *PhD Thesis*, University of Twente, the Netherlands, 1992
8. Tsay, C. S. and McHugh, A. J., *J. Polym. Sci., Polym Phys. Ed.* 28, 1327 (1990)
9. Tsay, C. S. and McHugh, A. J., *J. Polym. Sci., Polym Phys. Ed.* 29, 1261 (1991)
10. Tsay, C. S. and McHugh, A. J., *Chem. Eng. Sci.* 46, 1179 (1991)
11. Zeman, L. and Tkacik, G., *J. Membr. Sci.* 36, 119 (1988)
12. Pouchly, J.; Zivney, A. and Solc, K., *J. Polym. Sci. Polym. Symp.* 23, 245 (1968)
13. Altena, F. W. and Smolders, C. A., *Macromolecules*, 15, 1491 (1982)
14. Taylor, F. R. S., *Proc. Roy. Soc.* A219, 186 (1953)
15. Taylor, F. R. S., *Proc. Roy. Soc.* A225, 473 (1954)

16. Chapter 2 of this thesis
17. Altena, F. W., *PhD Thesis*, University of Twente, the Netherlands, 1982
18. Wienk, I. M., *PhD Thesis*, University of Twente, the Netherlands, 1993
19. Chapter 5 of this thesis
20. Zettlemoyer, A. C., *Nucleation*, Marcel Dekker, New York, 1969

---

CHAPTER 4

---

**PREPARATION OF HOLLOW FIBER MEMBRANES BY A  
MODIFIED DUAL BATH SPINNING PROCESS**

---

S.-G. Li, I.G.M. Pünt, H.M.M. Rolevink, Th. van den Boomgaard,  
C.A. Smolders, H. Strathmann

**4-1. ABSTRACT**

The dual bath process as developed by Van't Hof has been modified by the use of a triple orifice spinneret. The modification simplified the spinning process and improved the ability to control the contact time between the polymer solution and the first coagulant. This is critical for obtaining a fiber with a thin skin. Furthermore, with the use of the triple orifice spinneret the amount of first coagulant required for the spinning process was drastically reduced, which makes the modified dual bath process economically and technically more feasible as well as environmentally acceptable. With the modified dual bath spinning process, hollow fiber spinning could be performed as simple as with a traditional single bath spinning process, and adding more flexibilities for the development of new membranes. With this method hollow fibers having a skin thickness of about 0.3  $\mu\text{m}$  could be obtained. The skin is defect-free making a coating step unnecessary.

In this study, the effects of using different types of nonsolvents as the first coagulant on the properties of the resulting fibers were investigated. For the choice of the first coagulant it was found that delayed demixing was a necessary condition in order to obtain a highly gas selective fiber. However, delayed demixing did not necessarily result in a fiber with gas separation properties. Based on the solubility parameter concept an empirical rule concerning the choice of first coagulant for the spinning of hollow fibers for gas separation was obtained.

The type of solvent was shown to have a significant influence on the properties of the resulting fibers. For a given first coagulant, the fluxes of hollow fibers changed with the change of the solvent in the order of NMP > DMAC > DMSO. It seems that the experimental observations are related to the vitrification phenomenon as well as to the concentration profiles of the related systems as created in the first bath.

## 4-2. INTRODUCTION

In 1988, Van't Hof [1] developed a dual bath process for the spinning of integrally skinned hollow fibers for gas separation based on Reuvers model [2,3,4]. With this dual bath process, gas separation hollow fibers showing the intrinsic properties of the membrane forming polymer could be readily obtained without the necessity of coating. In this process [1,5] hollow fibers were spun by contacting the spinning solution with two coagulants successively. First, the polymer solution was brought into contact with a nonsolvent (the so called first coagulant). This nonsolvent has a relatively poor interaction with the solvent. By contacting the first coagulant with the polymer solution for a short time a thin layer of high polymer concentration at the interface can be formed while the rest of the solution remains unchanged. When such a solution with a highly anisotropic concentration distribution is then brought into contact with a second nonsolvent which shows a strong interaction with the solvent, instantaneous demixing occurs. Because of the polymer concentration distribution of the solution created in the first bath, a membrane with a gas tight skin and an open support layer can be obtained after immersion into the second bath.

Although the dual bath process could be used to prepare hollow fiber membranes showing high selectivity in gas separation, the flux was too low. Therefore this has to be improved in order to meet the requirements of both high selectivity and high flux for an industrially acceptable membrane. Furthermore, it was shown by Van't Hof [5] that the formation of macrovoids in the support layer of hollow fibers made by the dual bath process was quite significant. To improve the mechanical strength of the membrane it is necessary to eliminate the formation of such macrovoids in the support layer

Unlike ultrafiltration and microfiltration membranes whose fluxes are normally improved by increasing the porosity (mainly by increasing the amount of pores instead of the size of the pores) of the skin, for a gas separation membrane the improvement of the flux has to be done by reducing the skin thickness and/or by minimizing the resistance of the support layer. According to the resistance model proposed by Henis and Tripodi [6] it can be shown that if the resistance of the support layer of a membrane is not negligible compared to the resistance of the skin, the membrane does not possess the intrinsic selectivity of the polymer material used for preparing the membrane. It has been shown by Van't Hof [1,5] that fibers made by the dual bath process showed the intrinsic selectivity of the polymer material. This indicates that the resistance of the support layer of the fibers was negligible compared to the resistance of the skin. Therefore, to improve the flux of gas separation hollow fibers made by the dual bath process, attention has to be paid to the reduction of the skin thickness while maintaining a highly permeable support layer.

In order to reduce the skin thickness of an asymmetric membrane, in principle, fast precipitation of the polymer solution is demanding. According to the model of Reuvers [2,3,4], fast precipitation of a polymer solution can be achieved in different ways. The addition of a nonsolvent into the polymer solution and/or the use of a coagulant interacting strongly with the solvent are the most effective ways. However, a method which favours fast precipitation is, in general, unfavourable for the formation of a dense skin. This is why the dual bath process has been developed. So, the general rules of reducing the skin thickness of a membrane may not be followed strictly as the dual bath process is concerned. Van't Hof [1,5] proposed that it is most important to minimize the contact time between the first coagulant and the polymer solution in order to reduce the skin thickness of a fiber made by the dual bath process. However, in the way Van't Hof [1,5] applied the dual bath technique, he was unable to control the contact time adequately. Therefore a modification of the dual bath process has been developed in our laboratory which makes use of a triple orifice spinneret [7,8].

With the use of the triple orifice spinneret, the dual bath spinning process can be performed as simple as with the traditional single bath wet spinning process, but it adds more flexibilities to the process which is favourable for the development of new membranes.

In this chapter, the effect of controlling the contact time on the properties of the fibers is studied. The influences of using different first coagulants and solvents are also investigated. The delayed demixing phenomenon in relation to membrane formation by the dual bath process is described based on established membrane formation models [2, 9]. An empirical rule concerning the choice of the first coagulant is given. The study on macrovoid formation in the dual bath spinning process will be presented in the next chapter.

### 4-3. THEORY

It was observed by Reuvers [2,3] that during membrane formation by immersion precipitation liquid-liquid demixing process in polymer solutions may take place in two different ways. One is delayed demixing and the another is instantaneous demixing.

Delayed demixing occurs under two different conditions. One is that delayed demixing will occur when the polymer solution is immersed into a 'mild' coagulation bath containing high amounts of solvent. In this case, membranes with a porous skin and closed cell structure in the sublayer will be formed. The mechanism for the formation of the porous skin could be explained by Reuvers diffusion model [2,5]. According to the model calculations [2,3], it was shown that the polymer concentration at the top surface of the polymer solution is very low when demixing takes place. Delayed demixing may also be observed when the nonsolvent shows a poor affinity to

the solvent. In the latter case, model calculations showed that during the delay time the diffusion of solvent out of the solution is much faster than the diffusion of nonsolvent into the solution. The result of the difference in the diffusion rates is the increase of polymer concentration at the interface. The thickness of this layer of high polymer concentration increases proportional to the square root of time while the composition of this layer remains constant as long as the polymer solution can be considered as infinitely thick. It could be expected that when the solution can no longer be treated as infinitely thick the polymer concentration at the top surface will increase further with time. Before demixing starts to occur, the polymer concentration at the top surface may reach such a high value that this concentrated polymer layer vitrifies. It has actually been observed [10] that for a certain system liquid-liquid demixing may even not be able to take place at all and a vitrified transparent film could be obtained.

The net loss of liquid in the latter type of delayed demixing process will lead to a decrease in thickness of the polymer solution layer and in its turn to raise the polymer concentration in the solution beneath the top layer, which will cause the formation of closed cell structure in the support layer of the ultimate membrane. In general, membranes formed with a nonsolvent as the coagulant that shows a poor affinity to the solvent exhibit a gas selective skin and in combination a support layer with high resistance to mass transport.

Instantaneous demixing will take place in a polymer solution when the coagulant shows a strong interaction with the solvent. In this case the difference in the rate of solvent outflow and nonsolvent inflow becomes relatively small, and consequently a membrane with a thin skin and a highly permeable support layer will be formed. However, the skin of this type of membrane generally contains small pores, which results in a very low gas selectivity of the membrane. Macrovoids are often observed in the support layer of this type of membranes too.

It is noticed that instantaneous demixing can also take place in a polymer solution even when the coagulant shows a poor affinity to the solvent when a high amount of nonsolvent is present in the polymer solution. Apparently, in this case a membrane with a support layer of high resistance to mass transport is expected.

The dual bath process developed by Van't Hof [1,5] is actually using the combination of the two different membrane formation processes, raising the polymer concentration at the top surface by a delayed demixing process rapidly followed by an instantaneous demixing process to create a thin but very dense skin as well as a highly permeable support layer.

Modification of the dual bath process by applying a triple orifice spinneret [7,8] simplifies the spinning process. More important is that the use of the triple orifice



spinneret enhances our ability to control a short contact time between the first coagulant and the polymer solution. A short contact time is critical for obtaining a thin skin.

#### 4-4. EXPERIMENTAL

##### 4-4-1. Materials

Polyethersulfone (PES, VICTREX® 5200P from ICI) was used as the polymer material for the preparation of gas separation hollow fibers. Before use the polymer was dried at 150 °C under vacuum over night. Water-free glycerol (from Merck) was used as the additive in the spinning solutions. The other solvents and nonsolvents were synthesis grade, purchased from Merck and used without further treatment.

##### 4-4-2. Cloud point and delay time measurements

Cloud point data of ternary polymer solutions were determined by titration as being described in chapter 2.

Delay time measurements were performed in a similar procedure as being shown in literature [3].

##### 4-4-3. Measurements of the temperature change due to mixing

To have an indication of the affinity between NMP and a nonsolvent, the temperature change due to the mixing of NMP with the nonsolvent was measured. The device shown in figure 1 was used. The experiments were performed by adding NMP into a well stirred nonsolvent solution contained in a Dewar vessel. The temperature change was recorded as the temperature difference between the temperature before the addition of NMP and the highest temperature after the addition of NMP. The total

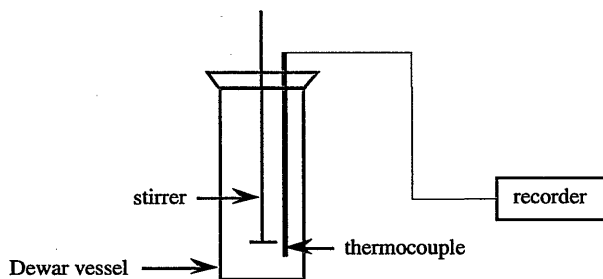


**Figure 1.** Apparatus used to measure the temperature change of mixing NMP with different nonsolvents.

weight of NMP and the nonsolvent for each measurement was kept constant at 350 grams, with a molar ratio of 1:1. It was noticed that the temperature increase due to stirring could be neglected under our experimental conditions. Before each measurement, the nonsolvent and NMP were kept at the same temperature. The temperature change due to mixing could be measured in an accuracy of 0.01 °C.

#### 4-4-4. Spinning of hollow fibers

The spinning solutions were prepared by adding the polymer to a well stirred NMP/glycerol mixture or a pure solvent at a temperature of 60-80 °C. After the polymer was dissolved the solution was filtered over a 25 µm stainless steel filter and degassed at the ultimate spinning temperature overnight.

The spinning process was performed with the aid of a triple orifice spinneret (see figure 2). During the spinning the first coagulant (nonsolvent) was pumped through the outer orifice of the spinneret; the polymer solution and the bore liquid were pumped through the other two orifices, with the bore liquid in the inner orifice. Various nonsolvents were used as first coagulant, and water or mixtures with NMP were used as bore liquid. Water was always used in the second bath. The spinning speed was kept at 7 m/min.

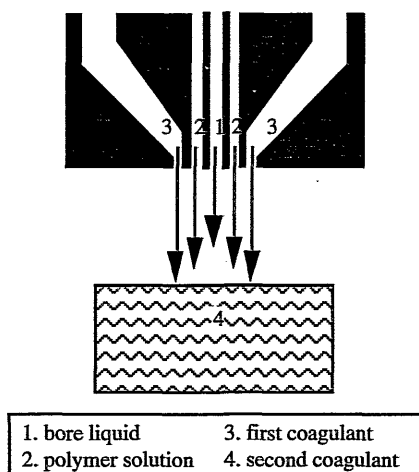


**Figure 2.** Schematic representation of the triple orifice spinneret with coagulation bath.

In general, the obtained fibers were dried with a liquid exchange method [11]. First, the fibers were rinsed with running water for two days, then immersed into ethanol for one day followed by immersion in a hexane bath for another day before

drying in air at room temperature. When other drying methods are applied, they will be specified.

#### **4-4-5. Fiber characterization**

Gas separation characteristics were measured with a permeation set-up described by Van't Hof [1]. A test module was composed of three fibers with a known length between 10 to 14 cm. For each type of fiber, at least three modules were made and were measured with a feed gas of 25 vol-% CO<sub>2</sub> in CH<sub>4</sub> at a pressure of 8 bars and a temperature of 22-24 °C. Before each measurement the time for conditioning of the fibers was at least 30 minutes.

The structures of the fibers were examined with a scanning electron microscopy (SEM). Samples for SEM examination were made by cryogenic breaking of the fibers. The broken samples were dried under vacuum and coated with a thin gold layer by means of sputtering. A JEOL JSM-T 220A Scanning Microscope was used.

The concentration units used in this chapter is weight fraction. The fluxes of the fibers are in units of 10<sup>-6</sup> cm<sup>3</sup>/cm<sup>2</sup> s cmHg, denoted as GPU (Gas Permeation Unit).

## **4-5. RESULTS AND DISCUSSION**

### **4-5-1. Choice of first coagulant**

It was proposed by Van't Hof [1,5] that the first coagulant should be able to induce delayed demixing in the polymer solution to obtain a gas separation fiber. The delay times for a polymer solution of 30 % PES, 10 % glycerol (a nonsolvent for PES) in NMP, immersed in various nonsolvents are presented in table 1. The molar volumes and the viscosities of the nonsolvents are also listed in this table. Except for 1-butanol and 1-pentanol the other nonsolvents are completely miscible with water. The addition of glycerol into the polymer solution is due to the viscosity requirement for spinning as well as for easy phase separation.

According to the estimations made by Van't Hof [1,5] for the diffusion coefficients of NMP in various nonsolvents, in general the diffusion coefficients are lower in high molecular weight alcohols than in low molecular weight alcohols. From the model calculations presented in chapter 3 of this thesis, it is shown that when the diffusivity of the solvent in the nonsolvent bath is low or the diffusivity of the nonsolvent in the polymer solution is low, delayed demixing may take place.

From table 1 as well as from the results presented by Van't Hof [5], it can be seen that water, acetone, THF, organic acids and small alcohol molecules give instantaneous

demixing while ethers and alcohols with large molar volume as well as high viscosity intend to induce delayed demixing. It was observed in literature [5] that for a polymer solution of 35 % PES and 10 % glycerol in NMP immersed in methanol, ethanol, 1-butanol, 1-pentanol and 1-octanol, respectively, the delay time of demixing increased following the size sequence of the alcohols. A similar phenomenon could also be found in table 1 by comparing the delay times of diethylene glycol, triethylene glycol and tetraethylene glycol.

**Table 1** Delay times for a polymer solution of 30 % PES and 10 % glycerol in NMP, immersed in various nonsolvents, together with the molar volumes and viscosities (at 20°C) of the nonsolvents, as well as the temperature changes occurring when mixing NMP with the nonsolvents.

| nonsolvent                     | molar volume<br>(cm <sup>3</sup> /mol) | viscosity<br>(cPoise) | $\Delta T_{\text{mix}}$<br>(°C) | delay time<br>(min) |
|--------------------------------|--|-----------------------|---------------------------------|---------------------|
| water                          | 18.1                                   | 0.998                 | 15.4                            | 0                   |
| acetic acid                    | 57.1                                   | 1.314 <sup>c</sup>    | —                               | 0                   |
| propionic acid                 | 75.0                                   | 1.175 <sup>c</sup>    | 17.35                           | 0                   |
| butyric acid                   | 110.0                                  | 1.814 <sup>c</sup>    | —                               | 0                   |
| methanol                       | 40.7                                   | 0.595                 | —                               | 0                   |
| ethanol                        | 58.5                                   | 1.117                 | -0.06                           | 0                   |
| 1-propanol                     | 74.8                                   | 2.26                  | -0.55                           | —                   |
| 1,2-propanediol                | 73.6                                   | 56.0                  | 2.53                            | 0                   |
| 1,4-butanediol                 | 84.3                                   | 88.8                  | 2.73                            | 0                   |
| ethylene glycol                | 55.8                                   | 25.66 <sup>d</sup>    | 4.68                            | 0                   |
| diethylene glycol              | 95.3                                   | 35.7                  | 3.29                            | 0                   |
| acetone                        | 74.0                                   | 0.316 <sup>e</sup>    | 1.01                            | 0                   |
| THF                            | 81.7                                   | 0.55                  | —                               | 0                   |
| triethylene glycol             | 114.0                                  | 49.0                  | 2.77                            | 2.15                |
| tetraethylene glycol           | 172.7                                  | 55.0                  | 2.43                            | 11.3                |
| DEGMME <sup>a</sup>            | 118.0                                  | 3.48                  | 2.72                            | 29.5                |
| DEGMEE <sup>b</sup>            | 130.9                                  | 3.85                  | 2.40                            | 4.40                |
| 2-propanol                     | 76.8                                   | 2.431                 | -2.41                           | 1.90                |
| 1-butanol                      | 91.5                                   | 2.95                  | -1.31                           | *                   |
| 1-pentanol                     | 108.2                                  | 3.31 <sup>e</sup>     | -2.60                           | 4.20                |
| 1,3-butanediol                 | 89.9                                   | 130.3                 | 1.60                            | 3.86                |
| 2-methyl-2,4-pentanediol (MPD) | 123.0                                  | 34.4                  | 0.43                            | 18.2                |
| 2 % H <sub>2</sub> O in MPD    |  |                       | —                               | 13.5                |
| 5 % H <sub>2</sub> O in MPD    |  |                       | —                               | 0                   |
| glycerol                       | 73.3                                   | 1412                  | 4.51                            | 15.0                |
| 1,2,6-hexanetriol (HT)         | 121.7                                  | 2584                  | 2.60                            | 11.9                |

\* delayed demixing was observed for a polymer solution of 35 % PES, 10 % glycerol in NMP in literature [5].

a: diethyleneglycolmonomethylether; b: diethyleneglycolmonoethylether  
c: at 15 °C; d: at 16 °C; e: at 25 °C

The above discussions are related only to the possible kinetic aspects. Thermodynamic aspects (as the driving force) may play an even more important role in determining whether delayed demixing or instantaneous demixing will take place, which have been shown by several authors [4,9]. The interaction parameter of the nonsolvent and the solvent  $\chi_{12}$  has the most significant effect on the demixing behaviour. When this parameter is small (*i. e.*  $< 1.5$  [4]), instantaneous demixing is often observed. As presented in table 1, the viscosities of ethylene glycol, diethylene glycol, 1,2-propanediol and 1,4-butanediol are comparable to those of 1,3-butanediol or MPD, however, they did not show any delay time for demixing. It could be expected that this is caused by a better thermodynamic interaction between ethylene glycol, diethylene glycol, 1,2-propanediol and 1,4-butanediol with NMP than that between 1,3-butanediol and MPD with NMP. From literature data on vapor-liquid equilibrium of the system NMP-ethylene glycol [12] and of the system NMP-diethylene glycol [12], the interaction parameters of these two systems could be calculated. They are shown in figure 3. From this figure, it is clear, indeed, a rather good interaction exists between NMP and ethylene glycol as well as between NMP and diethylene glycol, which is characterized by negative values for the interaction parameters through

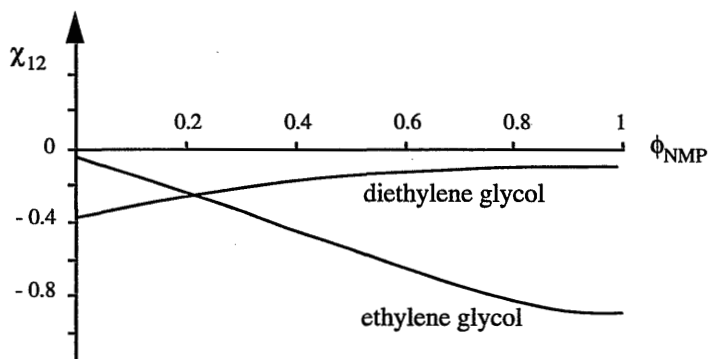


**Figure 3.** Concentration dependent interaction parameters for ethylene glycol-NMP and diethylene glycol-NMP systems at 50 °C, calculated from literature data [12].

the whole concentration range. Unfortunately, literature data on binary NMP-alcohol systems are rather limited, which prohibits a systematic thermodynamic analysis of the observed phenomena shown in table 1.

It was attempted to estimate the interaction parameters between NMP and the nonsolvents listed in table 1 by using the UNIFAC method. It was found, however, that the estimated values differed significantly from experimental values for systems of which literature data are available. Actually, it had been concluded by Gierycz [13] that the UNIFAC method could only be used to correlate already available experimental

results and is unable to predict the thermodynamic properties with reasonable accuracy in mixtures containing NMP. This is because the UNIFAC parameters obtained for the same pairs of groups differed considerably when computed from different systems and it was impossible to find reasonable mean values for them. The failing of using the UNIFAC method to predict the thermodynamic properties of mixtures containing NMP might be due to the ability of NMP to associate and to coassociate with other hydroxyl compounds, as suggested by Gierycz [13].

It has been shown by Strathmann [14] that the heat of mixing of solvent with nonsolvent can be used to predict the type of membrane to be formed. The temperature changes ( $\Delta T_{\text{mix}}$ ) of mixing NMP with the above nonsolvents have been measured in this study, which are also presented in table 1. It was realized that the trend of temperature change of mixing can only give a rough approximation for the trend of the heat of mixing. Still, it can be seen from table 1 that the interaction between NMP and organic acids must be rather strong, characterized by a considerable temperature increase during mixing. It was shown by Kesting [15] that relatively stable complexes can be formed between NMP and organic acids. The strong interaction between NMP and organic acids can explain why instantaneous demixing occurs when organic acids are used as the coagulant.

Table 1 also shows that the presence of water in a nonsolvent has a very strong effect on reducing the delay time. For MPD as a coagulant the addition of a few percent (< 5 %) of water is sufficient to induce instantaneous demixing, although pure MPD gives a quite long delay time for demixing.

Gas separation properties of hollow fibers spun from the same polymer solution as used for the delay time measurements in combination with the nonsolvents mentioned in table 1 as the first coagulant are shown in table 2. The contact time between the first coagulant and the polymer solution was kept constant as 0.34 second, which was calculated from the spinning speed (7 m/min) and the gap length (40 mm) between the spinneret and the second bath. Water was used as the bore liquid, except when glycerol was used as the first coagulant. Table 2 clearly shows that to obtain a highly selective fiber, it is necessary to use nonsolvents that may induce delayed demixing (see table 1) as the first coagulant. Using 1,3-butanediol, MPD, glycerol and HT as the first coagulant, the obtained fibers showed high selectivities. It is anticipated that the intrinsic selectivity could be obtained if those fibers would be dried completely. It will be shown later that the fiber spun with MPD as the first coagulant exhibited the intrinsic selectivity after completely drying it.

The intrinsic selectivity of PES for  $\text{CO}_2/\text{CH}_4$  was obtained to be 52 ~ 55 and the  $\text{CO}_2$  permeability to be  $3.0 \times 10^{-10} \text{ cm}^3 \text{ cm}/(\text{cm}^2 \text{ s cmHg})$ , when homogeneous flat films were measured at room temperature and a pressure of 5 bars.

**Table 2** *The gas permeation properties of hollow fibers made from a polymer solution of 30 % PES and 10 % glycerol in NMP by using various nonsolvents as the first coagulant.*

| nonsolvent                     | $P/l_{(CO_2)}$<br>(GPU) | $\alpha_{(CO_2/CH_4)}$ | external skin* |
|--------------------------------|-------------------------|------------------------|----------------|
| water                          | >300                    | 0.90                   | UF             |
| acetic acid                    | >300                    | 0.91                   | UF             |
| propionic acid                 | >300                    | 0.90                   | UF             |
| butyric acid                   | 230                     | 1.1                    | UF             |
| methanol                       | >300                    | 1.0                    | UF             |
| ethanol                        | 260                     | 1.0                    | UF             |
| 1,2-propanediol                | 210                     | 1.2                    | UF             |
| 1,4-butanediol                 | >300                    | 1.0                    | UF             |
| ethylene glycol                | >300                    | 0.90                   | UF             |
| diethylene glycol              | >300                    | 1.0                    | UF             |
| acetone                        | >300                    | 0.90                   | MF             |
| THF                            | >300                    | 0.91                   | MF             |
| triethylene glycol             | >300                    | 0.90                   | MF             |
| tetraethylene glycol           | >300                    | 0.90                   | MF             |
| DEGMME                         | >300                    | 0.91                   | MF             |
| DEGMEE                         | >300                    | 0.93                   | MF             |
| 2-propanol                     | 43                      | 3.4                    | GS             |
| 1-pentanol                     | 37                      | 3.8                    | GS             |
| 1,3-butanediol                 | 8.0                     | 44                     | GS             |
| 2-methyl-2,4-pentanediol (MPD) | 15                      | 38                     | GS             |
| glycerol <sup>a</sup>          | 12                      | 32                     | GS             |
| 1,2,6-hexanetriol (HT)         | 11                      | 42                     | GS             |

<sup>a</sup>: a mixture of 50 % NMP in water was used as the bore liquid.

\*: The type of external skin is defined as MF type when pores were observed (by SEM) on the skin (see figure 4 and 5). For UF type skin, no pores were detected by SEM under a magnification of 50,000. Fibers with these types of skin showed nonselective properties.

Spinning conditions:

spinning temperature, room temperature;  
 flow rate of the first coagulant, 2.0 ml/min;  
 gap length, 40 mm;  
 bore liquid, water (flow rate, 0.6 ml/min)

Compared to the previously mentioned four nonsolvents (1,3-butanediol, MPD, glycerol and HT), 2-propanol and 1-pentanol gave fibers with low selectivity, which could be due to the fact that the contact time between the polymer solution and these two nonsolvents was not long enough. By applying a contact time of 4.5 seconds, Van't Hof [5] was able to obtain PES fibers with nearly the intrinsic selectivity by using 1-pentanol as the first coagulant. Koops [16] also showed that polysulfone hollow fibers with the intrinsic selectivity could be obtained by using 1-pentanol as the

first coagulant, but quite a long contact time (5.7 seconds) had to be applied. It was argued by Koops [16] that for a nonsolvent giving a short delay time a long contact time is required to obtain a high selectivity.

1,3-Butanediol gives a shorter delay time than 1-pentanol. The reason for obtaining a high selectivity of the fiber made with 1,3-butanediol as the first coagulant is thought to be that due to the high viscosity of 1,3-butanediol its actual contact time with the polymer solution was much longer than the calculated contact time.

For all the nonsolvents giving instantaneous demixing, fibers showing nonselective properties were obtained. The fibers made with acetone and THF in the first bath are denoted as MF type because pores with sizes between 5  $\mu\text{m}$  to 20  $\mu\text{m}$  were present on the external skin of the fibers, as is shown in figure 4. Because of limitation of the gas permeation apparatus, fibers with fluxes higher than 300 GPU (gas permeation units:  $10^{-6} \text{ cm}^3/\text{cm}^2 \text{ s cmHg}$ ) could not be measured accurately.

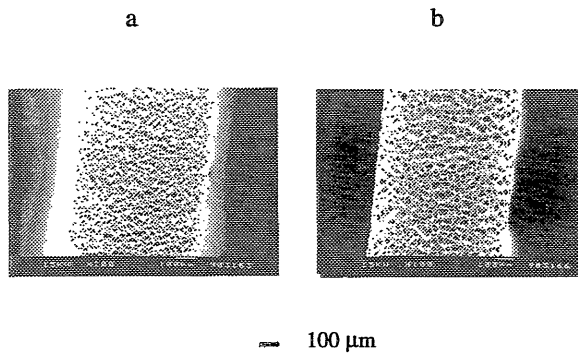


**Figure 4.** The external skin of hollow fibers spun with acetone (a) and THF (b) as the first coagulant.

Surprisingly, hollow fibers made with triethylene glycol, tetraethylene glycol, DEGMME and DEGMEE (see table 1) as the first coagulant showed completely nonselective properties. Considering the high viscosities and long delay times of these nonsolvents, it would be expected that highly selective fibers should be obtained. SEM examinations revealed that pores with sizes between 0.1  $\mu\text{m}$  to 0.5  $\mu\text{m}$  were present on the external skin of those fibers, as shown in figure 5. Those are the typical pore sizes for microfiltration membranes. In figure 5, only the SEM pictures for the external skins of fibers made with tetraethylene glycol and DEGMME are presented. The structures of the fibers made with triethylene glycol and DEGMEE as the first coagulant are similar to the structure obtained with DEGMME. SEM pictures taken from flat sheet membranes made from the same solution and the same nonsolvents displayed nearly the same structures. It is very interesting to see that for tetraethylene glycol the porosity of the skin of the resulting fiber is very high and the pore sizes are rather uniform, which



gives a strong indication that the modified dual bath spinning process offers a very effective way for the preparation of MF hollow fibers as well.

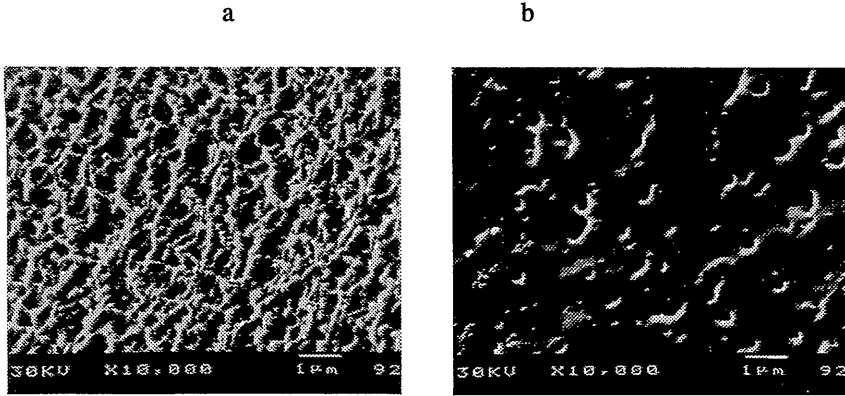


**Figure 5.** The external skin surfaces of hollow fibers spun with tetraethylene glycol (a) and DEGME (b) as the first coagulant.

It was also reported in literature [17] that polysulfone hollow fibers spun with NMP as the solvent and tetraethylene glycol or DMSO as the coagulant showed similar skin structure as those shown in figure 5. Because of the similarity of PES and polysulfone it is expected that tetraethylene glycol and DMSO should induce delayed demixing in a solution of polysulfone in NMP.

These experimental observations can actually be explained with the established models for membrane formation. According to the calculations of Tsay *et al.* [9], it was shown that in case the interaction parameter ( $\chi_{13}$ ) between the nonsolvent and the polymer is relatively small (implying that the nonsolvent is a rather strong swelling agent for the polymer) a long delay time is expected. With the decrease of  $\chi_{13}$  values the polymer concentration at the interface becomes lower and lower upon demixing, which was also shown by Reuvers [3]. In correspondence with this demixing behaviour, the binodals of the related systems shift more and more close to the nonsolvent-polymer axis in the ternary phase diagram. It is reasonable to expect that a membrane formed from such a system with a low  $\chi_{13}$  value will have a porous skin because of the low polymer concentration at the interface at the moment liquid-liquid demixing starts.

It is a general experimental fact that the addition of a high amount of solvent into a nonsolvent bath may induce delayed demixing in the related polymer solution. The membranes formed by such a delayed demixing process are characterized by a porous skin [18]. Providing the mixture of solvent and nonsolvent can be considered as a new

single nonsolvent, the interaction parameter of this "nonsolvent" and the polymer must be relatively small.

From the above considerations, it is pointed out that the formation of a porous skin of the fibers made with nonsolvents like triethylene glycol, tetraethylene glycol and DEGMME as the coagulant are most likely related to relatively low  $\chi_{13}$  values. In principle,  $\chi_{13}$  can be measured by swelling experiments. It was attempted to measure the  $\chi_{13}$  values for those systems in this study, however, it was found that to reach the equilibrium swelling state for those systems too long a time (years) is required. This is due to the large molar volumes and relatively high viscosities of those nonsolvents. So, direct data for the  $\chi_{13}$  values could not be obtained. But, according to the model calculations performed by Altena [19], a ternary polymer solution with a low  $\chi_{13}$  value is characterized by a binodal lying close to the polymer-nonsolvent axis in the ternary phase diagram. For the reason of comparison, cloud point data were measured at 25 °C for various systems. The data are presented in table 3.

**Table 3** Cloud point data for PES-NMP-nonsolvents systems at 25 °C.

| nonsolvent                     | PES % | NMP % | NS <sup>a</sup> % | NS/NMP         |
|--------------------------------|-------|-------|-------------------|----------------|
| water                          | 11.1  | 78.4  | 10.5              | <b>0.134</b>   |
| acetic acid                    | 12.3  | 49.0  | 38.7              | <b>0.789</b>   |
| propionic acid                 | 11.1  | 44.4  | 44.5              | <b>1.00</b>    |
| butyric acid                   | 5.5   | 49.6  | 44.8              | <b>0.90</b>    |
| methanol                       | 14.5  | 57.7  | 27.7              | <b>0.482</b>   |
| ethanol                        | 14.4  | 57.7  | 27.9              | <b>0.484</b>   |
| 1-propanol                     | 14.5  | 58.1  | 27.4              | <b>0.471</b>   |
| 1,2-propanediol                | 13.8  | 55.1  | 31.1              | <b>0.564</b>   |
| 1,4-butanediol                 | 14.2  | 56.8  | 29.0              | <b>0.511</b>   |
| ethylene glycol                | 14.0  | 56.2  | 29.8              | <b>0.530</b>   |
| diethylene glycol              | 9.3   | 37.1  | 53.6              | <b>1.45</b>    |
| acetone                        | 14.4  | 35.8  | 49.8              | <b>1.39</b>    |
| triethylene glycol             | 6.3   | 25.2  | 68.5              | <b>2.72</b>    |
| tetraethylene glycol           | 4.9   | 6.4   | 88.7              | <b>13.8</b>    |
|                                | 15.0  |       |                   | <b>&gt;3.5</b> |
| DEGMME                         | 2.4   | 3.2   | 94.4              | <b>29.5</b>    |
|                                | 15.0  |       |                   | <b>&gt;3.5</b> |
| DEGMEE                         | 5.5   | 21.8  | 72.7              | <b>3.33</b>    |
| 2-propanol                     | 15.0  | 60.0  | 25.0              | <b>0.416</b>   |
| 1-butanol                      | 14.7  | 58.7  | 26.6              | <b>0.452</b>   |
| 1,3-butanediol                 | 14.2  | 56.7  | 29.1              | <b>0.513</b>   |
| 2-methyl-2,4-pentanediol (MPD) | 13.9  | 55.6  | 30.5              | <b>0.549</b>   |
| glycerol                       | 15.0  | 61.5  | 23.5              | <b>0.382</b>   |
| 1,2,6-hexanetriol (HT)         | 14.6  | 58.6  | 26.8              | <b>0.457</b>   |

a: nonsolvent

According to literature [20], for a considerable number of ternary membrane-forming systems, the ratio of nonsolvent to solvent at the cloud point does not change too much with the change in polymer concentration. So, this ratio is an approximation of the position of the binodal. A higher value means that the binodal is more close to the polymer-nonsolvent axis. In the last column of table 3, this ratio is presented. The data clearly show that for triethylene glycol, tetraethylene glycol, DEGMME and DEGMEE, the cloud point curves of the related systems must be much more close to the polymer-nonsolvent axis compared to the other systems listed in this table, which means that the  $\chi_{13}$  values of those four systems are smaller than that of the others.

Here it can be concluded that for the choice of the first coagulant for the spinning of hollow fibers for gas separation, delayed demixing is a necessary but not a sufficient condition. When the nonsolvent is a strong swelling agent for the polymer, characterized by a relatively small  $\chi_{13}$  value, membranes with a porous skin will be obtained even though the related system shows delayed demixing.

Basically, the demixing behaviour of a polymer solution immersed in a nonsolvent bath is determined by both the interactions between the components and the kinetic factor of the related system. So, for the choice of the first coagulant both thermodynamic and kinetic parameters of the related systems have to be considered, instead of considering the type of demixing.

It has been shown in the above illustrations that based on the established models [3,9] for membrane formation, available literature data and the data measured in our laboratory, the experimentally observed membrane formation phenomena could be explained reasonably well in a qualitative way. This indicates that those models can be used to predict what kind of nonsolvent is suitable as the first coagulant for the spinning of hollow fibers with the dual bath process. However, for a practical use of those models, a considerable amount of experiments are required to obtain the interaction parameters and friction coefficients necessary for the model predictions. In literature, binary system data are rather limited, which limits the practical use of those models.

In this study, an empirical rule concerning the choice of the first coagulant for the spinning of gas separation hollow fibers with the dual bath process is proposed, which is based on the three dimensional solubility parameter concept [21]. The solubility parameter diagram of  $\delta_p$  versus  $\delta_h$  of the various nonsolvents listed in table 1 is shown in figure 6, provided with different symbols related to the membrane types from table 2 and from literature [5]. A fairly clear trend can be observed: nonsolvents suitable as a first coagulant for the spinning of gas separation hollow fibers are all located in the area

facing the right-down corner of the diagram. The nonsolvents which give delayed demixing but result in a MF type skin are near to the solubility envelope of the polymer.

Conceptually, the trend shown in figure 6 is actually in accordance with the model predictions [3,9]. The nonsolvents situated near to the solubility envelope, according to the solubility parameter concept, are strong swelling agents for the polymer. For the nonsolvents located in the right-down area, poor interactions with the solvents are expected because this area is far away from the envelope where the solvents are located.

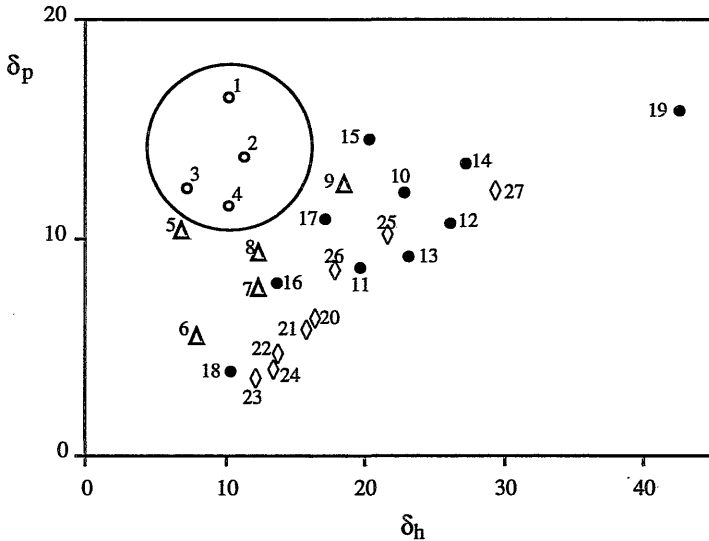


**Figure 6.** The solubility parameter map of  $\delta_p$  versus  $\delta_h$  of various solvents and nonsolvents for PES. The unit for  $\delta_p$  and  $\delta_h$  is  $\text{MPa}^{1/2}$ . The large circle schematically represents the solubility envelope for PES. (o): Solvents for PES; ( $\Delta$ ): nonsolvents resulting in MF skin; ( $\bullet$ ): nonsolvents inducing instantaneous demixing and resulting in UF skin; ( $\diamond$ ): nonsolvents causing delayed demixing and resulting in GS skin. For 1-butanol, 1-octanol and cyclohexanol, delayed demixing was observed in literature [5]. The solvents and nonsolvents are denoted as:

- |                       |                       |                    |
|-----------------------|-----------------------|--------------------|
| 1. DMSO               | 10. methanol          | 19. water          |
| 2. DMF                | 11. ethanol           | 20. 2-propanol     |
| 3. NMP                | 12. ethylene glycol   | 21. 1-butanol      |
| 4. DMAC               | 13. 1,2-propanediol   | 22. 1-pentanol     |
| 5. acetone            | 14. 1,4-butanediol    | 23. 1-octanol      |
| 6. THF                | 15. diethylene glycol | 24. cyclohexanol   |
| 7. DEGMME             | 16. acetic acid       | 25. 1,3-butanediol |
| 8. DEGMEE             | 17. propionic acid    | 26. MPD            |
| 9. triethylene glycol | 18. butyric acid      | 27. glycerol       |

It is worth while noticing that organic acids are also close to the envelope, indicating that the interaction parameters between those compounds and the polymer would be relatively small as well, which is reflected by the relatively high amount of

those compounds necessary to reach the cloud point as shown in table 3. Because of the strong special interaction with the solvent, which is characterized by a significant exothermic effect of mixing with the solvent shown in table 1, instantaneous demixing occurs in the polymer solution.

The interaction parameter between acetone and PES is probably relatively small as well, because acetone is also very close to the envelope. The cloud point data shown in table 3 support this speculation.

The empirical rule seems to hold also for polysulfone systems, as investigated by Koops [16]. At this stage it is not clear whether this rule can be applied to other polymer systems.

It has to be mentioned here that for spinning, an additive (glycerol) was used in the polymer solution. Because the polymer solution was the same for spinning as for the determination of the delay times of demixing (presented in table 1), the above reasoning concerning the relation between the type of membrane and the type of demixing process can be extrapolated to a situation in which no additive is present in the polymer solution.

#### *4-5-2. The effect of contact time*

According to Radovanovic [22], for systems resulting in a gas tight skin the delay time for demixing is proportional to the initial flux ratio of solvent outflow and nonsolvent inflow through the polymer solution interface. The higher the ratio, the longer is the delay time. It can be expected then that for a nonsolvent giving a long delay time as the first coagulant, the contact time between the nonsolvent and the polymer solution required for the polymer concentration at the interface to reach a certain high value will be short.

Koops [16] and Van't Hof [5] have, indeed, shown that in the dual bath spinning process, a long contact time is required to obtain a highly selective hollow fiber when a nonsolvent giving a short delay time, such as 1-pentanol, is used. On the other hand, a long contact time is unfavourable for the achievement of a thin skin. To obtain a fiber with both high selectivity and a thin skin, it is desirable to choose a nonsolvent giving a long delay time, such as MPD, glycerol or HT.

Van't Hof [5] used glycerol as the first coagulant for the spinning of PES hollow fibers for gas separation. However, fibers with a relatively thick skin (about 0.5  $\mu\text{m}$ ) were obtained. The formation of such a relatively thick skin is due to the practical difficulty on controlling a short contact time. It was observed by Van't Hof [5] that when glycerol was used as the first coagulant, during spinning after the fiber had been brought into the second bath glycerol stuck firmly to the nascent fiber surface for quite

a long time, which increased the actual contact time to a large extent. This observation was explained to be due to the high viscosity of glycerol, which makes its removal from the fiber surface in the second bath difficult.

To solve this problem, the dual bath process as used by Van't Hof has been modified by the use of a triple orifice spinneret. In this way, the amount of nonsolvent used as the first coagulant could be drastically reduced, which makes the removal of the first coagulant from the nascent fiber easier and hence diminishes the actual contact time. It has been demonstrated [7] that fibers with a thinner skin and the intrinsic selectivity could be obtained with this modified dual bath process.

Apparently, for the choice of the optimum first coagulant, not only the delay time has to be considered but also the viscosity of the first coagulant. It is preferred to choose a nonsolvent which gives a long delay time and has a low viscosity.

MPD seems to be a good candidate, because of its long delay time and relatively low viscosity compared to that of glycerol or HT.

In principle, in the modified dual bath spinning process, the contact time can be controlled by changing the gap length between the spinneret and the second bath. In figure 7, the gas separation properties of hollow fibers spun with MPD or HT as the first coagulant are presented as a function of the gap length.

From figure 7, it can be seen that when HT was used as the first coagulant the change in the gap length between the spinneret and the second bath hardly had any influence on the properties of the resulting fibers. With MPD as the first coagulant, however, the change in gap length had a considerable influence on the fluxes of the final fibers, while the selectivities of the fibers were nearly constant. The difference in behaviour can be explained by comparing the viscosities of the two nonsolvents. HT has an extremely high viscosity so it was very difficult to remove from the fiber surface in the second bath. Therefore the actual contact time between HT and the polymer solution was much longer than the "apparent" contact time calculated from the spinning speed and the gap length. MPD has a relatively low viscosity so it could easily be removed from the fiber in the second bath and then, as expected, the fluxes of the related fibers increased with the decrease of the gap length.

It is very interesting to see that with MPD as the first coagulant the flux of the fiber could be improved by reducing the contact time but without losing the selectivity. Apparently, for this system, the polymer concentration at the interface increases very quickly to a very high value after contacting the polymer solution with the coagulant, and remains constant regardless of the change in contact time. This fast increase of the polymer concentration at the interface should be related to a very high ratio of NMP outflow and MPD inflow, characterized by the long delay time for demixing.

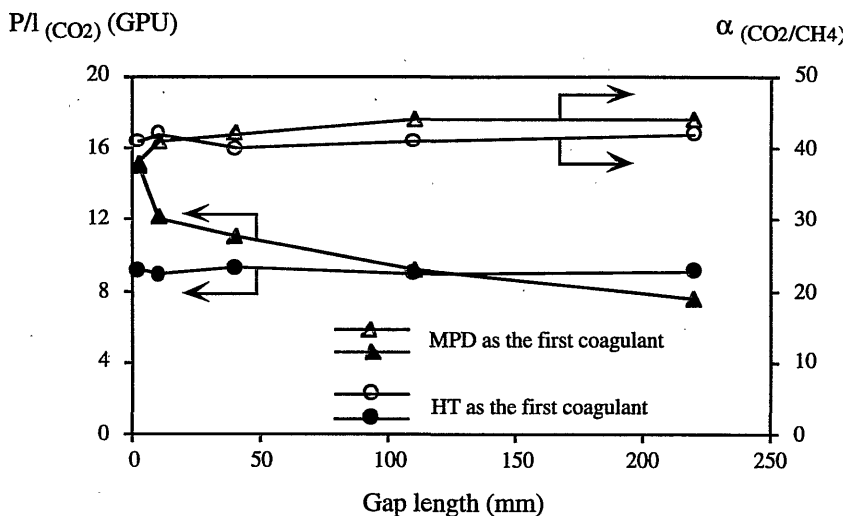


**Figure 7.** The gas separation properties of hollow fibers as a function of the gap length between the spinneret and the second bath. MPD and HT are used as the first coagulant, respectively. Other spinning parameters are: spinning solution: 30 % PES, 10 % glycerol and 60 % NMP; spinning temperature: room temperature; flow rate of the first coagulant: 2.0 ml/min; bore liquid: water (flow rate: 0.6 ml/min).

When the viscosity of the first coagulant is high, other methods instead of simply changing the gap length between the spinneret and the second bath should be used to reduce the actual contact time between the polymer solution and the first coagulant. Possible methods include using a smaller amount of first coagulant so that the thickness of the first coagulant layer surrounding the fiber will be thinner, and stirring in the second bath. In principle, increasing the temperature of the second bath could also enhance the removal of the first coagulant from the fiber surface, but the change in temperature would also change the thermodynamic and kinetic behaviour of the membrane formation process. Therefore the effect of changing temperature in the second bath is not discussed here.

It was found, in practice, that disturbing the second bath was not a positive way to improve the properties of the fiber. When the second bath was disturbed the nascent fiber was shaking in the second bath and the spinning process became unstable.

The influence of changing the flow rate of the first coagulant on the properties of the fibers is presented in figure 8. With MPD as the first coagulant, the properties of the resulting fibers were not influenced by changing its flow rate. This can be understood since it is easy to remove MPD from the fiber surface because of the relatively low viscosity, thus the contact time is dominated by the gap length. With HT as the first coagulant, fluxes of the fibers increased with the decrease of its flow rate meanwhile

the selectivities remained unchanged. According to figure 8, it is preferable to use a low flow rate of the first coagulant (*i. e.* a thinner layer) to obtain a fiber with both high selectivity and high flux. However, further reduction of the flow rate of the first coagulant resulted in nonselective fibers. This is probably due to incomplete coverage of the fiber surface by the first coagulant when the flow rate of the first coagulant is too low.

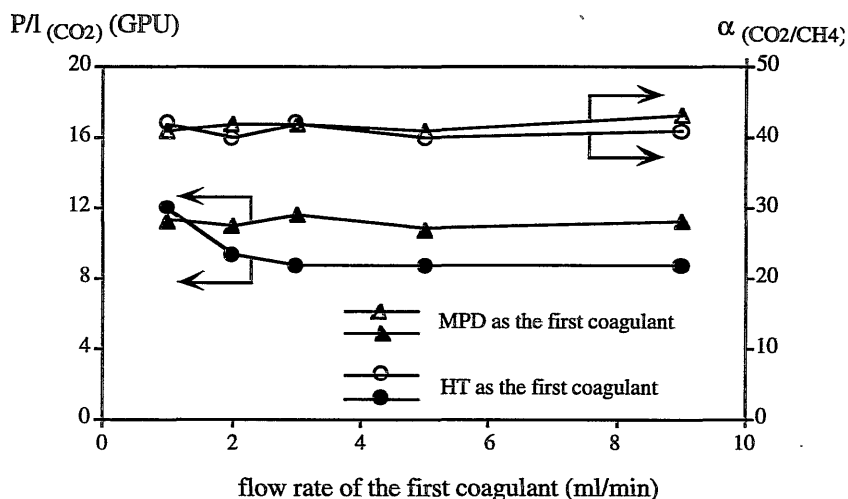


**Figure 8.** Gas separation properties of hollow fibers as a function of the flow rate of the first coagulant. MPD and HT are used as the first coagulant, respectively. Other spinning parameters are: spinning solution: 30 % PES, 10 % glycerol and 60 % NMP; spinning temperature: room temperature; gap length: 40 mm; bore liquid: water (flow rate: 0.6 ml/min).

The results presented in figure 7 and figure 8 show that the selectivities of the fibers are almost the same regardless of the change in contact time and the use of MPD or HT as the first coagulant, which indicates that the polymer concentrations at the interface are the same. It appears that with a first coagulant giving a long delay time, the polymer concentration at the interface raises to a very high value in a rather short time, and actually reaches the vitrification composition. The polymer concentration can only remain constant for a relatively long time during membrane formation when the vitrification composition is approached, since in a vitrified polymer solution the movement of the polymer chain is greatly retarded. Such a vitrified polymer solution resembles a highly swollen state before the solvent is completely replaced by the nonsolvent, which explains why relatively fast mass transfer between the polymer solution and the coagulation bath can still take place.



Figure 9 shows the structure of the fiber spun from the same polymer solution as in figure 7 with MPD as the first coagulant.

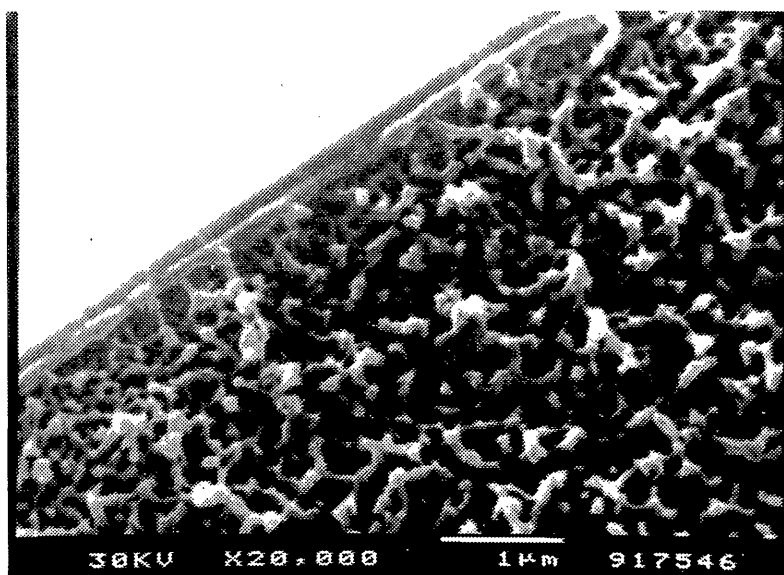


*Figure 9. The structure of hollow fiber spun with MPD as the first coagulant.*

From figure 9, it can be seen that the fiber has a very remarkable structure. A dense and thin skin directly supported by a highly porous sublayer. In general for membranes formed by immersion precipitation, a transition layer in between the skin and the highly porous support layer is present, which causes additional resistance to gas transport. The structure shown in figure 9 guarantees a negligible resistance of the support layer, which will be shown in the next chapter. It is believed that the absence of the transition layer in the fiber shown in figure 9 must be related to a very steep polymer concentration profile created by the first coagulant. When the polymer solution showing a highly anisotropic concentration distribution is in contact with the second coagulant (water), the ratio of solvent outflow and nonsolvent inflow is reduced drastically. The result is that the polymer concentration just underneath the concentrated layer hardly has changed when demixing starts and consequently a very porous structure is formed. Further down to the bore side of the fiber, many macrovoids are present, which will be shown in the next chapter as well.

### 4-5-3. The effect of bore liquid

The influence of the bore liquid on the properties of the fibers is dependent on the type of first coagulant and the composition of the spinning solution.

Figure 10 shows the influence of the addition of solvent to water as the bore liquid on the properties of the fibers. MPD and HT were used as the first coagulant, respectively. The spinning solution consisted of 30 % PES, 10 % glycerol and 60 % NMP. It can be seen that there is no change of the gas separation properties of the fibers when the concentration of NMP in the bore liquid is changed.

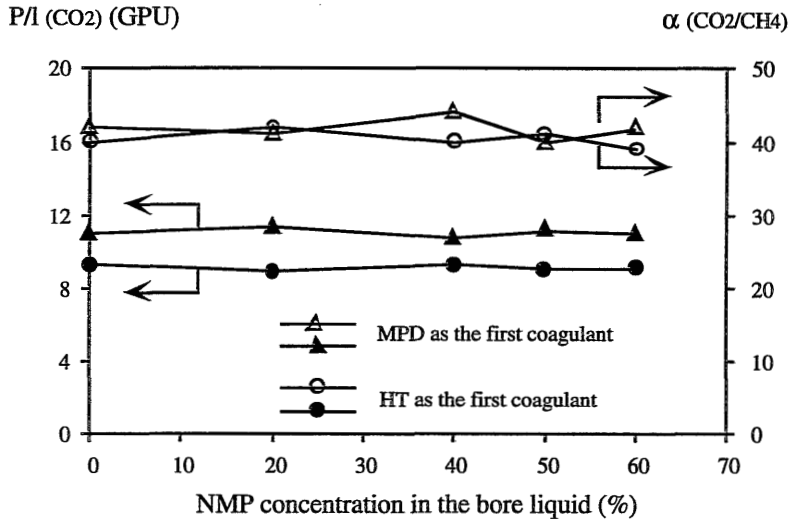


**Figure 10.** The influence of changing NMP concentration in the bore liquid on the properties of the resulting fibers. HT and MPD were used as the first coagulant, respectively. Other spinning parameters are:  
 spinning solution: 30 % PES, 10 % glycerol and 60 % NMP;  
 spinning temperature: room temperature;  
 flow rate of the first coagulant: 2.0 ml/min;  
 bore liquid: water (flow rate: 0.6 ml/min);  
 gap length: 40 mm.

For the same spinning solution, however, a drastic effect of the composition of the bore liquid on the properties of the fibers could be observed when glycerol was used as the first coagulant. Table 4 shows that with pure water as the bore liquid, a very low selectivity was obtained. To achieve a high selectivity, a certain amount of NMP had to be added to the bore liquid.

**Table 4.** *The influence of changing NMP concentration in the bore liquid on the properties of the fibers spun from a polymer solution of 30 % PES, 10 % glycerol in NMP. Glycerol was used as the first coagulant. Other spinning parameters are the same as that given in figure 10.*

| NMP % in bore liquid | $P/l_{(CO_2)}$ (GPU) | $\alpha_{(CO_2/CH_4)}$ |
|----------------------|----------------------|------------------------|
| 0                    | 15                   | 4.3                    |
| 20                   | 11.7                 | 14                     |
| 40                   | 10                   | 38                     |
| 50                   | 10.5                 | 35                     |
| 60                   | 10.2                 | 37                     |

According to the results presented in table 4, it appears that the formation of the external skin was influenced by the bore liquid. With glycerol as the first coagulant, the polymer concentration increase at the interface seems to be relatively slow. So, when pure water was used as the bore liquid, the diffusion of water from the bore side might already reach the external interface before the polymer concentration there became high enough to form a gas tight skin. The addition of solvent to the bore liquid decreased the driving force for water to diffuse into the polymer solution from the bore side. Then a long enough time was allowed for the polymer concentration at the external interface to increase before there was any interference by water from the bore side and thus a gas selective fiber could be obtained. It is worthwhile noticing that the flux of those fibers did not differ so much although the selectivity of the fiber spun with pure water as the bore liquid was much lower than that with mixtures of NMP and water as the bore liquid. This means that the skin thickness of those fibers was in a comparable range but the densities varied considerably.

With HT or MPD as the first coagulant, the polymer concentration at the interface increased rather fast so the formation of the external skin was hardly disturbed by the bore liquid.

It has to be mentioned here that although the gas separation properties of hollow fibers spun with HT or MPD as the first coagulant were not influenced by the bore liquid under the experimental conditions presented in figure 10, the substructures of those fibers changed significantly with the change of the bore liquid as will be shown in the next chapter.

#### 4-5-4. Solvent effect

In the previous sections, it has been demonstrated that the choice of the first coagulant is very important with respect to membrane formation by the dual bath process. In this section, the influence of using different solvents (NMP, DMAC and DMSO) on the properties of the resulting fibers is discussed.

For spinning hollow fibers with the dual bath process glycerol, HT, 1,3-butanediol and MPD were used as the first coagulant.

Cloud point data of the four different nonsolvents in PES-NMP solutions are given in table 5. The data in table 5 are plotted in the ternary phase diagram shown in figure 11. From figure 11, it can be seen that with NMP as the solvent, the amount of nonsolvent required to induce liquid-liquid demixing in the polymer solution is increasing in the order of glycerol < HT < 1,3-butanediol < MPD. This indicates that the interaction parameters ( $\chi_{12}$ ) between the nonsolvents and NMP are increasing in the same order, *i. e.*, glycerol < HT < 1,3-butanediol < MPD. The same trend was observed when DMAC or DMSO was used as the solvent, as shown by the data listed in table 6 and table 7. A lower interaction parameter means a stronger interaction between the two components. As presented in table 1, the  $\Delta T_{\text{mix}}$  of NMP with glycerol is 4.51 °C and that with MPD is 0.43 °C, which suggests that the interaction between glycerol and NMP should be stronger than that between MPD and NMP. This is in accordance with the conclusion drawn from the cloud point data.

The ternary phase diagram of one of the four nonsolvents, HT, in polymer solutions of different solvents is shown in figure 12. This figure shows that the amount of HT required to induce liquid-liquid demixing in the polymer solutions with respect to the solvents is decreasing in the order of NMP > DMAC > DMSO, which indicates that the interaction parameters between HT and the solvents are also decreasing in the order of NMP > DMAC > DMSO. With glycerol or 1,3-butanediol as the nonsolvent the same trend was found. However, with MPD as the nonsolvent, the sequence changes to NMP > DMSO > DMAC.

The gas separation properties of fibers spun from polymer solutions of 32 % PES in the different solvents (without additive) by using different first coagulants are given in figure 13 and figure 14. From figure 13, it can be seen that all the fibers have quite high selectivities, which clearly shows that the dual bath process is a very effective method for the preparation of gas separation hollow fiber membranes. A very clear trend can be observed in figure 14 that with NMP, DMAC and DMSO as the solvent, respectively, the fluxes of the fibers are decreasing in the same trend: NMP > DMAC > DMSO, for each of the first coagulants.

**Table 5.** Cloud point data for ternary systems of PES/NMP/nonsolvent at 25 °C.

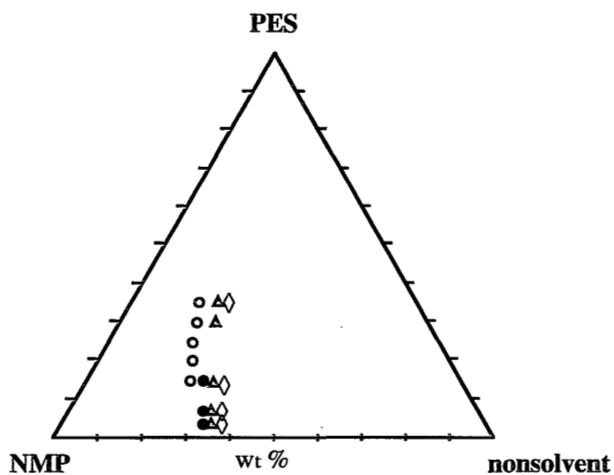
| nonsolvent     | PES % | NMP % | NS % | NS/NMP |
|----------------|-------|-------|------|--------|
| glycerol       | 35.0  | 49.5  | 15.5 | 0.313  |
|                | 30.0  | 52.7  | 17.3 | 0.328  |
|                | 25.0  | 55.7  | 19.3 | 0.346  |
|                | 20.0  | 58.7  | 21.3 | 0.363  |
|                | 15.0  | 61.5  | 23.5 | 0.382  |
| HT             | 14.6  | 58.6  | 26.8 | 0.457  |
|                | 7.0   | 62.5  | 30.5 | 0.488  |
|                | 3.4   | 64.4  | 32.2 | 0.500  |
| 1,3-butanediol | 35.0  | 45.0  | 20.0 | 0.444  |
|                | 30.0  | 47.9  | 22.1 | 0.461  |
|                | 14.2  | 56.7  | 29.1 | 0.513  |
|                | 6.7   | 60.7  | 32.6 | 0.537  |
|                | 3.3   | 62.6  | 34.1 | 0.545  |
| MPD            | 35.0  | 43.5  | 21.5 | 0.494  |
|                | 13.9  | 55.6  | 30.5 | 0.549  |
|                | 6.6   | 59.1  | 34.3 | 0.580  |
|                | 3.2   | 61.1  | 35.7 | 0.584  |

**Table 6.** Cloud point data for ternary systems of PES/DMAC/nonsolvent at 25 °C.

| nonsolvent     | PES % | DMAC % | NS % | NS/DMAC |
|----------------|-------|--------|------|---------|
| glycerol       | 15.6  | 64.9   | 19.5 | 0.300   |
|                | 7.7   | 69.7   | 22.5 | 0.323   |
|                | 3.8   | 72.3   | 23.9 | 0.331   |
| HT             | 15.5  | 62.1   | 22.4 | 0.361   |
|                | 7.5   | 67.4   | 25.1 | 0.372   |
|                | 3.7   | 69.7   | 26.6 | 0.382   |
| 1,3-butanediol | 15.3  | 61.2   | 23.4 | 0.383   |
|                | 7.4   | 66.3   | 26.3 | 0.397   |
|                | 3.6   | 68.8   | 27.6 | 0.401   |
| MPD            | 15.0  | 60.1   | 24.8 | 0.413   |
|                | 7.2   | 65.2   | 27.5 | 0.422   |
|                | 3.6   | 67.5   | 28.9 | 0.428   |

**Table 7.** Cloud point data for ternary systems of PES/DMSO/nonsolvent at 25 °C.

| nonsolvent     | PES % | DMSO % | NS % | NS/DMSO |
|----------------|-------|--------|------|---------|
| glycerol       | 17.9  | 72.7   | 9.4  | 0.129   |
|                | 9.0   | 80.8   | 10.2 | 0.126   |
|                | 4.4   | 84.4   | 11.1 | 0.132   |
| HT             | 17.3  | 69.3   | 13.4 | 0.193   |
|                | 8.5   | 76.1   | 15.5 | 0.204   |
|                | 4.2   | 79.4   | 16.4 | 0.207   |
| 1,3-butanediol | 16.3  | 65.2   | 18.5 | 0.284   |
|                | 7.9   | 71.4   | 20.6 | 0.289   |
|                | 3.9   | 74.6   | 21.5 | 0.288   |
| MPD            | 14.8  | 59.1   | 26.1 | 0.441   |
|                | 7.1   | 64.1   | 28.7 | 0.448   |
|                | 3.5   | 66.5   | 30.0 | 0.451   |

**Figure 11.** Cloud point data for ternary systems of PES/NMP/nonsolvents at 25 °C. (o) glycerol; (●) HT; (Δ) 1,3-butanediol; (◊) MPD.

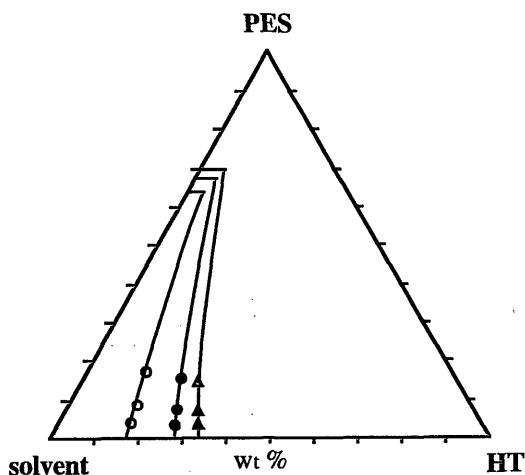


**Figure 12.** Cloud point data for ternary systems of PES/solvents/HT at 25 °C. (o) DMSO; (●) DMAC; (Δ) NMP. Horizontal lines on top of the cloud point curves are the vitrification boundaries of the related systems.

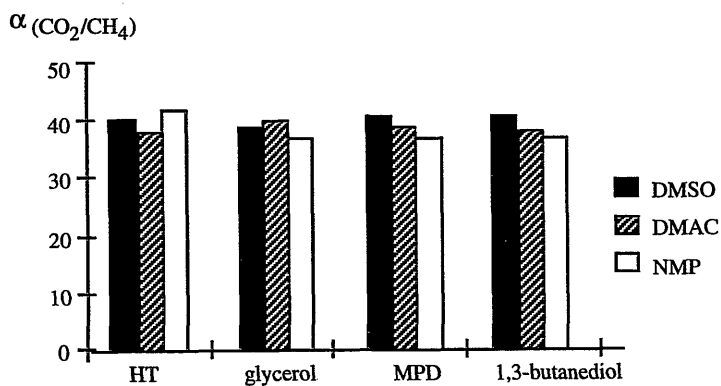


**Figure 13.** The selectivities of hollow fibers spun from polymer solutions of 32 % PES in different solvents (DMSO, DMAC, NMP) by using different first coagulants (HT, glycerol, MPD, 1,3-butanediol). Other spinning parameters: spinning temperature: room temperature; flow rate of the first coagulant: 2.0 ml/min (for glycerol, MPD, 1,3-butanediol), 1.0 ml/min (for HT); bore liquid: water (flow rate: 0.6 ml/min); gap length: 100 mm.

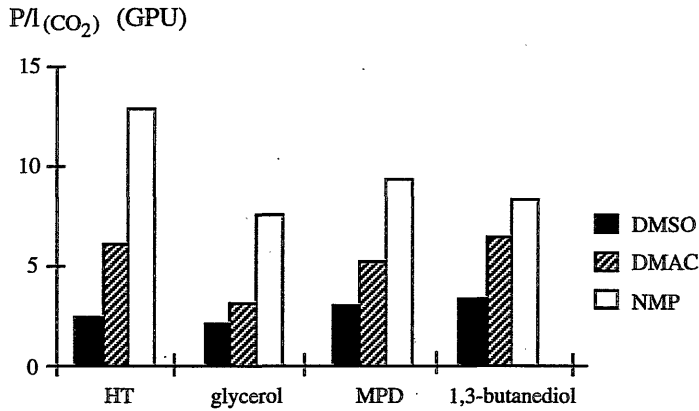


Figure 14. The fluxes of the hollow fibers presented in figure 13.

In chapter 2 of this thesis, vitrification compositions of PES in the three solvents have been measured. The data are presented in table 8. The vitrification concentration of PES in the different solvents are in the order of NMP > DMAC > DMSO as is listed in table 8. A high vitrification concentration means that a high polymer concentration is required for the polymer solution to become a glass at room temperature.

Table 8. Vitrification concentrations of PES in different solvents at 25 °C. Data are taken from chapter 2.

| solvent | PES vitrification concentration |
|---------|---------------------------------|
| NMP     | 70 %                            |
| DMAC    | 67 %                            |
| DMSO    | 64 %                            |

Comparing the data presented in table 8 with the data presented in figure 14, it appears that the skin thickness of a membrane prepared by the dual bath process is related to the vitrification concentration of the polymer solution. This relation is schematically shown in figure 15. As made clear in chapter 2, PES membranes can be formed by vitrification prior to liquid-liquid demixing from a solution with NMP as the solvent and MPD as the coagulant, which may also be extrapolated to systems with DMAC or DMSO as solvent and glycerol, HT or 1,3-butanediol as coagulant. According to figure 13 and the discussions presented in the previous sections, a vitrified skin can already be formed at the external interface of the polymer solution before the solution is brought into contact with the second coagulant. As illustrated in



figure 15, when the vitrification concentration of the polymer solution is high, only a thin layer of the solution near the interface may become a glass. Below this the solution is still in a liquid state and here liquid-liquid demixing can take place when the solution is brought into the second bath. When the vitrification concentration of the polymer solution is low, a relatively thick layer of the solution near the interface may already become a glass before coming into the second bath, and consequently a membrane with a relatively thick skin will be formed.

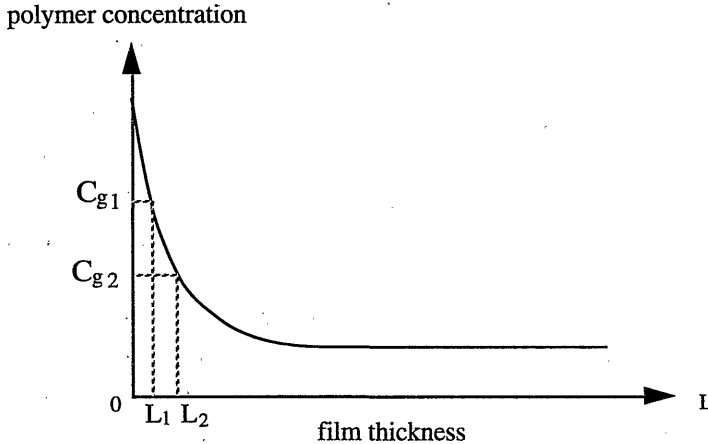


**Figure 15.** A schematic illustration of the relationship between skin thickness and the vitrification concentration of a polymer solution for a dual bath process. The curve represents the polymer concentration profile created in the first bath.  $C_{g1}$  and  $C_{g2}$  are the possible polymer vitrification concentrations, above which a polymer solution is in a glassy state. Liquid-liquid demixing cannot take place in the region where the polymer concentration is above its vitrification concentration when the solution is brought into contact with a second coagulant.  $L_1$  and  $L_2$  are the skin thicknesses of the membranes.

Certainly, for the same first coagulant, the created polymer concentration profiles in polymer solutions of different solvents will not be the same, because the change of the solvent in the spinning solution will change the interaction between the solvent and the coagulant. This will influence the polymer concentration profile and consequently complicates the effect of the vitrification concentration on the skin thickness. Considering the small differences in the vitrification concentrations of the different polymer solutions as listed in table 8, the rather significant differences in the fluxes of the related membranes may not only be caused by the mechanism illustrated in figure 15. It seems that the low flux of hollow fibers prepared with DMSO as the solvent should be due to the low vitrification concentration as well as to a less steep concentration profile. It is obvious that the influence of the vitrification concentration on

the skin thickness of a membrane will become more pronounced when the polymer concentration profile is less steep.

According to the cloud point data, the sequence of the values of the interaction parameters between a nonsolvent and the solvents could be estimated to be in the order of NMP > DMAC > DMSO, still it is difficult to correlate the concentration profile to the interaction parameter  $\chi_{12}$ , because the position of the binodals and the concentration profiles are related to  $\chi_{12}$  in a very complex way as has been argued by Reuvers [4].

For the same solvent, the influence of changing the first coagulant on the skin thickness of the fiber is difficult to explain, because the change of nonsolvent will change both the interaction parameters of  $\chi_{12}$  and  $\chi_{13}$  simultaneously, and both parameters have a strong effect on the position of the binodals and the concentration profiles. Furthermore, the change of first coagulant will also affect the actual contact time between the coagulant and the spinning solution due to differences in viscosity. This makes it nearly impossible to find a satisfactory explanation for the influence of the nonsolvent on the skin thickness of the membrane.

Nevertheless, from the results presented in this section it can be concluded that in the dual bath spinning process a solvent which leads to a high vitrification concentration of the polymer solution is preferred in order to obtain a hollow fiber with a thin skin. It is suggested that more effort should be put in the investigations of the vitrification phenomena of membrane forming systems in order to further improve the performance of hollow fibers prepared by the dual bath process.

#### *4-5-5. The effect of drying procedure*

With the dual bath spinning process, a completely dense skin can be formed on the external surface of a fiber, which is necessary to obtain a membrane with satisfactory gas separation properties. However, the presence of this dense skin greatly retards the complete removal of residual solvent from the resulting fiber during the rinsing procedure and the drying procedure. It is known that the presence of residual solvent can reduce the selectivity of a fiber [23]. In this section the effect of the drying procedure on the properties of the fibers is investigated.

In our study hollow fibers were normally dried at ambient temperature in air after a liquid exchange treatment [11]. The use of the liquid exchange treatment is to prevent changes in structure and properties of membranes caused by large capillary forces during drying. As shown previously, fibers with the intrinsic selectivity could not be obtained with this drying method. The same phenomenon was also observed by Van't Hof [5]. The SEM pictures of those fibers showed that the skin was very dense and no nodular structure was present. So, the relatively low selectivity of the membrane

compared to the intrinsic selectivity of the polymer cannot be explained as the presence of defects in the skin layer. A reasonable explanation might be the presence of residual solvent and/or additive (glycerol) in the fibers.

The properties of hollow fibers dried in three different ways are given in table 9.

**Table 9.** Gas separation properties of hollow fibers dried by three different methods.

| drying method           | $P/l$ (CO <sub>2</sub> ) (GPU) | $\alpha_{\text{(CO}_2\text{/CH}_4\text{)}}$ |
|-------------------------|--------------------------------|---|
| air                     | 4.5                            | 52  |
| EtOH/hexane/air         | 15                             | 38  |
| EtOH/hexane/air (80 °C) | 9.5                            | 52  |

Fibers presented in this table were prepared with MPD as the first coagulant. The gap length was 5 mm. Other spinning conditions were the same as that given in figure 7.

The first method was drying the fibers in ambient air directly after rinsing with water. The second one was the normal procedure (with a liquid exchange treatment before drying in air). The third one was to dry the fibers at a temperature of 80 °C for one night after applying the liquid exchange treatment. Drying the fibers by the first method, the intrinsic selectivity could be obtained, but the flux was rather low. Actually, selectivities higher than the intrinsic one were often obtained with the first drying method. For example a selectivity as high as 63 could be obtained. The reason is not clear. Drying the fibers by the third method, the intrinsic selectivity and a rather good flux were obtained. The skin thickness, calculated from the flux of the fiber and the intrinsic permeability of PES, is in agreement with the skin thickness observed by SEM, which is about 0.3  $\mu\text{m}$  as is shown in figure 9. Apparently, the achievement of the intrinsic selectivity by drying at elevated temperature is due to a complete removal of the residual solvent. In our experiments, some fibers were further dried at 150 °C under vacuum and the properties of those fibers were the same as of the ones dried by method three.

Remeasuring the fibers presented in table 9 after leaving the fibers under ambient conditions for about half a year yielded different results, which are given in table 10. For the fibers dried by the first method, the selectivity dropped slightly, but virtually no change in flux was observed. For fibers dried by the second method, selectivity increased and flux decreased. No change in properties was found for the fibers dried by the third method.

**Table 10.** Gas separation properties of the hollow fibers presented in table 9, remeasured after half a year.

| drying method           | $P/l$ (CO <sub>2</sub> ) (GPU) | $\alpha_{\text{(CO}_2\text{/CH}_4\text{)}}$ |
|-------------------------|--------------------------------|---|
| air                     | 4.2                            | 46  |
| EtOH/hexane/air         | 11                             | 47  |
| EtOH/hexane/air (80 °C) | 9.5                            | 52  |

#### 4-6. CONCLUSIONS

The dual bath process developed by Van't Hof has been modified by the use of a triple orifice spinneret, which simplifies the spinning process and improves the ability to control the contact time between the polymer solution and the first coagulant. Furthermore, with the use of the triple orifice spinneret the amount of first coagulant required for the spinning was drastically reduced, which makes the modified dual bath process economically and technically more feasible.

It was found that delayed demixing can result in two completely different membranes. When the interaction parameter  $\chi_{13}$  is relatively small, delayed demixing may occur and MF type membranes are obtained. Delayed demixing caused by a poor interaction between nonsolvent and solvent will result in gas separation type membranes when the contact time between the nonsolvent and the polymer solution is sufficiently long. For instantaneous demixing, MF membranes can also be obtained when  $\chi_{13}$  is small.

The choice of the first coagulant for the preparation of gas separation hollow fibers can reasonably well be predicted by using the solubility map of  $\delta_p$  versus  $\delta_h$ . It has been shown that predictions obtained from the solubility map are in agreement with predictions based on Reuvers model for membrane formation. Although predictions from the solubility map might be rough, it is very useful in a practical point of view because solubility parameters are easy to obtain from literature.

MPD has been shown to be a very good candidate to be used as the first coagulant for the preparation of gas separation hollow fibers from PES/NMP solutions. Its relatively low viscosity enables the control of a short contact time and the high ratio of

NMP flow out of the polymer solution and MPD flow into the solution ensures the achievement of a dense and thin skin in a short contact time.

With the dual bath process, hollow fibers with a favourable structure could be obtained, which was composed of a completely dense skin directly supported by a very porous sublayer. This is probably caused by a very steep polymer concentration profile created in the first bath.

The influence of the bore liquid on the properties of the resulting fibers is dependent on the type of first coagulant and the composition of the polymer solution. For a polymer solution of 30 % PES, 10 % glycerol in NMP, the properties of the fibers spun with HT or MPD as the first coagulant were not affected by the variation of the composition of the bore liquid. With glycerol as the first coagulant, a certain amount of NMP had to be added to the bore liquid to obtain a high selectivity from the same polymer solution.

The type of solvent has a significant influence on the properties of the resulting fibers. For the same first coagulant, the flux of hollow fibers changed with the change of solvent in the order of NMP > DMAC > DMSO. The experimental observations are most likely related to the vitrification phenomenon as well as the polymer concentration profile of the related system as created in the first bath.

Hollow fibers spun from the dual bath process have to be dried at a high temperature after the liquid exchange treatment in order to obtain the intrinsic selectivity and a relatively high flux.

#### 4-7. REFERENCES

1. Van't Hof, J. A., *PhD Thesis*, University of Twente, the Netherlands, 1988
2. Reuvers, A. J.; Van den Berg, J. W. A. and Smolders, C. A., *J. Membr. Sci.* 34, 45 (1987)
3. Reuvers, A. J. and Smolders, C. A., *J. Membr. Sci.* 34, 67 (1987)
4. Reuvers, A. J., *PhD Thesis*, University of Twente, the Netherlands, 1987
5. Van't Hof, J. A.; Reuvers, A. J.; Boom, R. M.; Rolevink, H. H. M and Smolders, C.A., *J. Membr. Sci.*, 70, 17-30 (1992)
6. Henis, J. M. S and Tripodi, M. K., *J. Membr. Sci.* 8, 233 (1981)
7. Li, S.-G.; Koops, G. H.; Mulder, M. H. V.; Boomgaard, Th. v. d. and Smolders, C.A., To be published in *J. Membr. Sci.*

8. Koops, G. H.; Li, S.-G.; Boomgaard, Th. v. d.; Mulder, M. H. V. and Smolders, C. A., *Dutch Patent* 91.02151 (1991)
9. Tsay, C. S. and McHugh, A. J., *J. Polym. Sci., Polym Phys. Ed.* 28, 1327 (1990)
10. Chapter 2 of this thesis
11. MacDonald, U. S. Pat 3,842,515 (1974)
12. Surovy, J.; Graczova, E. and Oveckova, J., *Collect. Czech. Chem. Commun.* 54, 2856 (1989)
13. Gierycz, P., *Thermochimica Acta*, 108, 229 (1986)
14. Strathmann, H.; Kock, K.; Amar, P. and Baker, R.W., *Desalination*, 16(1975), 179
15. Kesting, R. E; Fritzsche, A. K; Murphy, M. K; Cruse, C. A.; Handermann, A. C.; Malon, R. F. and Moore, M. D., *J. Appl. Polym. Sci.* 40, 1557 (1990)
16. Koops, G. H., *PhD Thesis*, University of Twente, the Netherlands, 1992
17. Doi, S. and Hamanaka, K. *Desalination*, 80, 167 (1991)
18. Wijmans, J. G.; Baaij, J. P. B. and Smolders, C. A., *J. Membr. Sci.* 14, 263 (1983)
19. Altena, F. W. and Smolders, C. A., *Macromolecules*, 15, 1491 (1982)
20. Boom, R. M., *PhD Thesis*, University of Twente, the Netherlands, 1992
21. Barton, A. F. M., *Handbook of solubility parameters and other cohesion parameters*, 2nd Edn, CRC Press, Inc. 1991
22. Radovanovic, P.; Thiel, S. W. and Hwang, S.-T., *J. Membr. Sci.* 65, 231 (1992)
23. Brown, P. J.; East, G. C. and McIntyre, J. E., *Polym. Commun.* 31, 156 (1990)

---

**CHAPTER 5**

---

**ELIMINATION OF MACROVOIDS IN DUAL-BATH FIBERS  
BY A THERMAL INVERSION PROCESS**

---

S.-G. Li, H.M.M. Rolevink, I.G.M. Pünt, Th.van den Boomgaard,  
C.A. Smolders, H. Strathmann

**5-1. ABSTRACT**

The formation of macrovoids in the support layer of hollow fibers prepared with a dual bath process has been studied. The mechanism for the formation of these macrovoids could be explained reasonably well on the basis of a model proposed by Smolders. Furthermore, a new spinning method based on this model has been developed for the preparation of gas separation hollow fiber membranes. Macrovoid free and highly selective hollow fibers could be obtained by using this method which combines the dual bath process with a thermally induced phase inversion process. In this so-called DB & TIPI process a polymer solution is spun into hollow fibers by contacting it with two successive nonsolvent baths. The polymer solution has a cloud point temperature that is higher than the temperature of the second bath. When the polymer solution is immersed into the second bath, liquid-liquid demixing spreads through the solution quickly due to the fast drop in temperature. This rules out the possibility for macrovoid formation. Besides a macrovoid free support layer, the obtained fibers showed a very thin and dense skin. Scanning electron microscopic studies showed that the skin was thinner than 0.1  $\mu\text{m}$ . The formation of the thin and dense skin was interpreted as a result of instantaneous demixing of the polymer solution in combination with fast depletion of solvent from the solution, when the solution was in contact with the first coagulant.

However, the effective skin thickness, calculated according to the flux of the fiber and the intrinsic permeability of the polymer used for preparation of the fiber, was 0.19  $\mu\text{m}$  which is about two times higher than the skin thickness as observed by SEM. This indicates that the resistance of the support layer of these fibers is still profound.

## 5-2. INTRODUCTION

Macrovoids are often found in the support layer of polymeric membranes prepared by immersion precipitation process [1-8]. The presence of macrovoids can reduce the mechanical strength of the membranes. For gas separations, membranes are often used under high pressures. Therefore, a support layer free of macrovoids is one of the important requirements for a gas separation membrane.

In literature [1-5], several empirical rules are described, which can be used to eliminate the formation of macrovoids. Those empirical rules can be summarized as follows:

- 1) Using a solvent-nonsolvent pair with a low tendency of mixing [1-3];
- 2) Increasing the polymer concentration in the polymer solution [2,3];
- 3) Adding large amounts of nonsolvent (or a second polymer [4]) to the polymer solution [5];
- 4) Adding large amounts of solvent to the coagulation bath [3].

In practice, those rules are used in combination. Very often, nonsolvent additives are used in the polymer solution in order to obtain a gas separation membrane with a macrovoid-free as well as an open porous support layer.

It was shown by Van't Hof [6] that using a high polymer concentration only is not always an effective way for eliminating the formation of macrovoids. It was found that a considerable number of macrovoids were still formed when a polymer concentration as high as 43.6 wt % was used without any nonsolvent additive. In the study of Van't Hof, the polymer used was polyethersulfone (PES) and the solvent was N-methylpyrrolidone (NMP). The addition of 10 wt % glycerol (a nonsolvent) into a polymer solution of 35 wt % PES resulted in macrovoid-free hollow fibers. Those macrovoid-free hollow fibers were obtained with a traditional single bath spinning process, where a polymer solution is spun into hollow fibers by passing the solution through air for a short time before entering into a coagulation bath. To obtain a high selectivity for gas separation, those fibers had to be coated with a layer of silicon rubber.

With a dual bath spinning process, Van't Hof *et al.* [9] were able to prepare fibers showing the intrinsic selectivity of the polymer by using the same polymer solution mentioned above (*i.e.*, 35 % PES, 10 % glycerol in NMP) without the necessity of a silicon rubber coating. However, many macrovoids were formed in the support layer of those highly selective fibers. It appears that macrovoids are more easily formed in fibers spun from the dual bath process than in fibers spun from the traditional single bath process. It was suggested by Van't Hof [6] that the addition of more glycerol to



the spinning solution or the addition of NMP in the bore liquid might help to eliminate the formation of macrovoids.

In chapter 4 of this thesis, it is shown that the dual bath process developed by Van't Hof can be modified by the usage of a triple orifice spinneret. The modified dual bath process resulted in gas separation hollow fibers with improved flux while maintaining the same selectivity compared to the fibers obtained by Van't Hof. However, those fibers still contained many macrovoids in the support layer. In this study we adopted the suggestions made by Van't Hof and investigated the effect of adding nonsolvent to the polymer solution and solvent to the bore liquid on the formation of macrovoids in hollow fibers spun with the modified dual bath process.

It will be shown that the formation of macrovoids in those fibers can be explained by using a mechanism for macrovoid formation proposed by Smolders *et al.* [10]. This mechanism will be described in details in the next section. Based on this mechanism a new spinning method has been developed to prepare gas separation hollow fibers with a macrovoid-free support layer and high selectivity. The method combines the dual bath process with a thermally induced phase inversion process, called DB & TIPI process. In this process a polymer solution is spun into hollow fibers by contacting two successive nonsolvent baths. The polymer solution is formulated in such a way that its cloud point temperature is higher than the temperature of the second coagulation bath. During spinning the polymer solution is kept at a temperature which is higher than the cloud point temperature. Therefore, when the polymer solution is immersed into the second bath, liquid-liquid demixing spreads quickly through the solution due to the fast drop in temperature. This rules out the possibility for macrovoid formation. Besides showing a macrovoid free support layer, the obtained fibers showed a very thin and dense skin.

Plasma etching technique was used to obtain information on the resistance of the support layer of the hollow fibers obtained in this study.

### 5-3. THEORY

Different mechanisms were proposed to be responsible for the formation of macrovoids, which have been reviewed by Smolders [10]. Normally, the formation of macrovoids is observed in systems undergoing instantaneous demixing. Based on this general experimental observation and Reuvers' model [11] for membrane formation, Smolders [10] proposed a new mechanism to explain the formation of macrovoids. A brief summary of the most important points of this mechanism is given as follows:

(1) The initiation of macrovoids is the nucleation of the polymer lean phase created during instantaneous demixing.

(2) The growth of macrovoids is corresponded by the expansion of the polymer lean phase nuclei. These nuclei can expand into macrovoids as a result of diffusional flow only when the following two conditions are fulfilled simultaneously: the first condition is that the polymer solution in front of the nuclei must remain in a thermodynamically stable state for a relatively long time period and the second condition is that the solvent concentration in the nuclei must be high enough to locally induce delayed demixing in front of the already formed nuclei.

According to this mechanism, the formation of a dense skin in the nascent membrane will favour the formation of macrovoids in the sublayer. The dense skin will drastically reduce the diffusion of solvent out of the polymer solution and the diffusion of nonsolvent into the solution. The result will be a low supersaturation of nonsolvent in the solution and a high solvent concentration in the formed nuclei underneath the skin, which will prevent the formation of new nuclei and promote the formed nuclei to grow into macrovoids.

Based on this model, the effect of variation of polymer concentration and the effect of addition of nonsolvent to the polymer solution on the occurrence of macrovoids were examined in the literature [10]. It was explained that the elimination of macrovoids by the addition of nonsolvent to the polymer solution was due to the suppression of local delay of demixing. The same explanation could also be applied to explain the elimination of macrovoids by increasing the polymer concentration.

According to this mechanism, the formed polymer lean phase nuclei will not be able to grow into macrovoids if liquid-liquid demixing has already taken place in the polymer solution in front of the formed nuclei. This forms the base for the development of the new spinning method.

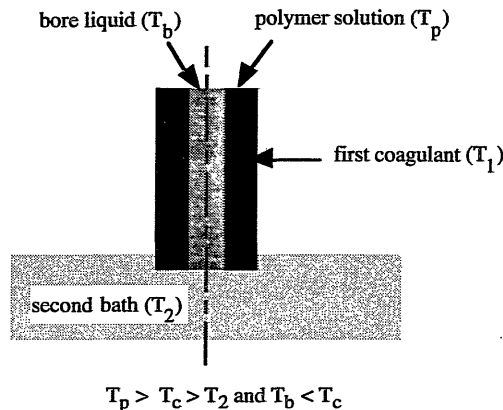


**Figure 1.** A schematic demonstration of the new spinning process.  $T_c$  is the cloud point temperature of the spinning solution.

The new spinning process is schematically demonstrated in figure 1. The key point of this process is that the polymer solution is formulated in such a way that it has a cloud point temperature ( $T_c$ ) higher than the temperature ( $T_2$ ) of the second bath. During spinning the polymer solution is kept at a temperature ( $T_p$ ) which is higher than  $T_c$ . When the polymer solution together with the first coagulant are brought into the second bath liquid-liquid demixing will progress very quickly through out the entire polymer solution, before any formed nuclei can grow into macrovoid. This is due to the fact that heat transfer is generally several orders of magnitude faster than mass transfer.

Because of the fast demixing process, it is expected that hollow fibers with a very thin skin can be formed as well.

## 5-4 EXPERIMENTAL

### 5-4-1. *Materials*

Polyethersulfone (PES, VICTREX® 5200P from ICI) was used as the polymer for the preparation of gas separation hollow fibers. Before use the polymer was dried at 150 °C under vacuum over night. Water-free glycerol (from Merck) was used as the additive in the spinning solutions. Other solvents and nonsolvents were synthesis grade, purchased from Merck and used without further treatment.

### 5-4-2. *Cloud point measurements*

Glycerol was used as an additive in the spinning solutions. To formulate the spinning solutions with cloud point temperatures higher than room temperature, cloud point data were measured at different temperatures for the system PES-NMP-glycerol. A cooling method was used to determine the cloud point temperature, in which a polymer solution was homogenized at high temperature (96 °C) overnight then cooled down stepwise. First the solution was cooled down quickly to a certain temperature a few degrees higher than the expected cloud point temperature. Then the solution was cooled down at a slow speed (1 °C in 20 minutes) until the cloud point temperature was observed visually.

### 5-4-3. *Fiber spinning and characterizations*

A triple orifice spinneret was used in the spinning process as described in chapter 4. Water was used in the second bath. Spinning speed was kept constant at 7 m/min for all experiments.

The obtained fibers were normally dried using a liquid exchange method [12], in which fibers having been rinsed with water were immersed into an ethanol bath for one day followed by immersion in a hexane bath for another day before drying at ambient conditions. When other drying methods are applied, they are specified.

Characterization of the obtained fibers was performed according to the descriptions given in chapter 4. In addition, burst pressure tests were carried out. Each module used for the burst pressure tests contained only one fiber with a length of 10 cm. Pressurized N<sub>2</sub> was used for the burst pressure tests. The fibers were pressurized from the bore side. The pressure was increased in an interval of 5 bars and kept for 10 minutes. The outlet of the module was connected to a stainless steel tube which was immersed in a water bath. The burst pressure could easily be determined by observing the gas flow in the water bath.

After measuring the gas permeability, some of the fibers were coated with a thin layer of a silicon rubber (polydimethylsiloxane, PDMS) and the permeation through these fibers was measured again. The coating procedure has been described in literature [13]: the bore side of the fibers was evacuated and after 1 minute the fibers were immersed into a solution of 2 % (w/w) PDMS (Sylgard 184, DOW Corning) in hexane for 2 minutes. The coated fibers were dried at 80 °C overnight.

#### ***5-4-4. Plasma etching***

Plasma etching experiments were performed with a PLASMAFAB-508 etching apparatus. The etching power was 50 Watts. The flow rate of oxygen as the etching gas was kept at 45 ml/min. During etching the pressure in the etching chamber was kept constant at 0.1 Torr. Because of no temperature control system in the etching chamber of the apparatus, the temperature of the etching procedure could not be controlled. When a long etching time was required, the etching process was divided into several time intervals to reduce the change in temperature during the etching process. In this case, after one minute etching the chamber was purged with N<sub>2</sub> for two minutes. Such a procedure was repeated until the required etching time was reached. It was found that the final permeation properties of the etched fiber were significantly dependent on the position of the fibers placed in the etching chamber. To ensure a good reproducibility, each etching experiment was performed by using three fibers placed in the same position in the chamber.

For the etched fibers with fluxes higher than 300 GPU (gas permeation units, 10<sup>-6</sup> cm<sup>3</sup>/cm<sup>2</sup> s cmHg), the fluxes were measured with a soap bubble flow meter under a pressure of 1 bar at room temperature.

## 5-5. RESULTS AND DISCUSSION

### 5-5-1. *The use of different first coagulants*

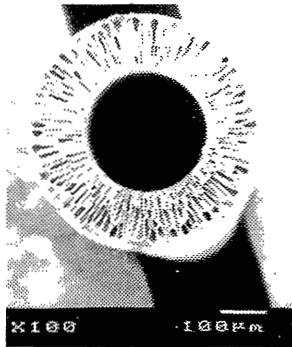
With the dual bath spinning process, hollow fibers with a very dense external skin could easily be obtained [9,14]. Due to the formation of this dense skin it is expected that macrovoids will be formed from the external side of the fiber wall according to the mechanism proposed by Smolders *et al.*[10].

It is shown in chapter 4 that with 1,2,6-hexanetriol (HT), 1,3-butanediol or 2-methyl-2,4-pentanediol (MPD) as the first coagulant defect-free hollow fibers could be prepared from a polymer solution of 30 % PES, 10 % glycerol and 60 % NMP when water with a flow rate of 0.6 ml/min was used as the bore liquid. The structures of these fibers and the structure of the fiber spun with glycerol as the first coagulant are shown in figure 2. From this figure it can be seen that these fibers contained many macrovoids in the support layer. The macrovoids, however, are initiated from the bore side.

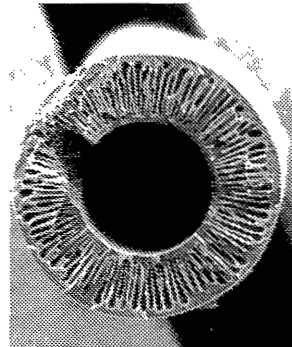
Hollow fibers with similar structures were also obtained by Van't Hof [6]. It was explained that the absence of macrovoids initiated from the external side is due to retarded penetration of water from the external side in combination with liquid-liquid demixing induced by penetration of water from the bore side. The slow penetration of water from the external side was caused by the slow removal of glycerol from the fiber surface when the fiber was in the second bath. This promotes the growth of macrovoids from the bore side. The result is that the demixing front induced from the external side already meets the macrovoids initiated from the bore side before the solvent concentration in the nuclei of the demixing front reaches the level necessary for the nuclei to be able to grow into macrovoids. When 1-pentanol, which has a low viscosity and therefore can easily be removed from the fiber surface, was used as the first coagulant macrovoids indeed appeared from both sides of the fiber wall [6].

### 5-5-2. *Addition of solvent to the bore liquid*

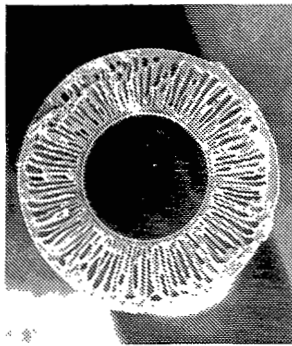
Addition of solvent to the bore liquid will reduce the density of the internal skin, which will then reduce the tendency to form macrovoids from the bore side. Furthermore, the driving force for water to diffuse into the polymer solution from the bore side will be reduced as well. Hence, the chance for macrovoid formation from the external side is increased. It was shown in literature [11,15] that when the solvent concentration in the coagulation bath is above a certain value, delayed demixing will occur in the polymer solution. In general, no macrovoids are formed in systems showing delayed demixing.



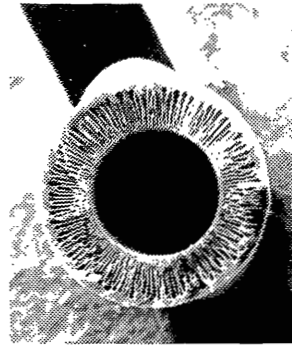
2a). first coagulant: HT



2b). first coagulant: glycerol



2c). first coagulant: 1,3-butanediol

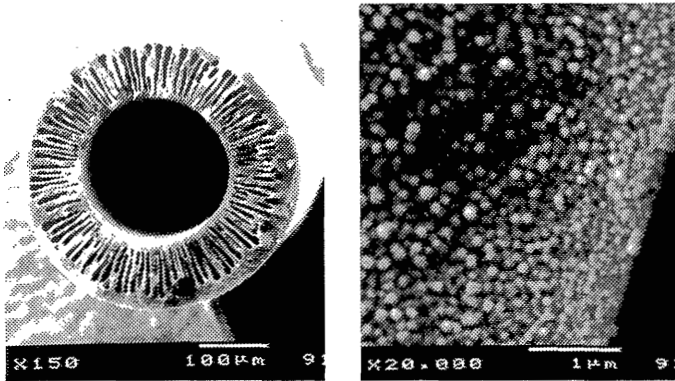


2d). first coagulant: MPD

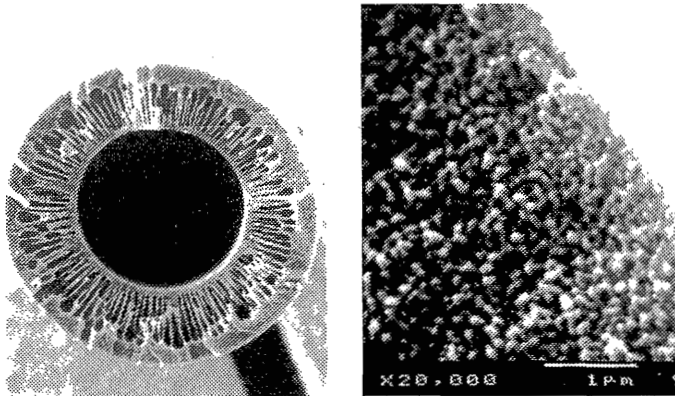
**Figure 2.** Cross sections of hollow fibers spun by using different first coagulant. spinning solution: 30 % PES, 10 % glycerol and 60 % NMP; spinning temperature: room temperature; gap length: 40 mm; flow rate of the first coagulant: 2.0 ml/min; bore liquid: water (0.6 ml/min)

Figure 3 shows that below the concentration of 40 wt % NMP in the bore liquid, macrovoids are formed only from the bore side. With 60 wt % NMP in the bore liquid, macrovoids appeared from both sides of the fiber wall and the length of macrovoids formed from the internal side was shorter. It can also be seen in figure 3 that with an increase of the NMP concentration in the bore liquid, the internal skin becomes more and more porous. Similar observations were obtained by Koops [16] for the spinning of polysulfone (PSF) hollow fibers.

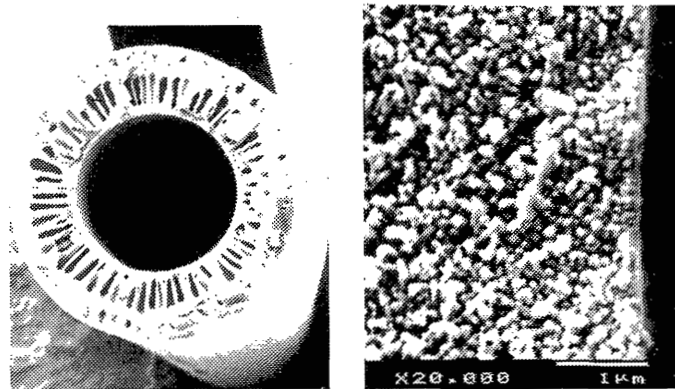
Although significant differences in the support layer and the internal skin of the fibers were observed in figure 3, the gas separation properties of those fibers were nearly identical. The gas separation properties of the fibers are presented in chapter 4.



3a). bore liquid: 20 % NMP/80 % H<sub>2</sub>O



3b). bore liquid: 40 % NMP/60 % H<sub>2</sub>O



3c). bore liquid: 60 % NMP/40 % H<sub>2</sub>O

**Figure 3.** Cross sections of entire fiber wall (left) and of bore side skin layer (right) of PES hollow fibers spun with various NMP concentrations in the bore liquid. HT was used as the first coagulant. Other spinning parameters are the same as indicated in figure 2.

However, it is described in literature [16] that selectivities and fluxes of PSF hollow fibers increased with increase of the NMP concentration in the bore liquid. The differences in the separation properties of the fibers presented here and those in literature [16] are due to the fact that the resistance of the support layer of hollow fibers presented in literature [16] had a significant effect on the properties of the fibers. The resistance of the support layer of the fibers developed here is negligibly low compared to the resistance of the dense external skin, as will be shown later. Thus no influence on gas separation properties was observed when the internal layer became more open.

Increasing the NMP concentration further to 80 wt % in the bore liquid made a continuous spinning impossible. The fiber broke down due to the fact that the polymer solution could not solidify at the bore side. This was confirmed by preparing flat film membranes under the same conditions. The mechanical strength of the formed membrane was then tested with an elongation method described previously [17].

With MPD as the first coagulant, the formation of macrovoids from the external side is more pronounced than with HT as the first coagulant. The cross section of the fiber spun with MPD as the first coagulant and 60 % NMP in water as the bore liquid is shown in figure 4.

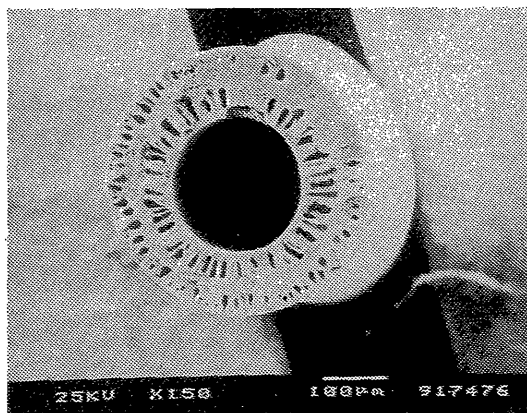
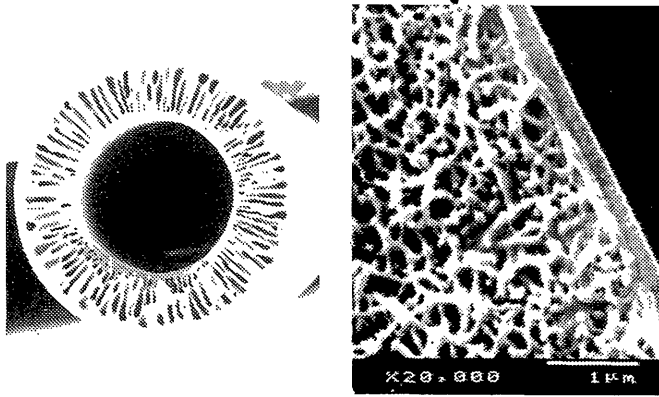


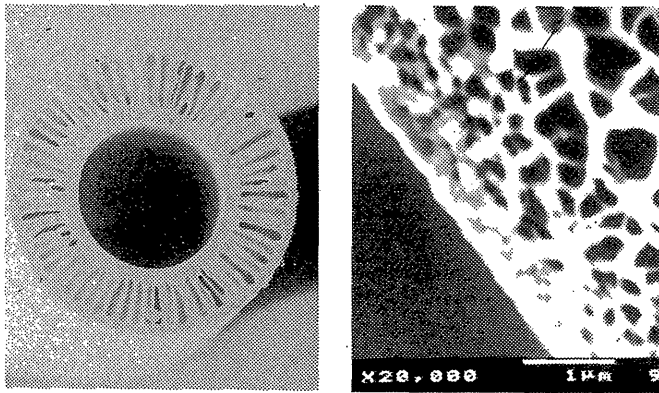
**Figure 4.** Cross section of a hollow fiber spun with MPD as the first coagulant and 60 % NMP in water as the bore liquid. Other spinning parameters are the same as indicated in figure 2.

The viscosity of MPD ( 34.4 cPs. at 20 °C) is much lower than the viscosity of HT ( 2584 cPs. at 20 °C). So, during the spinning process MPD can be removed more easily from the fiber surface than HT. In case MPD is used the formation of macrovoids from the external side of the fiber occurs earlier and more time is allowed for growth of those macrovoids before they meet the demixed solution induced from the bore side of the fiber.

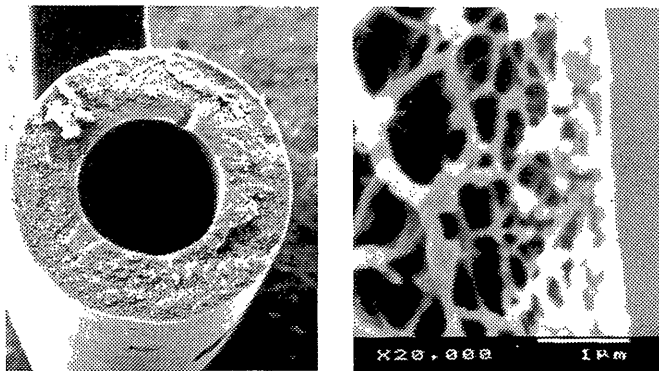




5a). 10 % glycerol in the polymer solution



5b). 14 % glycerol in the polymer solution



5c). 17 % glycerol in the polymer solution

**Figure 5.** Cross section and external skin of hollow fibers spun from polymer solutions with identical polymer concentration (30 % PES) but various glycerol concentrations. HT was used as the first coagulant. Water was used as the bore liquid. Other spinning parameters are the same as indicated in figure 2.

It was observed by Strathmann *et al.*[3] that under certain conditions macrovoids can be initiated from defects of the skin. Both fiber 3c) in figure 3 and the fiber in figure 4 contained macrovoids formed from the external skin side. Even so, these fibers showed nearly the intrinsic selectivity of the polymer for the separation of CO<sub>2</sub> and CH<sub>4</sub>. This gives a strong indication that the formation of macrovoids is not necessarily related to defects of the skin.

### 5-5-3. Addition of nonsolvent to the polymer solution

In the previous section it has been shown that it is not an effective way to reduce or eliminate the formation of macrovoids by simply increasing the solvent concentration in the bore liquid. In this section, the influence of changing the additive concentration in the polymer solution on the formation of macrovoids is investigated.

Figure 5 shows that with 10 % or 14 % glycerol in the polymer solution, many macrovoids are present in the fibers. Macrovoids disappeared when the concentration of glycerol in the solution was increased to 17 %. The cross section of the external skin of these fibers are also presented in figure 5. It can be seen that the skin structure of the fiber spun from the solution with 10 % glycerol is significantly different from the skin structure of the fiber with 14 % or 17 % glycerol in the solution. Gas separation properties of the fibers are presented in table 1.

**Table 1.** The gas separation properties of hollow fibers shown in figure 5.

| fiber | PES  | glycerol | NMP  | $\alpha_{(CO_2/CH_4)}$ | $PI_{(CO_2)}$ (GPU) |
|-------|------|----------|------|------------------------|---------------------|
| 1     | 30 % | 10 %     | 60 % | 42                     | 11                  |
| 2     | 30 % | 14 %     | 56 % | 1.3                    | 34                  |
| 3     | 30 % | 17 %     | 53 % | 0.9                    | >300                |

The results presented in table 1 show that addition of a high amount of glycerol to the polymer solution gave rise to the formation of nonselective hollow fibers. The low selectivity is thought to be caused by the fact that with a glycerol concentration higher than 14 %, in the top layer of the fiber liquid-liquid demixing occurred prior to vitrification. Since the contact time between the polymer solution and the first coagulant was the same for the spinning of the three fibers presented in table 1, it seems that the increase in glycerol concentration of the polymer solution reduces the raising rate of the polymer concentration at the interface when the solution is in contact with the first

coagulant. This is confirmed by the experimental results presented in table 2. By reducing the water flow rate at the bore side from 0.7 ml/min to 0.4 ml/min, the selectivities of the fibers increased. For hollow fiber spinning, the amount of bore liquid is limited, which means that the change in solvent concentration in the bore cannot be neglected during spinning. When the flow rate of the bore liquid is low the solvent concentration in the bore increases rapidly, thus reducing the driving force for water to diffuse from the bore side into the solution. The result then is that the formation of the external skin layer is less affected by the water from the bore side.

**Table 2.** *The influence of changing the flow rate of bore liquid on the properties of the resulting fibers.*

| flow rate of the bore liquid (ml/min) | $\alpha_{(\text{CO}_2/\text{CH}_4)}$ | P/l ( $\text{CO}_2$ ) (GPU) |
|---------------------------------------|--------------------------------------|-----------------------------|
| 0.7                                   | 1.4 (4.0)                            | 30 (10)                     |
| 0.6                                   | 1.3 (3.5)                            | 34 (9.5)                    |
| 0.5                                   | 14 (41)                              | 10 (6.0)                    |
| 0.4                                   | 23 (40)                              | 10 (5.9)                    |
| 0.3                                   | 7.5 (38)                             | 12 (6.7)                    |

(-): Data were measured after coating the fiber with a layer of silicon rubber  
 spinning solution: 30 % PES, 14 % glycerol, 56 % NMP;  
 spinning temperature: room temperature;  
 bore liquid: water;  
 first coagulant: HT (2.0 ml/min);  
 gap length: 40 mm

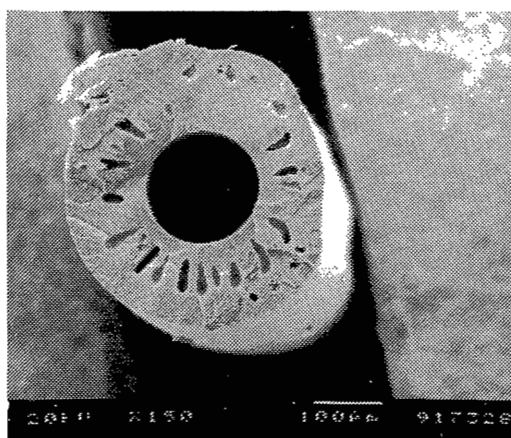


**Figure 6.** *Cross section of the fiber spun with a water flow rate of 0.3 ml/min in the bore. Other spinning parameters are the same as those given in table 2.*

Consequently, a denser skin can be formed. Further reduction of the bore flow rate to 0.3 ml/min resulted in a fiber with a slightly deformed external skin (see figure 6). The deformation is probably due to the contact of an unsolidified external skin with the guiding wheel in the second bath. This may be the reason for the decreased selectivity of the fiber. Comparing figure 6 and figure 5b), it can be seen that the number of macrovoids in the fiber reduces with decreasing the bore liquid flow rate.

From the results presented in this section, it can be concluded that the formation of macrovoids in hollow fibers can be suppressed or even eliminated by the addition of a certain amount of nonsolvent to the polymer solution. However, this may result in the formation of nonselective hollow fibers. It is believed that the increase in glycerol concentration of the polymer solution reduces the raising rate of polymer concentration at the interface when the solution is in contact with the first coagulant. In this case, the polymer concentration in the external skin layer is lower than the vitrification concentration when the solution is getting in contact with water and, consequently, small pores are created in the skin of the resulting fiber.

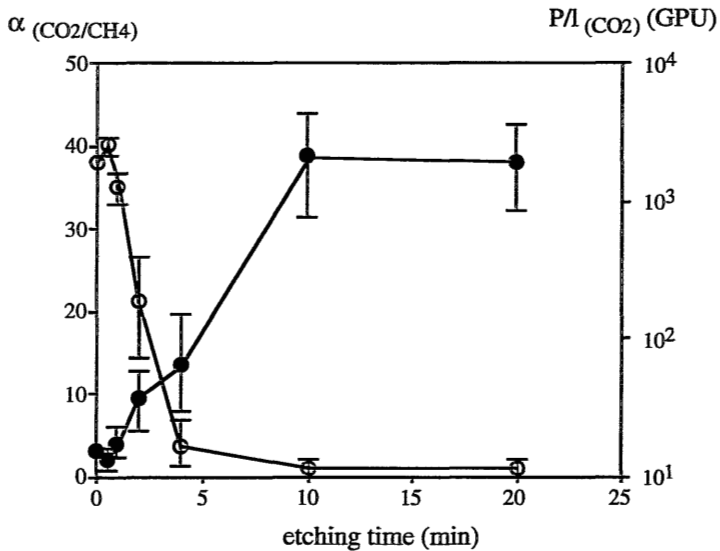


**Figure 7.** The gas separation properties of hollow fibers as a function of etching time. The fibers were spun from a polymer solution of 30 % PES, 10 % glycerol and 60 % NMP with MPD as the first coagulant. Other spinning parameters: spinning temperature: room temperature; gap length: 5 mm; flow rate of the first coagulant: 1.0 ml/min; bore liquid: water (0.6 ml/min)

#### **5-5-4. Support layer resistance**

It has been shown in chapter 4 that hollow fibers spun with MPD as the first coagulant possessed a remarkable structure. It is expected that the resistance of the support layer of those fibers would be very low. In this study a plasma etching technique was used to investigate the properties of the support layer of hollow fibers spun with the dual bath process. With plasma etching, the skin of a fiber can be gradually removed. By measuring the gas separation properties of the etched fibers as a function of etching time, information concerning the resistance of the support layer can be obtained. Figure 7 gives the gas separation results of etched fibers spun from a polymer solution of 30 % PES, 10 % glycerol and 60 % NMP with MPD as the first coagulant. After 10 minutes etching time the fluxes of the etched fibers reached a plateau value. According to literature [18], this plateau value represents the flux of the support layer of the fiber. This flux is inversely proportional to the resistance of the support layer. The flux of the support layer of these fibers have an average value of about 2100 GPU, which is more than 100 times higher than the flux of the unetched fiber. Based on the resistance model [19] it was shown in literature [20] that generally the resistance of the support layer of a membrane can be neglected when the flux of the support layer is more than 10 times higher than the flux of the membrane.

#### **5-5-5. Hollow fibers spun with the DB&TIPI process**

In the previous discussion, it is shown that macrovoid formation in fibers prepared with the dual-bath process can be explained with the mechanism proposed by Smolders [10]. This suggests that it should also be possible to apply this mechanism to design a spinning process for the production of macrovoid free hollow fibers. Based on this mechanism, a new spinning method was developed, which combines the dual bath process with a thermally induced phase inversion process, called DB & TIPI process. Primary results of hollow fibers spun with this process are presented in this section.

The system PES-NMP-glycerol was used for preparation of the spinning solutions. To formulate the polymer solution for the new spinning process, cloud point data at different temperatures were determined. The cloud point data of this system are given in figure 8. In this figure it can be seen that the cloud point temperature of the system is very sensitive to variations of the glycerol concentration. For example, for 30 % PES solutions the cloud point temperature is 35 °C with 17.3 % glycerol. It is increased to 90 °C when the glycerol concentration is raised to 18.8 %.

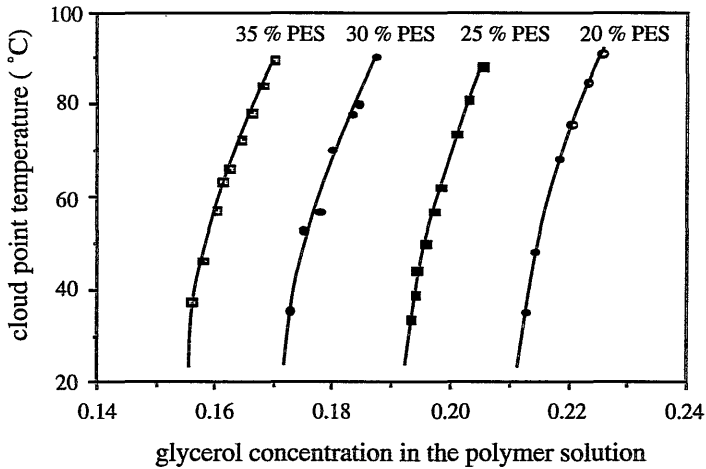


**Figure 8.** Cloud point data for the system PES-NMP-glycerol.

Hollow fibers have been spun from a polymer solution consisting of 30 % PES, 18 % glycerol and 52 % NMP. The cloud point temperature of this solution is 70 °C. The temperature of the spinning solution was kept at 100 °C. HT was used as the first coagulant. The first coagulant was heated to 95 °C before entering the spinneret. Table 3 shows the gas separation properties of the obtained fibers.

**Table 3.** The gas separation properties of hollow fibers spun with the new spinning process.

| fiber | $\alpha_{(\text{CO}_2/\text{CH}_4)}$ | $P/l_{(\text{CO}_2)}$ (GPU) |
|-------|--------------------------------------|-----------------------------|
| 1     | 22                                   | 19                          |
| 2*    | 40                                   | 16                          |
| 3**   | 44                                   | 15                          |

\*: Fiber 1 dried in an oven at 80 °C over night

\*\* : Fiber 1 coated with a layer of silicon rubber.

polymer solution: 30 % PES, 18 % glycerol and 52 % NMP ( $T_c = 70$  °C)

first coagulant: HT (2.0 ml/min)

bore liquid: water (0.6 ml/min)

gap length: 40 mm

temperature of the spinning solution: 100 °C

temperature of the first coagulant: 95 °C

temperature of the second bath: 18 °C

temperature of the bore liquid: room temperature

Although the temperature of the spinning solution and the temperature of the first coagulant are about 30 °C higher than the cloud point temperature of the spinning

solution, instantaneous demixing occurred when the polymer solution was in contact with the first coagulant. This was observed when casting a flat sheet film of the same solution followed by immersion of the film into a HT bath. Instantaneous demixing was observed visually when the film was immersed into the HT bath. The experiment was performed in an oven at 100 °C. Before the casting process the polymer solution, the casting knife and the support plate as well as the HT bath were stored in the oven overnight at 100 °C.

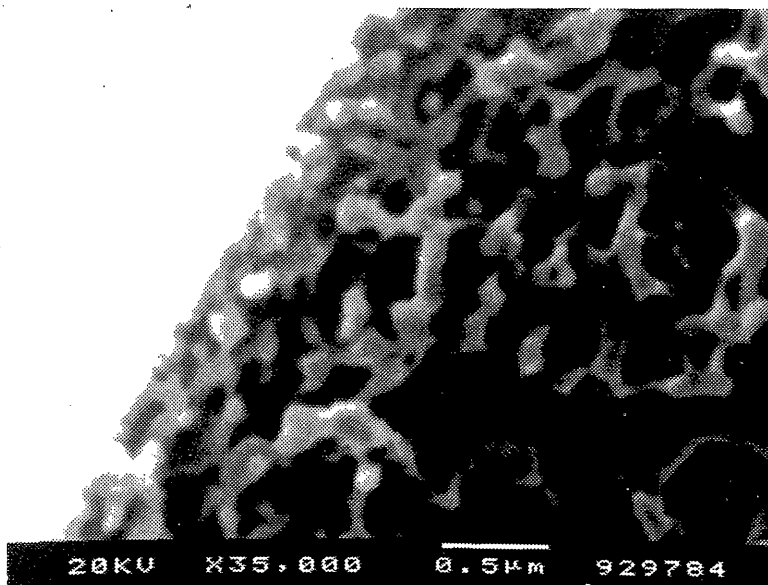
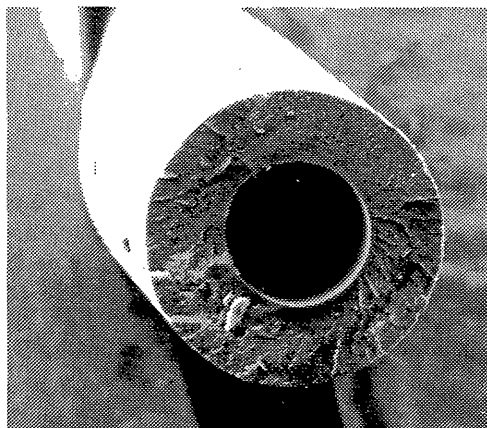


**Figure 9.** Cross section and of the external skin region of fiber 1 in table 3.

After drying at 80 °C overnight, the fiber showed a selectivity of 40 for a mixture of CO<sub>2</sub> and CH<sub>4</sub> and a flux of 16 GPU for CO<sub>2</sub>. The effective skin thickness of this fiber was estimated to be about 0.19 μm. The skin thickness was calculated from the flux of the fiber and the intrinsic permeability of the polymer. The intrinsic permeability of PES for CO<sub>2</sub> is 3.0 x 10<sup>-10</sup> cm<sup>3</sup> cm/cm<sup>2</sup> s cmH<sub>g</sub> at room temperature as measured with a homogeneous, dense film [14]. High temperature drying removed residual solvent from the fiber and might also anneal the fiber. These two effects are both favourable for achieving a high selectivity. After coating, the selectivity is 44 and the flux is 15 GPU. The intrinsic selectivity (52~55) was not obtained. The reason for this will be discussed later.

Figure 9 shows a cross section and the external skin region of the fiber. Indeed, the fiber is macrovoid free. The SEM picture shows that the thickness of the skin is somewhat less than 0.1 μm.

The observed skin thickness is significantly smaller than the effective skin thickness, which means that the resistance of the support layer has a strong influence on the properties of the fiber. Assuming the external skin is completely dense with a thickness of 0.1 μm, estimations based on the resistance model [19] showed that the resistance of the support layer is nearly half of the total resistance of the fiber. The fact that the intrinsic selectivity of the coated fiber cannot be achieved also indicates a certain resistance of the support layer. The reason for the formation of a highly resistant support layer at high temperature is not clear.

The differences in properties of fiber 3 in table 1 and fiber 1 in table 3 are striking. Although the additive concentrations in the two spinning solutions are not the same, the high selectivity of fiber 1 in table 3 is not likely to be caused by the high additive concentration because the results presented in table 1 show that a high additive concentration does not favour formation of a dense skin. Comparing the other spinning parameters for the two fibers, it can be seen that there is a significant difference in spinning temperature. At high spinning temperature, the exchange of solvent and nonsolvent becomes fast. The differences in properties of the two fibers suggest that for our membrane forming system the polymer concentration at the interface increases faster when the spinning temperature is higher. It is very interesting to see that although instantaneous demixing occurred when the polymer solution was in contact with the first coagulant, highly selective fibers could still be obtained. A hypothesis about skin formation during this process will be given later.

Hollow fibers were also spun from a different solution at a temperature lower than that used for the spinning of fiber 1 in table 3. The polymer solution consisted of 30 % PES, 17.3 % glycerol and 52.7 % NMP. The temperature of the polymer solution and the temperature of the first coagulant were kept at 65 °C. The cloud point temperature of the solution is 35 °C. Other spinning parameters were the same as those



given in table 3. The resulting fiber showed a selectivity of 1.2 and a flux of about 200 GPU. Again this indicates that when a high amount of nonsolvent additive is present in the polymer solution, a high spinning temperature has to be applied in order to obtain a highly selective fiber.

Burst pressures of a hollow fiber without macrovoids and a fiber with macrovoids have been measured. Table 4 gives the results. The burst pressure of the fiber free of macrovoids is higher than that of the fiber with macrovoids. This was actually expected.

**Table 4.** Burst pressures of a fiber without macrovoids and a fiber with macrovoids

| fiber              | macrovoids | burst pressure (bar) |
|--------------------|------------|----------------------|
| fiber 1 in table 1 | yes        | 35 ~ 40              |
| fiber 1 in table 3 | no         | 55 ~ 60              |

#### 5-5-6. Skin formation in the new spinning process

It had been believed that instantaneous demixing process would result in membranes with a porous skin, suitable for UF or MF applications. The results obtained in this study indicate that this is not always true. In the new spinning process presented here instantaneous demixing takes place when the polymer solution is in contact with the first coagulant. Still, fibers with a very dense skin can be obtained.

To explain the formation of the dense skin, a mechanism is proposed which is strongly supported by experimental evidence.

It is often assumed that for membrane formation by immersion precipitation liquid-liquid demixing takes place by means of nucleation and growth of the polymer lean phase. Reuvers [8] has confirmed this experimentally for the system CA-acetone-H<sub>2</sub>O. Theoretically, *nucleation can not take place at the interface*. To be more specific, a nucleus can not be created in such a way that half of the nucleus is in the polymer solution and the other half is in the coagulation bath. This means that at the interface no pores can be formed by nucleation of the polymer lean phase when liquid-liquid demixing can take place by means of nucleation and growth. Pores *can* be formed at the interface, however, by coalescence of the formed nuclei. Apparently, the condition required for nuclei to be able to coalesce at the interface is a low enough polymer concentration at the interface. The result of breaking of the thin lamella between nuclei and coagulation bath will be the formation of an MF membrane. In literature [21], it

was reported that an MF membrane could be obtained by contacting a cast solution with a nonsolvent vapour phase saturated with the solvent, followed by immersion of the demixed solution into a nonsolvent bath. In this case, liquid-liquid demixing takes place in the polymer solution by adsorption of nonsolvent into the polymer solution. Since solvent outflow is negligible, the polymer concentration at the interface will still be low, which gives the chance for the growing nuclei to coalesce at the interface.

In the dual bath spinning process, no demixing will occur as long as the polymer solution is in contact with the first coagulant, if the nonsolvent additive concentration is relatively low. Before the solution contacts the second coagulant, the polymer concentration at the interface may already reach the vitrification concentration. As a result, fibers with a completely dense skin can be obtained as shown previously [14]. In the other hand if a high amount of additive is present in the polymer solution, liquid-liquid demixing will occur prior to vitrification of polymer at the interface during contact time of the polymer solution and the first coagulant. This will lead to three possible results, which are discussed with the aid of figure 10.

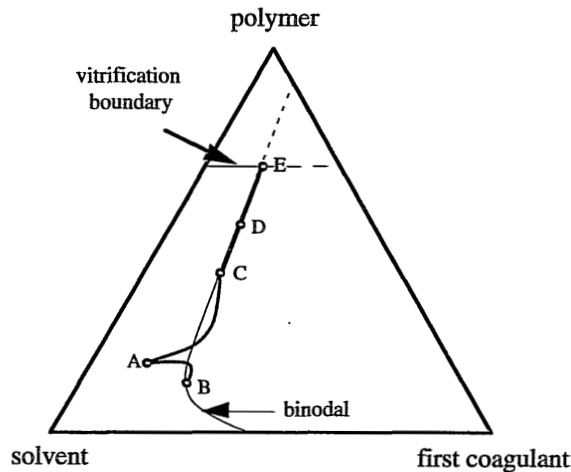


**Figure 10.** A schematic illustration of change of polymer concentration in the top region of a polymer solution as long as the solution is in contact with the first coagulant. A refers to the initial composition of the polymer solution. B or C represents the possible interface composition of the solution at the onset of liquid-liquid demixing. For the initial composition path AC, D or E is a possible interface composition at the moment when the demixed solution is getting in contact with a second coagulant. In this diagram, the additive in the polymer solution is the first coagulant.

The first possibility is that the formed nuclei may coalesce at the interface resulting in an MF membrane, provided that the initial composition path in the solution is characterized by the path AB in figure 10. This is apparently not true for the spinning

conditions used in this study, because at the skin of fiber 2 or fiber 3 in table 1 no pores were observed by SEM examination.

When liquid-liquid demixing starts, the polymer concentration at the interface may increase significantly, characterized by the composition path AC in figure 10. The high polymer concentration at the interface will drastically reduce the coalescence rate of the growing nuclei. Moreover, the polymer concentration at the interface increases continuously due to the fact that the first coagulant extracts solvent from the polymer solution. This eventually prevents coalescence at the interface. Depending on the mass transfer rate and the time allowed for the solution to remain in contact with the first coagulant, the polymer concentration at the interface may reach a value characterized by point D or a value characterized by point E in figure 10.

In case the demixed solution with an interface composition D is getting in contact with water (from the second bath or from the bore side of the fiber), the already occurred liquid-liquid demixing process suddenly changes its course because of the intrusion of water. The concentrated lamella between the nuclei and the coagulation bath vitrifies rapidly then. The result is the formation of nodular structure in the skin of the ultimate membrane, following the mechanism proposed in chapter 3. This is the second possibility for skin formation of the fibers spun with the new spinning process.

The third possibility is that the interface polymer concentration has reached the vitrification level (point E in figure 10) before the demixed solution gets in contact with water. The result will be the formation of a highly selective skin. This requires a fast outflow of solvent from the interface while the solution remains in contact with the first coagulant.

Fiber 1 in table 3 was spun at high temperature. Thus outdiffusion of solvent was enhanced. The skin of the obtained fiber is composed of nodules, as is shown in figure 9. The selectivity of the fiber before high temperature drying or coating was considerably lower than the intrinsic value. This indicates that the packing of the nodules is not completely dense. So, probably the outdiffusion rate of the solvent under our spinning conditions was not high enough to achieve a vitrified interface before the polymer solution was in contact with water, implying that the second possibility described above is most likely responsible for the skin formation of the fiber obtained with the new spinning process. The porosity of the skin, however, is very low (lower than  $10^{-6}$  percent of the surface area, estimated by applying the resistance model [19]). After drying at a temperature of 80 °C, the selectivity reached 40, nearly the same value as that of the coated fiber. As described previously, the failure in achieving the intrinsic selectivity is due to the rather high resistance of the support layer.

Recently, Pinnau *et al.* [22,23] developed a so-called dry/wet phase inversion process for the preparation of integrally-skinned and defect-free membranes for gas separation. In this process, instantaneous demixing occurs and defect-free membranes

with a skin as thin as 200 Å can be obtained. In principle the dry/wet phase inversion process is rather similar to the dual bath process. In the dry/wet phase inversion process evaporation of solvent is employed to increase the polymer concentration at the interface. In the dual bath process, the increase of the polymer concentration at the interface is realised by using a properly chosen nonsolvent to "extract" solvent out of the polymer solution. The results obtained by Pinnau and that obtained in this study suggest that to obtain a thin skin ( $< 0.1 \mu\text{m}$ ) with the dual bath process, instantaneous demixing has to be induced when the polymer solution is in contact with the first coagulant. This is because when no demixing occurs during the contact time not only the polymer concentration at the interface will increase but also the thickness of this concentrated layer will increase. This inevitably will limit the possibility to achieve an ultrathin skin, especially when a highly viscous nonsolvent is used as the first coagulant. By introducing instantaneous demixing in the polymer solution during contact with the first coagulant, the difficult removal of the viscous first coagulant from the fiber surface will no longer be the limiting step to obtain a thin skin since the formation of the nuclei underneath the interface will prohibit the increase of the thickness of the skin.

## 5-6. CONCLUSIONS

Plasma experiments carried out in this study have shown that the resistance of the support layer of fibers presented in chapter 4 is about 100 times lower than the resistance of the skin of the corresponding fiber. However, these highly selective hollow fibers contain many macrovoids in the support layer. The formation of these macrovoids is initiated from the bore side.

Addition of solvent to the bore liquid can reduce the size of the macrovoids initiated from the bore side, but this gives rise to the appearance of macrovoids initiated from the external skin side.

Macrovoids can be eliminated by the addition of a high amount of nonsolvent to the polymer solution. However, when those fibers are spun at a relatively low temperature (i. e. at room temperature), they show nonselective properties.

With a new spinning process, combining the dual bath process with a thermally induced phase inversion process (DB & TIPI process), highly selective hollow fibers free of macrovoids can be obtained. SEM examinations reveal that the apparent skin of those fibers is very thin ( $< 0.1 \mu\text{m}$ ). The formation of the thin skin is the result of instantaneous demixing when the polymer solution is brought in contact with the first coagulant. It is believed that achievement of the high selectivity is related to the high temperature applied in the spinning process. The effective skin thickness of the fibers prepared with the new spinning process is about two times the apparent skin thickness.

This means that further improvement of the properties of those fibers has to be focussed on reduction of the resistance of the support layer.

Burst pressure tests show that the mechanical strength of fibers without macrovoids is higher than that of fiber with macrovoids.

## 5-7. REFERENCES

1. Frommer, M. A. and Lancet, D., in Lonsdale, H. K. and Podall, H. E. (Eds), *Reverse Osmosis Membrane Research*, Plenum Press, New York, NY, 1972
2. Frommer, M. A. and Messalam, R. M., *Ind. Eng. Chem., Prod. Res. Dev.*, 12, 328 (1973)
3. Strathmann, H.; Kock, K.; Amar, P. and Baker, R. W., *Desalination*, 16, 179 (1975)
4. Cabasso, I.; Klein, E. and Smith, J. K., *J. Appl. Polym. Sci.*, 21, 165 (1977)
5. Kesting, R.E.; Fritzsche, A.K.; Murphy, M.K.; Cruse, C.A.; Handermann, A.C. and Malon, R.F., *Eur. Pat.*, 0259288, 1987
6. Van't Hof, J. A., *PhD Thesis*, University of Twente, the Netherlands, 1988
7. Broens, L.; Altena, F. W. and Smolders, C. A., *Desalination*, 32, 33 (1980)
8. Reuvers, A. J., *PhD Thesis*, University of Twente, the Netherlands, 1986
9. Van't Hof, J. A.; Reuvers, A. J.; Boom, R. M.; Rolevink, H. H. M and Smolders, C.A., *J. Membr. Sci.*, 70, 17 (1992)
10. Smolders, C. A.; Reuvers, A. J.; Boom, R. M. and Wienk. I. M., *J. Membr. Sci.*, 73, 259 (1992)
11. Reuvers, A. J.; Van den Berg, J. W. A. and Smolders, C. A., *J. Membr. Sci.* 34, 45 (1987)
12. MacDonald, *U. S. Pat.* 3,842,515 (1974)
13. Henis, J. M. S and Tripodi, M. K., *U. S. Pat.* 4,230,463, 1980
14. Chapter 4 of this thesis
15. Boom, R. M., *PhD Thesis*, University of Twente, the Netherlands, 1992
16. Kooops, G. H., *PhD Thesis*, University of Twente, the Netherlands, 1992
17. Chapter 2 of this thesis
18. Fritzsche, A. K.; Cruse, C. A.; Kesting, R. E. and Murphy, M. K., *J. Appl. Polym. Sci.*, 41, 713 (1990)
19. Henis, J. M. S and Tripodi, M. K., *J. Membr. Sci.* 8, 233 (1981)
20. Pinnau, I. and Koros, W.J., *Ind. Eng. Chem. Res.*, 30, 1837 (1991)
21. Kesting, R. E., *Synthetic polymeric membranes*, McGraw Hill, New York, 1985
22. Pinnau, I.; Wind, J. and Peinemann, K.-V., *Ind. Eng. Chem. Res.*, 29, 2028 (1990)
23. Pinnau, I. and Koros, W. J., *J. Membr. Sci.*, 71, 81 (1992)



---

**SUMMARY**

---

Today, immersion precipitation is the most often used process for the preparation of gas separation membranes from polymeric materials. In this process a polymer solution in the form of a thin liquid film or hollow fiber is immersed in a nonsolvent bath where the polymer precipitates and forms a membrane.

The immersion precipitation process can be performed by various means. The dual bath spinning process is one specific way which can be used, *e.g.*, for the preparation of hollow fiber membranes for gas separation. In this process hollow fibers are spun by contacting the polymer solution with two properly chosen coagulants successively. The first coagulant is used to "extract" solvent out of the polymer solution. The contact time is short in order to create a thin layer of high polymer concentration at the interface. The second coagulant is used to quickly precipitate the polymer solution to form the membrane. With this spinning process, hollow fibers with the intrinsic selectivity of the polymer material can be easily obtained without the necessity of coating.

This thesis is aimed on extending the knowledge on membrane formation and on further developing the dual bath spinning process for the preparation of gas separation hollow fibers with both high selectivity and high flux.

The term (physical) gelation is very often used to describe the skin formation of membranes by immersion precipitation. However, in literature a clear picture on the gelation mechanism during membrane formation is lacking. In chapter 2, the gelation process during the formation of a membrane from amorphous polymers is studied. A gelation mechanism based on a literature model is applied to membrane formation and tested experimentally. According to this mechanism, gelation results from liquid-liquid phase separation arrested by vitrification of the polymer rich phase. Gelation boundary for the system PES-NMP-H<sub>2</sub>O is obtained from DSC measurements and cloud point data. It is found that for this system, vitrification is the only mechanism for the fixation of the membrane structure. It is also shown that for some membrane forming systems, upon immersion precipitation vitrification can occur prior to liquid-liquid demixing. Such a process results in a completely dense skin suitable for gas separation.

In chapter 3, mass transfer during the membrane formation process is studied for the system H<sub>2</sub>O-NMP-PES. The study is based on a model developed by Reuvers to describe the immersion precipitation process. In the model both thermodynamic and kinetic parameters of a membrane forming system are taken into account. It is found that to describe accurately the thermodynamic properties of the system H<sub>2</sub>O-NMP-PES by using the Flory-Huggins theory, a ternary interaction parameter has to be taken into

account instead of considering binary interaction parameters only. It is shown that an accurate description of the thermodynamic properties of a membrane forming system is essential for obtaining useful information about the composition changes during membrane formation. Model calculations show that for the system H<sub>2</sub>O-NMP-PES, after the immersion of a PES/NMP solution into a water bath both liquid-liquid demixing and vitrification take place instantaneously near the interface. Based on model calculations, the reason for nodular structure formation is described. The effect of changing the friction coefficients (related to diffusion coefficients) on the liquid-liquid demixing behaviour is also simulated.

In chapter 4, the results for gas separation hollow fibers spun with a modified dual bath spinning process are presented. The modification is made by the usage of a triple orifice spinneret. This simplifies the spinning process and improves the ability to control the contact time between the polymer solution and the first coagulant, which is critical for obtaining a fiber with a thin skin. Using this modified dual bath process, completely defect-free PES hollow fibers with a skin thickness between 0.2 and 0.3  $\mu\text{m}$  could be obtained. The criteria for the choice of the first coagulant in relation to the membrane properties are also studied in this chapter. Based on the three dimensional solubility parameter concept, an empirical rule concerning the selection of the first coagulant for the preparation of gas separation membranes is proposed. It is shown that the dual bath process is also an effective method for the preparation of microfiltration membranes with high surface porosity and uniform pore size.

In chapter 5 the formation of macrovoids in the support layer of hollow fibers prepared with the dual bath process is studied. It is shown that the mechanism for the formation of these macrovoids can be explained on the basis of a model proposed by Smolders. Furthermore, a new spinning method based on this model has been developed for the preparation of gas separation hollow fibers. Macrovoid free and highly selective hollow fibers could be obtained by using this method which combines the dual bath process with a thermally induced phase inversion process. In this so-called DB & TIPI process a polymer solution is spun into hollow fibers by contacting two successive nonsolvent baths. The polymer solution has a cloud point temperature that is higher than the temperature of the second bath. When the polymer solution is immersed into the second bath, liquid-liquid demixing spreads through the solution quickly due to the fast drop in temperature. This eliminates the possibility for macrovoid formation. Hollow fibers prepared in this way show an apparent skin thickness about 0.1  $\mu\text{m}$  (observed by SEM). The effective skin thickness is, however, about 0.19  $\mu\text{m}$  (calculated according to the flux of the fiber and the intrinsic permeability of the polymer). This means that the resistance of the support layer of those fibers has to be reduced in order to further increase the flux.



---

## SAMENVATTING

---

Vandaag de dag is immersie-precipitatie het meest gebruikte proces voor het vervaardigen van gasscheidingsmembranen van polymere materialen. Bij dit proces wordt een polymeeroplossing in de vorm van een dunne film of een holle vezel ondergedompeld in een niet-oplosmiddel waardoor het polymeer precipiteert en het membraan wordt gevormd.

Het immersie-precipitatie proces kan op verschillende manieren worden uitgevoerd. Het twee-badsspinproces is een specifieke wijze waarop bijvoorbeeld holle vezel membranen voor gasscheiding kunnen worden vervaardigd. Bij dit proces worden holle vezels gesponnen door een polymeeroplossing achtereenvolgens in contact te brengen met twee zorgvuldig gekozen coagulatiemiddelen. Het eerste coagulatiemiddel wordt gebruikt om gedurende korte tijd het oplosmiddel uit de polymeeroplossing te extraheren om zodoende een dunne laag met een hoge polymeerconcentratie aan het grensvlak te creëren waarna de tweede coagulant zorgt voor een snelle precipitatie waarbij het membraan gevormd wordt. Met dit spinproces worden op eenvoudige wijze holle vezels verkregen met de intrinsieke selectiviteit van het membraanmateriaal zonder dat coating noodzakelijk is.

Dit proefschrift heeft als doel het vergroten van de kennis van membraanvorming en de verdere ontwikkeling van het twee-badsspinproces voor het vervaardigen van holle vezels voor gasscheiding met zowel een hoge selectiviteit als een hoge flux.

De term (fysische) gelering wordt vaak gebruikt om de vorming van de toplaag bij immersie-precipitatie te beschrijven. Echter, in de literatuur ontbreekt een duidelijk beeld van het geleringsmechanisme tijdens membraanvorming. In hoofdstuk 2 wordt het geleringsproces bestudeerd dat plaats vindt tijdens de vorming van een membraan van een amorf polymeer. Een geleringsmechanisme gebaseerd op een model uit de literatuur wordt toegepast op membraanvorming en experimenteel getest. Volgens dit mechanisme wordt gelering veroorzaakt door vloeistof-vloeistof ontmenging welke wordt gestopt door verglazing van de polymeerrijke fase. De geleringsgrens van het systeem H<sub>2</sub>O-NMP-PES wordt verkregen uit DSC-metingen en cloud-point data. Voor dit systeem is gevonden dat alleen de verglazing belangrijk is voor het fixeren van de membraan structuur. Ook is aangetoond dat voor sommige membraanvormende systemen verglazing optreedt tijdens immersie-precipitatie voordat vloeistof-vloeistof ontmenging plaats vindt. Een dergelijk proces resulteert in een dichte toplaag die geschikt is voor gasscheiding.

In hoofdstuk 3 wordt het massatransport tijdens membraanvorming bestudeerd voor het systeem H<sub>2</sub>O-NMP-PES. De studie is gebaseerd op een model ontwikkeld door Reuvers voor de beschrijving van het immersie-precipitatieproces. In het model worden zowel thermodynamische als kinetische parameters in beschouwing genomen. Het blijkt dat voor een nauwkeurige beschrijving van de thermodynamische eigenschappen van het systeem H<sub>2</sub>O-NMP-PES aan de hand van de Flory-Huggins theorie een ternaire interactieparameter in beschouwing moet worden genomen in plaats van alleen binaire interactieparameters. Er is aangetoond dat een nauwkeurige beschrijving van de thermodynamische eigenschappen essentieel is voor het verkrijgen van nuttige informatie over compositieveranderingen tijdens membraanvorming. Modelberekeningen tonen aan dat voor het systeem H<sub>2</sub>O-NMP-PES zowel vloeistof-vloeistof ontmenging en verglazing onmiddellijk plaats vinden aan het grensvlak na immersie van een PES/NMP-oplossing in een water bad. Een oorzaak voor de vorming van nodulaire structuren wordt beschreven op basis van modelberekeningen. Bovendien is het effect gesimuleerd van het veranderen van de frictiecoëfficiënten (welke gerelateerd zijn aan diffusiecoëfficiënten) op het vloeistof-vloeistofontmenggedrag.

In hoofdstuk 4 worden resultaten gepresenteerd van holle vezels voor gasscheiding welke zijn gesponnen volgens een gemodificeerd twee-badspinproces. De modificatie bestaat uit het gebruik van een spinkop met drie concentrische ringvormige openingen, hetgeen het spinproces vereenvoudigt en de mogelijkheid verbetert om de contacttijd tussen polymeeroplossing en het eerste coagulatiebad te controleren. Dit laatste is van cruciaal belang voor het verkrijgen van een dunne top laag. Met dit gemodificeerde twee-badsproces worden geheel defectvrije PES-holle vezels verkregen met een top laagdikte van ca. 0.2-0.3 µm. Ook wordt in dit hoofdstuk het criterium voor de keuze van het coagulatiebad in relatie tot de membraaneigenschappen bestudeerd. Op basis van het concept van driedimensionale oplosbaarheidsparementers wordt een empirische regel voorgesteld voor de keuze van het eerste coagulatiebad voor het vervaardigen van gasscheidingsmembranen. Aangetoond wordt dat het twee-badsproces ook een geschikte methode is voor het vervaardigen van microfiltratiemembranen met een hoge oppervlakteporositeit en een uniforme poriegrootte.

In hoofdstuk 5 wordt de vorming bestudeerd van macro voids in de steunlaag van holle vezels die vervaardigd zijn met het twee-badsproces. Aangetoond wordt dat de vorming van deze macrovoids uitgelegd kan worden aan de hand van van een model voorgesteld door Smolders. Verder is op basis van dit model een nieuwe spinmethode ontwikkeld voor het vervaardigen van holle vezels voor gasscheiding. Holle vezels zonder macrovoids en met een hoge selectiviteit konden worden verkregen met deze methode welke het "dual bath"-proces combineert met een

“thermally induced phase inversion”-proces. In dit zogenaamde DB&TIPI-proces worden holle vezels gesponnen door een polymeeroplossing achtereenvolgens in contact te brengen met twee niet-oplosmiddelbaden. De polymeeroplossing heeft een cloud point temperatuur die hoger is dan de temperatuur van het tweede bad. Wanneer de polymeeroplossing in het tweede bad wordt ondergedompeld, vindt een snelle vloeistof-vloeistof ontmenging plaats in het membraan ten gevolge van de snelle temperatuurdaling. Dit sluit de mogelijkheid voor vorming van macrovoids uit. Holle vezels die op deze wijze zijn vervaardigd hebben een schijnbare toplaagdikte van 0.1  $\mu\text{m}$  (bepaald met SEM). De werkelijke toplaagdikte is echter ongeveer 0.19  $\mu\text{m}$ , berekend aan de hand van de flux door de vezel en de intrinsieke permeabiliteit van het polymeer. Dit betekent dat de weerstand in de steunlaag verminderd moet worden om de flux verder te verhogen.



## **CURRICULUM VITAE**

Shu-Guang Li was born on May 19, 1960 at Guang Xi, China. After graduation from high school in 1977 he spent one year on a farm. From 1978 to 1982 he studied in the Chemical Engineering Department of Hunan University and obtained the degree of Bachelor of Engineering in 1982. The following three years he studied in the Dalian Institute of Chemical Physics, Chinese Academy of Sciences in the field of membrane technology and got his M.Sc. degree in Chemical Engineering in 1985. In the same institute he worked for other four years on the preparation and application of UF and MF membranes. In September 1989 he joined the Membrane Technology group (under supervision of Prof. Smolders and later Prof. Strathmann) of the Chemical Technology Department at the University of Twente (the Netherlands) and worked on preparation of hollow fiber membranes for gas separation.





